

Report No. FHWA-RD-75-77

**CORRELATION OF THEORETICAL AND EXPERIMENTAL
DATA FOR HIGHWAY BRIDGES**

Vol. II. Military Loading

H.A. Miklofsky



February 1975

Final Report

This document is available to the public
through the National Technical Information
Service, Springfield, Virginia 22161

Prepared for

FEDERAL HIGHWAY ADMINISTRATION

Offices of Research & Development

Washington, D.C. 20590

OCT 30 1975

DISCLAIMER NOTICE

This document is disseminated under the sponsorship of the Department of Transportation in the interest of information exchange. The United States Government assumes no liability for its contents or use thereof.

The contents of this report reflect the views of the Office of Research of the Federal Highway Administration, which is responsible for the facts and the accuracy of the data presented herein. The contents do not necessarily reflect the official views or policy of the Department of Transportation.

This report does not constitute a standard, specification, or regulation.

FHWA DISTRIBUTION NOTICE

Sufficient copies of this report are being distributed by FHWA Bulletin to provide a minimum of two copies to each regional office, two copies to each division office, and four copies to each State highway agency. Direct distribution is being made to the division offices.

1. Report No. FHWA-RD-75-77		2. Government Accession No.		3. Recipient's Catalog No.									
4. Title and Subtitle CORRELATION OF THEORETICAL AND EXPERIMENTAL DATA FOR HIGHWAY BRIDGES. Vol. II. Military Loading.				5. Report Date February 1975									
				6. Performing Organization Code									
7. Author(s) Haaren A. Miklofsky				8. Performing Organization Report No.									
9. Performing Organization Name and Address Bridge Structures Group, Structures & Applied Mech. Div. Office of Research Federal Highway Administration Washington, D. C. 20590				10. Work Unit No. (TRAIS) FCP 25F2-022									
				11. Contract or Grant No.									
12. Sponsoring Agency Name and Address Federal Highway Administration, Department of Transportation Washington, D. C. 20590				13. Type of Report and Period Covered Final Report									
				14. Sponsoring Agency Code 50376									
15. Supplementary Notes Staff Study (HRS-11)													
16. Abstract A computer program analytical routine "SSAP-2" is utilized to correlate a theoretical finite element analysis with experimental results for three typical two-lane multi-span girder and slab highway bridges in Tennessee. The programmed response for a fourth bridge is also included. All three bridges gave excellent correlation between predicted and experimental responses for deflection and moment distribution of the HET-70 loading to the main carrying members of the bridge. It is concluded that maximum stresses induced by future unique heavy military loads can be compared on a timely basis with the highway bridge structure's load carrying capability by use of the computerized theoretical method. This volume is the second of two reports. The other is: <table border="1"> <thead> <tr> <th>Vol. No.</th> <th>FHWA No.</th> <th>Short Title</th> <th>NTIS (PB) No.</th> </tr> </thead> <tbody> <tr> <td>I</td> <td>75-37</td> <td>Static Loading</td> <td>(not yet available)</td> </tr> </tbody> </table>						Vol. No.	FHWA No.	Short Title	NTIS (PB) No.	I	75-37	Static Loading	(not yet available)
Vol. No.	FHWA No.	Short Title	NTIS (PB) No.										
I	75-37	Static Loading	(not yet available)										
17. Key Words Finite element analysis, bridge analysis, computer programs, SSAP-2, HET-70			18. Distribution Statement No restrictions. This document is available through the National Technical Information Service, Springfield, Virginia 22151.										
19. Security Classif. (of this report) Unclassified		20. Security Classif. (of this page) Unclassified		21. No. of Pages 186									
22. Price													

ACKNOWLEDGEMENTS

The author wishes to express his thanks to Ron Theobald and Chris Folger, MTMTS, for their splendid assistance in helping to run the computer program on the Honeywell 6060 computer at MTMTS.

Special thanks are extended to Lynn Runt, Toni Wilbur, and Bob Feather, members of the Fairbank Highway Research Station computer team, for their assistance with JCL for the IBM 360 computer. The author also wishes to express his thanks to Val Radosevich, Fairbank Highway Research Station, and Francis Litavec, Federal Highway Administration, (IBM 360 operators) for their excellent cooperation in running the program on the IBM 360 computer.

The author appreciates the seminar and review sessions with Jeff Franklin, Tom Collingsworth, and Leon Heidebrecht during the summer of 1974, which led to many constructive suggestions.

It is always a pleasure to work for such people as Robert Varney, Charles Galambos, and Jim Cooper, who gave the author their full support and encouragement.

Finally, the author wishes to thank Linda Roberts for typing the final report within an almost impossible deadline.

TABLE OF CONTENTS

	<u>Page</u>
LIST OF ILLUSTRATIONS	v
LIST OF TABLES	xi
I. INTRODUCTION	1
1. Subject	1
2. Background	1
II. TABULATION OF MAXIMUM DEFLECTION AND STRESS LEVELS IN COMPARISON WITH EXPERIMENTAL DATA AND INFORMATION FROM PRELIMINARY REPORTS.	6
1. General	6
2. Bridge #1	6
3. Bridge #2	18
4. Bridge #3	23
5. Bridge #4	27
III. CONCLUSIONS AND LIMITATIONS.	30
IV. RECOMMENDATIONS.	31
APPENDIX A - Background Correspondence Pertaining to Establishment of Project	Omitted
APPENDIX B - Preliminary Research Reports	B-1
APPENDIX C - Details of Computer Input Data and Load Conditions	C-1
APPENDIX D - References	D-1
APPENDIX E - Calculations Regarding Computer Predictions and AASHTO Specifications	E-1

LIST OF ILLUSTRATIONS

	<u>Page</u>
FIGURE 1 - PHOTOGRAPH OF HET-70 TANK TRANSPORTER AND M-60 TANK	7
FIGURE 2 - LOADING KEY FOR BRIDGE NO. 1 SHOWING THE POSITION OF ALL TEST VEHICLES IN THEIR RESPECTIVE LANES	8
FIGURE 3 - LAYOUT OF STRAIN AND DEFLECTION GAGES FOR BRIDGE NO. 1	9
FIGURE 4 - LOADING KEY SHOWING ALL TEST VEHICLES IN THEIR LANE LOCATION FOR BRIDGE NO. 2	10
FIGURE 5 - STRAIN GAGE AND DEFLECTION LOCATIONS FOR BRIDGE NO. 2	11
FIGURE 6 - LOADING KEY FOR ALL TEST VEHICLES IN THEIR RESPECTIVE LANE LOCATION FOR BRIDGE NO. 3	12
FIGURE 7 - STRAIN GAGE AND DEFLECTION GAGE LOCATIONS FOR BRIDGE NO. 3	13
FIGURE 8 - LANE LOCATION OF VEHICLES FOR BRIDGE NO. 4.	14
FIGURE 9 - POSITION OF HET-70 TANK TRANSPORTER ALONG BRIDGE NO. 1 FOR DIFFERENT LOAD CASES	15
FIGURE 10 - CORRELATIONS BETWEEN COMPUTER AND EXPERIMENTAL DATA FOR BRIDGE NO. 1	16
FIGURE 11 - LOCATION OF HET-70 TANK TRANSPORTER ON BRIDGE NO. 2 FOR VARIOUS LOAD CASES	19
FIGURE 12 - CORRELATION BETWEEN COMPUTER AND EXPERIMENTAL DATA FOR BRIDGE NO. 2	20
FIGURE 13 - POSITION OF HET-70 TANK TRANSPORTER ON BRIDGE NO. 3 FOR VARIOUS LOAD CASES	24
FIGURE 14 - CORRELATION BETWEEN COMPUTER AND EXPERIMENTAL RESULTS FOR BRIDGE NO. 3	25
FIGURE 15 - LOCATION OF HET-70 TANK TRANSPORTER ON BRIDGE NO. 4 FOR VARIOUS LOAD CASES	27
FIGURE 16 - COMPUTER PREDICTIONS FOR LOAD DISTRIBUTION AND DEFLECTION FOR BRIDGE NO. 4	28

FIGURE B- 1 - HET-70 TANK TRANSPORTER ON FOUR SPAN CONTINUOUS STEEL BEAM BRIDGE	B-13
FIGURE B- 2 - BPR TEST VEHICLE ON REINFORCED CONCRETE T-BEAM BRIDGE	B-14
FIGURE B- 3 - M-60 TANK ON PRESTRESSED CONCRETE BEAM BRIDGE	B-14
FIGURE B- 4 - HET-70 AXLE LOADS IN KIPS FULLY LOADED	B-15
FIGURE B- 5 - VEHICLE PATHS AND STRAIN GAGE LOCATIONS FOR CONTINUOUS STEEL BEAM BRIDGE	B-16
FIGURE B- 6 - MAXIMUM BENDING STRESSES IN CONTINUOUS STEEL BEAM BRIDGE FOR VARIOUS PATHS OF BPR VEHICLE	B-17
FIGURE B- 7 - MAXIMUM BENDING STRESSES IN CONTINUOUS STEEL BEAM BRIDGE FOR VARIOUS PATHS OF M-60 TANK	B-18
FIGURE B- 8 - MAXIMUM BENDING STRESSES IN CONTINUOUS STEEL BEAM BRIDGE FOR VARIOUS PATHS OF HET-70 VEHICLE	B-19
FIGURE B- 9 - MAXIMUM BENDING STRESS FOR REINFORCED CONCRETE SIMPLE SPAN BRIDGE FOR VARIOUS VEHICLES AND VARIOUS PATHS	B-20
FIGURE B-10 - MAXIMUM BENDING STRESS FOR PRESTRESSED CONCRETE SIMPLE SPAN BRIDGE FOR VARIOUS VEHICLES AND VARIOUS PATHS	B-21
FIGURE B-11 - NEUTRAL AXIS LOCATION FROM MEASURED STRAINS WITH HET-70 LOADING, INTERIOR GIRDER NEAR MID-SPAN OF 90' SPAN, FOUR SPAN CONTINUOUS STEEL GIRDER BRIDGE	B-38
FIGURE B-12 - NEUTRAL AXIS LOCATION FROM MEASURED STRAINS WITH HET-70 LOADING, EXTERIOR GIRDER NEAR MID-SPAN OF 90' SPAN, FOUR SPAN CONTINUOUS STEEL GIRDER BRIDGE	B-39
FIGURE B-13 - STRAIN GAGE LOCATION IN PIER CAP FOR MEASURING LIVE LOAD EFFECTS TRANSMITTED BY EXTERIOR GIRDER BEARINGS	B-40
FIGURE B-14 - ELEVATIONS OF T-BEAM STEMS SHOWING MAXIMUM LIVE LOAD STRESSES AT GAGE POINTS AND BOTTOM REINFORCING BARS	B-57

	<u>Page</u>
FIGURE B-15 - ELEVATIONS OF PRESTRESSED GIRDERS SHOWING MAXIMUM LIVE LOAD STRAINS AT GAGE POINTS ON BOTTOM SURFACES PATH 2 CROSSINGS	B-58
FIGURE B-16 - ELEVATIONS OF PRESTRESSED GIRDERS SHOWING MAXIMUM LIVE LOAD STRAINS AT GAGE POINTS ON BOTTOM SURFACES PATH 3 CROSSINGS	B-59
FIGURE B-17 - ELEVATIONS OF PRESTRESSED GIRDERS SHOWING MAXIMUM LIVE LOAD STRAINS AT GAGE POINTS ON BOTTOM SURFACES PATH 4 CROSSINGS	B-60
FIGURE B-18 - TYPICAL VIBRATION RESPONSES AT MID-SPAN OF THE BRIDGE SUPERSTRUCTURE, PRESTRESSED CONCRETE GIRDER BRIDGE UNDER PASSAGE OF THE TRACK LAYING TANK	B-61
FIGURE B-19 - OBSERVED NATURAL FREQUENCIES IN MODE SHAPES OF BRIDGE SUPERSTRUCTURE VERTICAL VIBRATIONS, FOUR SPAN CONTINUOUS STEEL GIRDER BRIDGE	B-62
FIGURE B-20 - HET-70 BRIDGE LOADING CAPACITY NOMOGRAPH	B-63
FIGURE B-21 - LEGEND AND EXAMPLE FOR HET-70 BRIDGE LOADING CAPACITY NOMOGRAPH	B-64
FIGURE C- 1 - COORDINATE LOCATION OF NODES USED FOR BRIDGE NO. 1 FOR MILITARY LOADING	C- 4
FIGURE C -2 - HALF CROSS SECTION OF BRIDGE NO. 1 WITH BOUNDARY CONDITIONS ALONG CENTERLINE	C- 6
FIGURE C -3 - SAMPLE NODAL INPUT DATA FOR BRIDGE #1, ILLUSTRATING BOUNDARY CONDITION CODES FOR 1/2 SECTION OF BRIDGE	C- 7
FIGURE C- 4 - BEAM AND DIAPHRAGM NUMBERING FOR BRIDGE NO. 1 FOR MILITARY LOADINGS	C- 8
FIGURE C- 5 - PLATE SHELL NUMBERING FOR SLAB OF BRIDGE NO. 1 FOR MILITARY LOADING	C-10
FIGURE C- 6 - LOAD CONDITION 1, BRIDGE 1. CENTER OF GRAVITY OF HET-70 WHEEL LOADS IN LOCATION USED TO CALCULATE THE BRIDGE MOMENT OF TABLE 1	C-12
FIGURE C- 7 - LOAD CONDITION 2, BRIDGE 1. CENTER OF GRAVITY OF HET-70 WHEEL LOADS PLACED TO SATISFY SIMPLE BEAM CRITERIA AT CENTERLINE OF 70' SPAN	C-13
FIGURE C- 8 - LOAD CONDITION 3, BRIDGE 1. REAR WHEEL OF TRAILER AT FIRST INTERIOR SUPPORT ON 90' SPAN	C-14

FIGURE C- 9 - LOAD CONDITION 4, BRIDGE 1. CENTER OF GRAVITY OF WHEEL LOADS PLACED 5' TO THE RIGHT OF LOAD CONDITION 2.	C-15
FIGURE C-10 - LOAD CONDITION 5, BRIDGE 1. REAR WHEEL OF TRAILER AT CENTER OF BRIDGE.	C-16
FIGURE C-11 - LOAD INPUT DATA FOR BRIDGE NO. 1.	C-17
FIGURE C-12 - LOAD CONDITION 6, BRIDGE 1. STATIC LOADING.	C-18
FIGURE C-13 - COORDINATE LOCATION OF NODES USED FOR BRIDGE #2 FOR MILITARY LOADING	C-19
FIGURE C-14 - BEAM AND DIAPHRAGM NUMBERING FOR BRIDGE #2 FOR MILITARY LOADING	C-20
FIGURE C-15 - PLATE SHELL NUMBERING FOR SLAB OF BRIDGE #2 FOR MILITARY LOADING	C-21
FIGURE C-16 - LOAD CONDITION 1, BRIDGE 2. CENTER OF GRAVITY OF HET-70 WHEEL LOADS ON BRIDGE IN LOCATION USED TO CALCULATE THE BRIDGE MOMENT OF TABLE 1.	C-22
FIGURE C-17 - LOAD CONDITION 2, BRIDGE 2. REAR WHEEL OF TRAILER AT END OF INTERIOR GIRDER.	C-23
FIGURE C-18 - LOAD CONDITION 3, BRIDGE 2. CENTER OF GRAVITY OF HET-70 LOADS REMAINING ON INTERIOR GIRDER PLACED TO SATISFY MAXIMUM MOMENT CRITERIA FOR INTERIOR GIRDER	C-24
FIGURE C-19 - LOAD CONDITION 4, BRIDGE 2. STATIC LOADING	C-25
FIGURE C-20 - COORDINATE LOCATION OF NODES USED FOR BRIDGE #3 FOR MILITARY LOADING	C-26
FIGURE C-21 - BEAM AND DIAPHRAGM NUMBERING FOR BRIDGE #3 FOR MILITARY LOADING	C-27
FIGURE C-22 - PLATE SHELL NUMBERING FOR SLAB OF BRIDGE #3 FOR MILITARY LOADING	C-28
FIGURE C-23 - LOAD CONDITION 1, BRIDGE 3. CENTER OF GRAVITY OF HET-70 WHEEL LOADS ON BRIDGE IN LOCATION USED TO CALCULATE THE BRIDGE MOMENT OF TABLE 1.	C-29
FIGURE C-24 - LOAD CONDITION 2, BRIDGE 3. REAR WHEEL OF TRAILER AT END OF INTERIOR GIRDER.	C-30

	<u>Page</u>
FIGURE C-25 - LOAD CONDITION 3, BRIDGE 3. CENTER OF GRAVITY OF HET-70 LOADS REMAINING ON INTERIOR GIRDER PLACED TO SATISFY MAXIMUM MOMENT CRITERIA FOR INTERIOR GIRDER.	C-31
FIGURE C-26 - LOAD CONDITION 4, BRIDGE 3. STATIC LOADING	C-32
FIGURE C-27 - COORDINATE LOCATION OF NODES USED FOR BRIDGE #4 FOR MILITARY LOADING	C-33
FIGURE C-28 - BEAM AND DIAPHRAGM NUMBERING FOR BRIDGE #4 FOR MILITARY LOADING	C-34
FIGURE C-29 - PLATE SHELL NUMBERING FOR SLAB OF BRIDGE #4 FOR MILITARY LOADING	C-35
FIGURE C-30 - LOAD CONDITION 1, BRIDGE 4. CENTER OF GRAVITY OF HET-70 WHEEL LOADS AT THE CENTER OF THE FIRST INTERIOR 60' SPAN	C-36
FIGURE C-31 - LOAD CONDITION 2, BRIDGE 4. CENTER OF GRAVITY OF REAR FOUR WHEELS OF HET-70 TRAILER IS AT 18', THE 0.4 POINT OF THE EXTERIOR 45' SPAN	C-37
FIGURE C-32 - LOAD CONDITION 3, BRIDGE 4. CENTER OF GRAVITY OF HET-70 WHEEL LOADS REMAINING ON INTERIOR GIRDER IS AT 22.5', THE 0.5 POINT OF THE EXTERIOR 45' SPAN	C-38
FIGURE C-33 - LOAD CONDITION 4, BRIDGE 4. REAR WHEEL OF TRAILER IS AT THE FIRST INTERIOR SUPPORT ON 60' SPAN	C-39
FIGURE E- 1 - CALCULATIONS FOR STRINGER MOMENTS OF INERTIA FOR BRIDGE #1, ACCORDING TO AASHO SPECIFICATIONS	E- 5
FIGURE E- 2 - CALCULATIONS OF NEGATIVE MOMENTS AT INTERIOR SUPPORTS FOR BRIDGE #1 - FROM COMPUTER DATA, LOAD CONDITION 1	E- 6
FIGURE E- 3 - CALCULATIONS OF MOMENT OF INERTIA OF TRANSFORMED UNIT WIDTH OF SLAB FOR BRIDGE #1	E- 9
FIGURE E- 4 - MOMENT OF INERTIA CALCULATIONS FOR BRIDGE #2	E-14
FIGURE E- 5 - MAXIMUM FLEXURAL STRESS SUMMARIES FOR INTERIOR GIRDER OF BRIDGE #2	E-18

	<u>Page</u>
FIGURE E- 6 - CALCULATIONS OF MOMENT OF INERTIA OVER TRANSVERSE UNIT WIDTH OF SLAB FOR BRIDGE #2	E-23
FIGURE E- 7 - ONE POSSIBLE ARRANGEMENT OF REINFORCING STEEL FOR THE T-BEAM OF BRIDGE #3	E-25
FIGURE E- 8 - CALCULATIONS OF MOMENT OF INERTIA OVER TRANSVERSE UNIT WIDTH OF SLAB FOR BRIDGE #3	E-28
FIGURE E- 9 - CALCULATIONS OF DEAD LOAD MOMENTS AND SHEARS FOR THE INTERIOR GIRDER OF BRIDGE #4	E-31
FIGURE E-10 - MOMENTS OF INERTIA OF GIRDER AND COVER PLATES FOR BRIDGE #4	E-32
FIGURE E-11 - CALCULATIONS OF MAXIMUM NEGATIVE MOMENT AT ONE OF THE INTERIOR SUPPORTS FOR BRIDGE #4	E-32
FIGURE E-12- CALCULATIONS OF MOMENT OF INERTIA OVER TRANSVERSE UNIT WIDTH OF SLAB FOR BRIDGE #4	E-34

LIST OF TABLES

		<u>Page</u>
TABLE 1	COMPUTED BENDING MOMENTS AND STRESSES	B-12
TABLE 2	MAXIMUM MEASURED LIVE-LOAD DEFLECTIONS, FOUR-SPAN CONTINUOUS STEEL BRIDGE	B-54
TABLE 3	MAXIMUM MEASURED LIVE LOAD DEFLECTIONS, REINFORCED CONCRETE AND PRESTRESSED CONCRETE BRIDGE	B-55
TABLE 4	GIRDER RESPONSE DISTRIBUTION FACTORS, FOUR-SPAN CONTINUOUS STEEL BRIDGE	B-56
TABLE 5	SUMMARY OF ALLOWABLE TRANSVERSE SLAB STRESSES UNDER VARIOUS AASHO SPECIFICATIONS	E- 3

I. INTRODUCTION

1. Subject

This final report covers the investigation of a computerized methodology for accurately predicting stresses and deflections in straight and skew highway bridges under the HET-70 tank transporter military loading. Verification of the methodology is accomplished through a comparison of predicted responses and experimental results for three highway bridges in Tennessee loaded with the HET-70 tank transporter carrying the M-60 tank. The investigation was undertaken at the request of the Special Assistant for Transportation Engineering, Department of the Army. The purpose of this report is to provide the Department of the Army with a computerized theoretical methodology, so that maximum stresses induced by future, unique, heavy military loads can be compared on a timely basis with the highway bridge structure's load carrying capability.

Appendix B contains three preliminary reports by FHWA. Appendix C contains a detailed description of the computerized data input format and load conditions for the Tennessee bridge analyses for the HET-70 loading. Volume I contains a detailed description of the programming methodology.

2. Background

The transportation of many heavy military vehicle requires special state permits for crossing highway bridges. One of the fundamental problems in the issuance of these permits for the HET-70 tank transporter has been the establishment of the lateral load distribution of the transporter to the main load carrying girders. Various simplifications have been developed in the past, none of which has been acceptable to all the states. (1) (2)* The

* Numbers in () refer to references listed in Appendix D.

computer methodology presented herein will allow the direct determination of actual wheel loads to the longitudinal load carrying members of the bridge without the simplifying assumptions associated with empirical methods. For example, the AASHTO 1973 specifications presents empirical formulas for calculating the distribution of wheel loads to stringers for the "design of normal highway bridges." (3) It is also inferred, but not so stated, that this means normal loading as well. The HET-70 tank transporter, with its 8 1/2 ft. lateral c.c. distance between wheels, has a non-standard distance; hence, distribution factors based on normal loads may not be valid in this case.

After permission to move the HET-70 over public highways was denied by several states, the Army* requested the Bridge Committee of AASHTO, (then American Association of State Highway Officials) in December, 1967, to examine the problem and reconcile the different views of the highway departments. In January, 1968, the AASHTO Committee on Bridges and Structures received comments from several interested states that questioned the distribution of wheel loads to two lanes. Some states were concerned that a bridge designed for a H-15 or HS-15 loading could not safely carry the 195 kip HET-70 loading. Furthermore, different states suggested different load distribution factors for the HET-70 to the middle girders of the bridge. There was disagreement among several of the state highway department bridge engineers with the transverse distribution of the load used by BPR (formally the Bureau of Public Roads, now the Federal Highway Administration). Finally, the Bureau of Public Roads was asked to finalize plans in January, 1969, for actual field tests to move the tank transporter over certain bridges to determine the true transverse distribution of the wheel loads to the girders.

Accordingly, in April-May, 1969, a work plan was drawn up by BPR for a loading study of highway bridges near Winchester, Tennessee, to be conducted as a cooperative study by the Bureau of Public Roads, the Tennessee Department of Highways, and the Department of the Army. Essentially, four bridges in the Tennessee state highway system in the vicinity of Winchester, Tennessee, were available for research studies as a result of their planned inundation by the new Tims Ford Reservoir which had made necessary the relocation of the highway at a higher elevation. The opportunity to utilize full-size bridges as test specimens, one of which was built under H-15 specifications, came at an appropriate time for a planned study of the effect of the tank transporter on bridges.

* Military Traffic Management and Terminal Service (MTMTS); now the Military Traffic Management Command-Special Assistant for Transportation Engineering (MTMC-SA).

The objective of the test was to measure the strains and deflections on each main load carrying member at critical sections of the bridge, which would then be used to determine the actual moment distribution of various moving live loads among these members for comparisons with each other and with empirical design distributions predicted by analytical methods. The loads would consist of (1) a vehicle closely approximating an HS-20 design loading; (2) a late model Department of the Army tank transporter loaded to represent the maximum magnitude of such load likely to be required to transverse the Nation's highways; and (3) a Department of the Army 52-ton battle tank crossing under its own power. Each bridge would be subjected to carefully controlled crossings by each of the three prescribed vehicles in turn. The lane, speed, and direction of crossing would be the other variables included. Speeds would be varied in increments from crawl speed to the maximum attainable. The crossing lanes would be each of the two normal lanes and a centerline. The strains would be monitored continuously and simultaneously on recording oscillographs.

The testing of three of the Tennessee bridges with the HET-70 tank transporter and M-60 combat tank was conducted between April 18 and May 8, 1969. The bridges in question are identified as bridges 1, 2, and 3 of this report. In June, 1969, the first preliminary research report (Appendix B) was prepared, which gave an indication of the measured live load responses from the tests, and compared them to allowable bending moments and stresses for the entire cross section of the bridge.

The second preliminary BPR report (October, 1969) also presented in Appendix B, gave detailed consideration to the distribution of the total bending moment to the interior and exterior girders. Consideration was also given to the dynamic amplification of stress due to moving loads. Of fundamental importance to this report is the statement that "The crawl speed stress corresponds to the static live loading of the structure." *The crawl speed is taken to mean a speed less than 5 mph.* The second preliminary report also discussed in general terms the measured deck slab stresses and measured pier cap bending stresses. A brief motion picture film *Tennessee Bridge Test* was also prepared by the Bureau of Public Roads, depicting the conduct of the field study and illustrating some typical findings drawn from the research.

Preliminary Report No. 3 (Appendix B) was prepared in May, 1970, which completed the presentation of the field study findings. In this report the effect of skew on two concrete bridges was contrasted with the behavior of the unskewed steel bridge. Also live load deflections and vibration responses of the bridges were presented. Finally, a nomograph procedure for evaluating the capability of simple span bridges to carry the HET-70 loading was described.

During the summer of 1970, an additional field study was conducted by the Bureau of Public Roads, the Tennessee Highway Department, and the University of Tennessee, which culminated in the static live loading to failure of the three bridges heretofore mentioned plus one additional continuous three span bridge identified as bridge No. 4 in this report. The resulting tests are described in a report by the University of Tennessee published in December, 1971, reference (4). This report served as background information for the computer study of Volume I.

In 1972, the author of this report, during summer employment on earthquake analysis at the Fairbank Highway Research Station, began exploring the capabilities of various computer programs to analyze bridge structures by the Finite Element Analysis Method. Fortunately a copy of the SAP I program prepared by Dr. Wilson of the University of California (Berkeley) for the Corps of Engineers on a CDC 6400 computer was available in modified IBM form, furnished to FHWA by the Corps of Engineers. Unfortunately, some assembler additions to speed up I-O had been made to the IBM version that were inoperative on the FHWA computer; and the author, then being inexperienced in the JCL language, was unable to successfully correct the JCL code that summer. In the fall, the author cut the program back to a CDC version and successfully computed (under his own personal funding and additional funding from the University of Arizona) the mode shapes and frequencies for the Sitka Harbor Cable Stayed Bridge.*

The author then requested computer support only from FHWA (Federal Highway Administration) to further examine the possibilities of the SAP program series for bridge analyses. The author also proposed that the report on research should contain sufficient background information so that an engineer, unfamiliar with finite element analysis, might be able to make intelligent changes in the program to suit his own needs without repeating the extensive research performed by the author. There is an additional fringe benefit to understanding the program statements in detail. If a user wishes to hand check certain computations when experimental data is not available, he can use print statements at strategic locations in the program to greatly simplify the hand calculations. The SSAP2 program, then the latest available, was chosen as the basis for the investigation for static loading on bridges. Volume I is the result of the research performed from July, 1973 through May, 1974, and contains a correlation of theoretical and experimental data for

* The Bathe dynamic version was also added to replace the original Rayleigh-Ritz method to eliminate the trial and error procedure for evaluating the lowest fundamental frequency. (5)

the four Tennessee Highway Bridges under static loading. (6)
Also contained therein is an extensive description relating
finite element theory directly to the program statements of
SSAP2. Finally, a complete listing is presented of that part of
the SSAP2 program used for bridge analysis together with full
control statements for the CDC 6400, IBM 360/370, and Honeywell
6060 computers.*

FHWA invited the author to rejoin its ranks for the summer of
1974 to extend this research to the HET-70 loading, the results of
which are contained in Volume II of this report. In June, 1974,
the author

met with representatives of
MTMTS in seminar discussions to finalize plans for the additional
Volume II to complete the project. Volumes I and II, therefore,
will serve as the final report for this project to date. Copies
of the source statements, data decks for the four bridges and
computer printouts are now on file with MTMTS.

* The work on the Honeywell computer was performed in the summer
of 1974 at the MTMTS headquarters, Bailey's Cross Roads,
Virginia.

II. TABULATIONS OF MAXIMUM DEFLECTION AND STRESS LEVELS IN COMPARISON WITH EXPERIMENTAL DATA AND INFORMATION FROM PRELIMINARY REPORTS

1. General

Figure 1 shows the HET-70 tank transporter loaded with the M-60 tank. It has an overall length of approximately 60 feet, weighs 195 kips fully loaded and transmits its load through 8 tires in the cab section and 16 tires in the trailer section as shown on page A-12. Page A-2 also gives further design engineering data. In preliminary report 1 on page B-15 is a sketch showing the design axle loads in kips for the fully loaded vehicle. These are the axle loads used for analysis.

Figures 2 through 8 show the loading key, direction of travel, and location of strain gages for the four Tennessee bridges tested. We shall evaluate the correlation of information for each bridge in turn.

2. Bridge #1

Figure 9 shows the location of the tank transporter and direction of travel for each of the five loading conditions carried through in the computer analysis, while Figure 10 summarizes the pertinent information derived from computer results and compares them to the preliminary reports.

When preliminary report 1 was written, the calculated value of 1715 kips (page B-12) was based upon load condition 1 as the position of the transporter on the interior 90' span of the bridge. In Figure 10, the statics is first recompiled from the computer results for load condition 1 at a section 4.8' to the left of the centerline of the 90' span. The computer data shows a moment of 1653 kip feet for the bridge section versus the 1715 kip feet first calculated by simple beam procedures in preliminary report 1. The computer moment is within 4 percent of the hand calculated value.

At the same location we examine the percent of the total moment carried by the exterior and interior girders respectively. The computer results show 18% of the total moment carried by each exterior girder and 32% of the total moment carried by each interior girder, while the measured averaged distribution of moments carried by these girders (as shown on page B-26) is 21.5% for each exterior girder and 28.5% for each interior girder. Thus there is reasonable agreement between the computer theoretical method and the experimental data concerning the transverse distribution of the HET-70 tank transporter wheel loads to the main load carrying members of bridge #1.

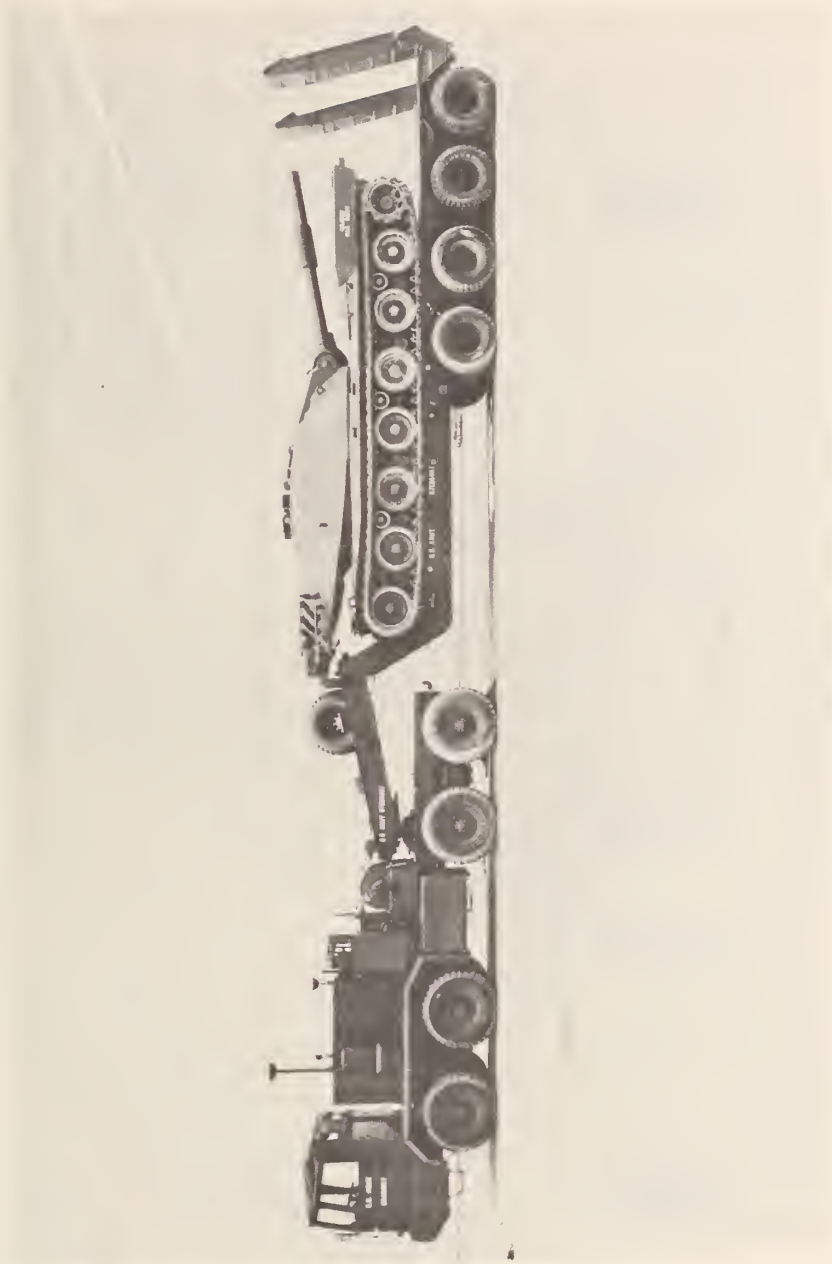


FIG. 1 - PHOTOGRAPH OF HET-70 TANK TRANSPORTER AND M-60 TANK

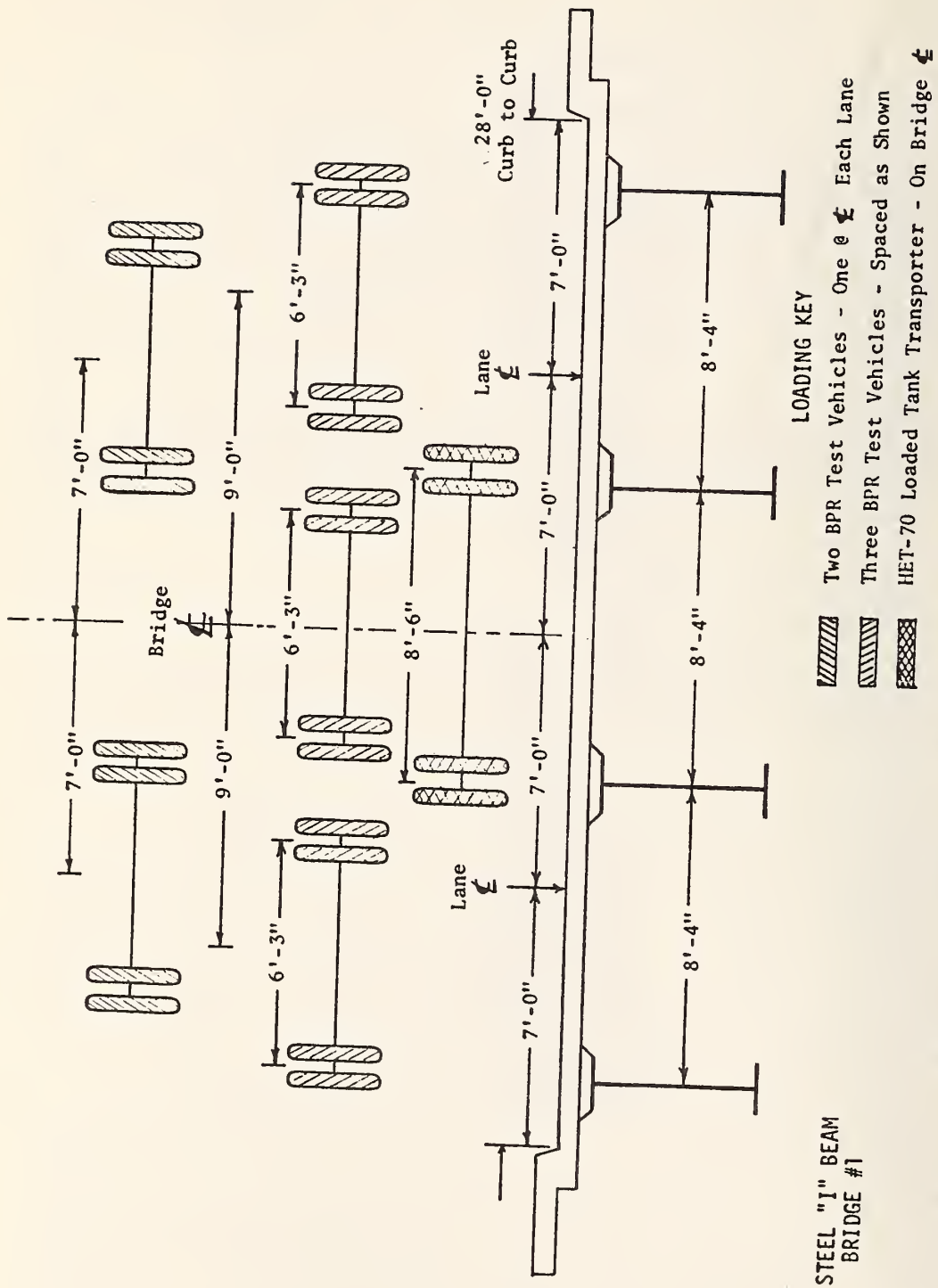
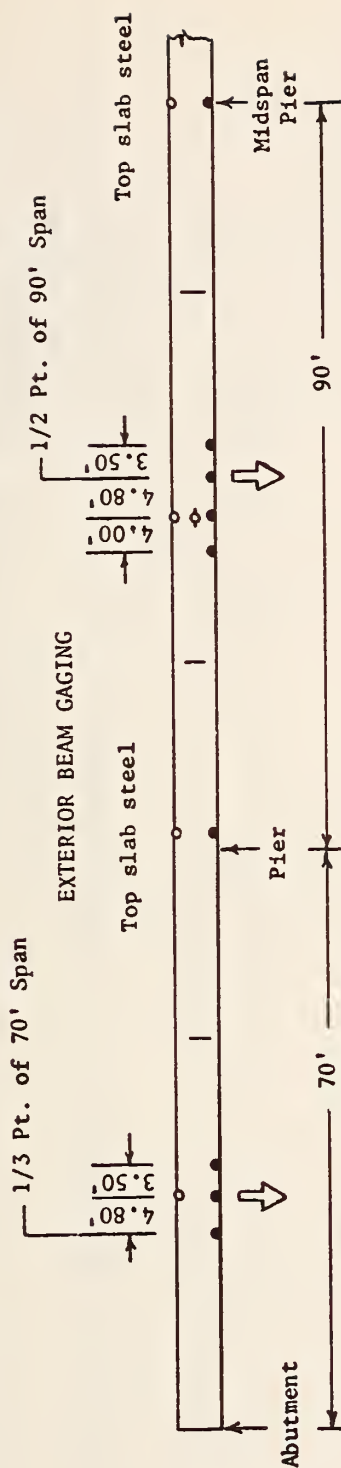


FIG. 2 - - LOADING KEY FOR BRIDGE NO. 1 SHOWING THE POSITION OF ALL TEST VEHICLES IN THEIR RESPECTIVE LANES

- Gages on Top Flange (Strain)
- ◊ Gages on Web (Strain)
- Gages on Bottom Flange (Strain)
- ⇓ Deflection Gages

GAGING LAYOUT



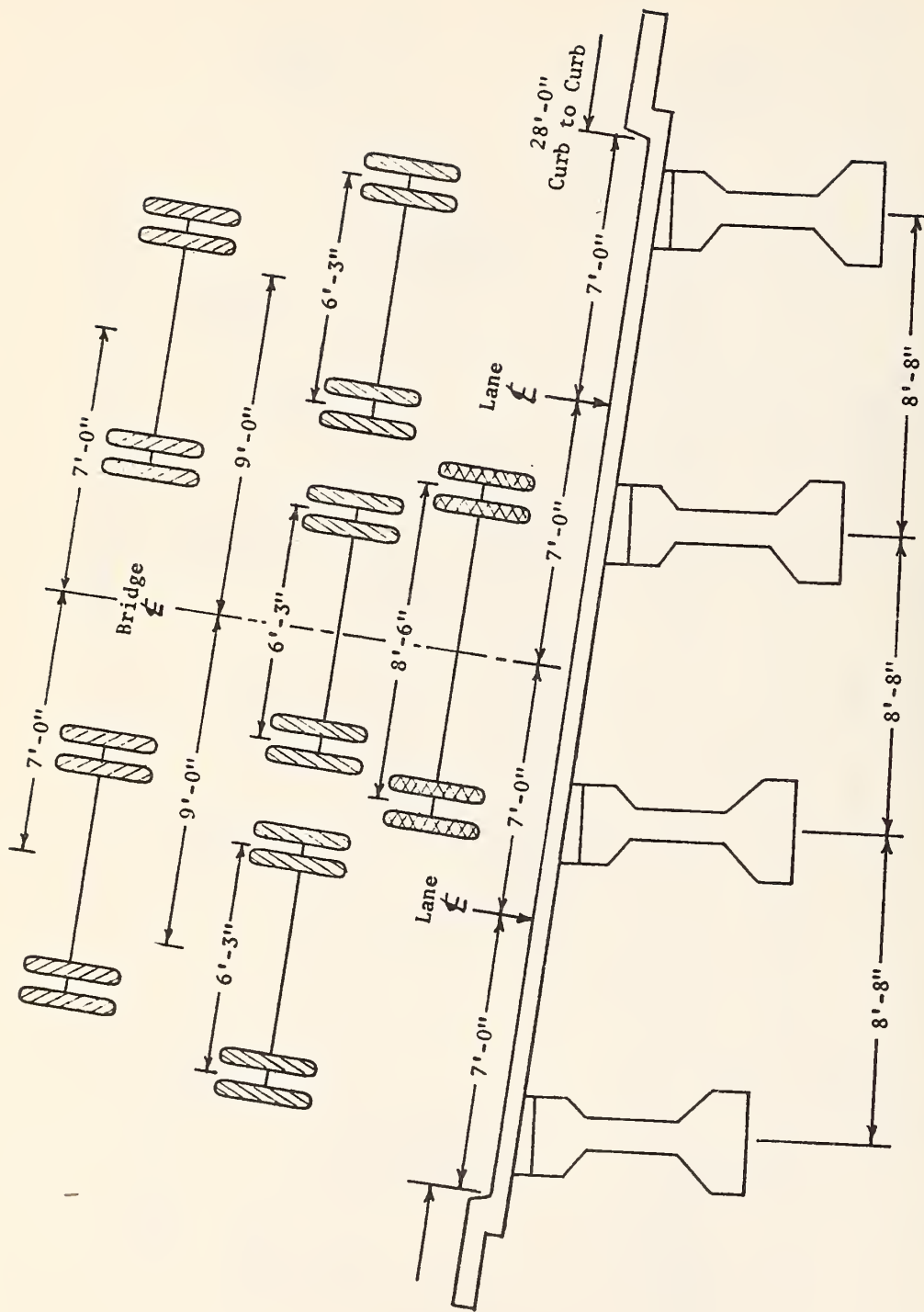
DIRECTION OF TRAVEL →
 HS20 M_{max} Section @ 5.50' from Midspan
 HET-70 M_{max} Section @ 4.80' from Midspan

INTERIOR BEAM GAGING



STEEL "I" BEAM
 BRIDGE #1

FIG. 3 - LAYOUT OF STRAIN AND DEFLECTION GAGES FOR BRIDGE NO. 1



LOADING KEY

PRESTRESSED CONCRETE
BEAM - BRIDGE #2



- Two BPR Test Vehicles - One @ Each Lane
- Three BPR Test Vehicles - Spaced as Shown
- HET-70 Loaded Tank Transporter - On Bridge

FIG. 4 - LOADING KEY SHOWING ALL TEST VEHICLES IN THEIR
LANE LOCATION FOR BRIDGE NO. 2

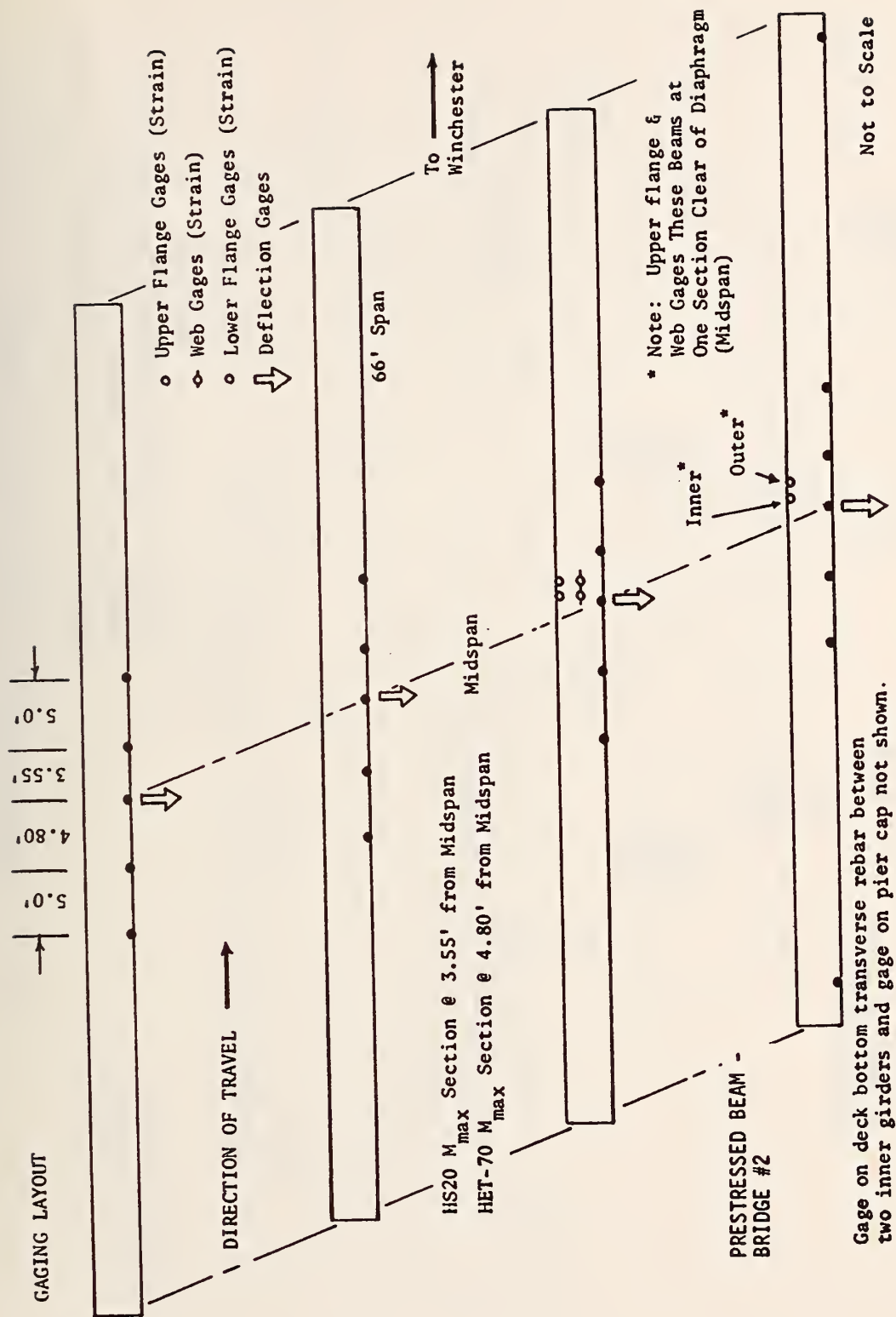


FIG. 5 - STRAIN GAGE AND DEFLECTION LOCATIONS FOR BRIDGE NO. 2

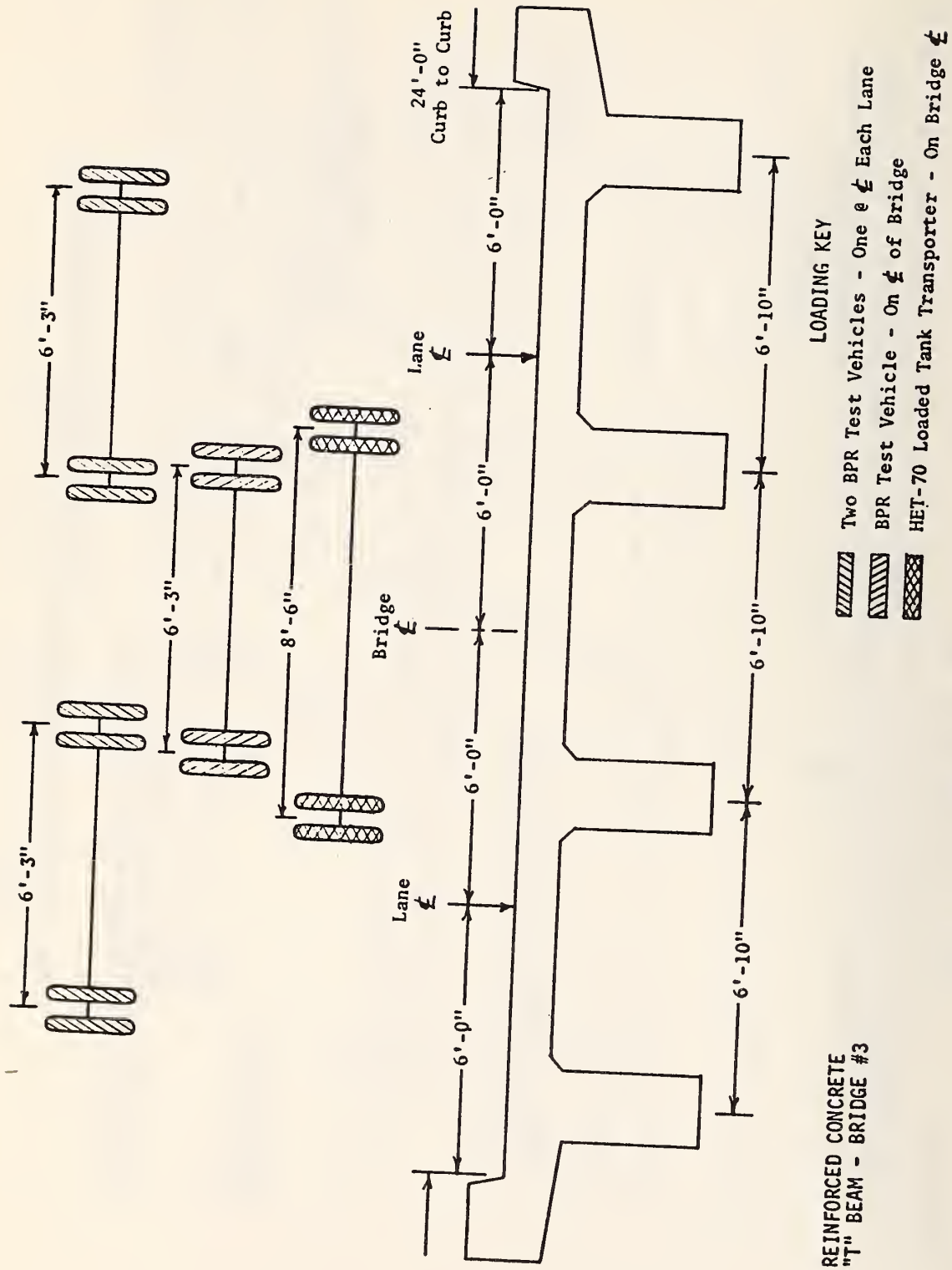


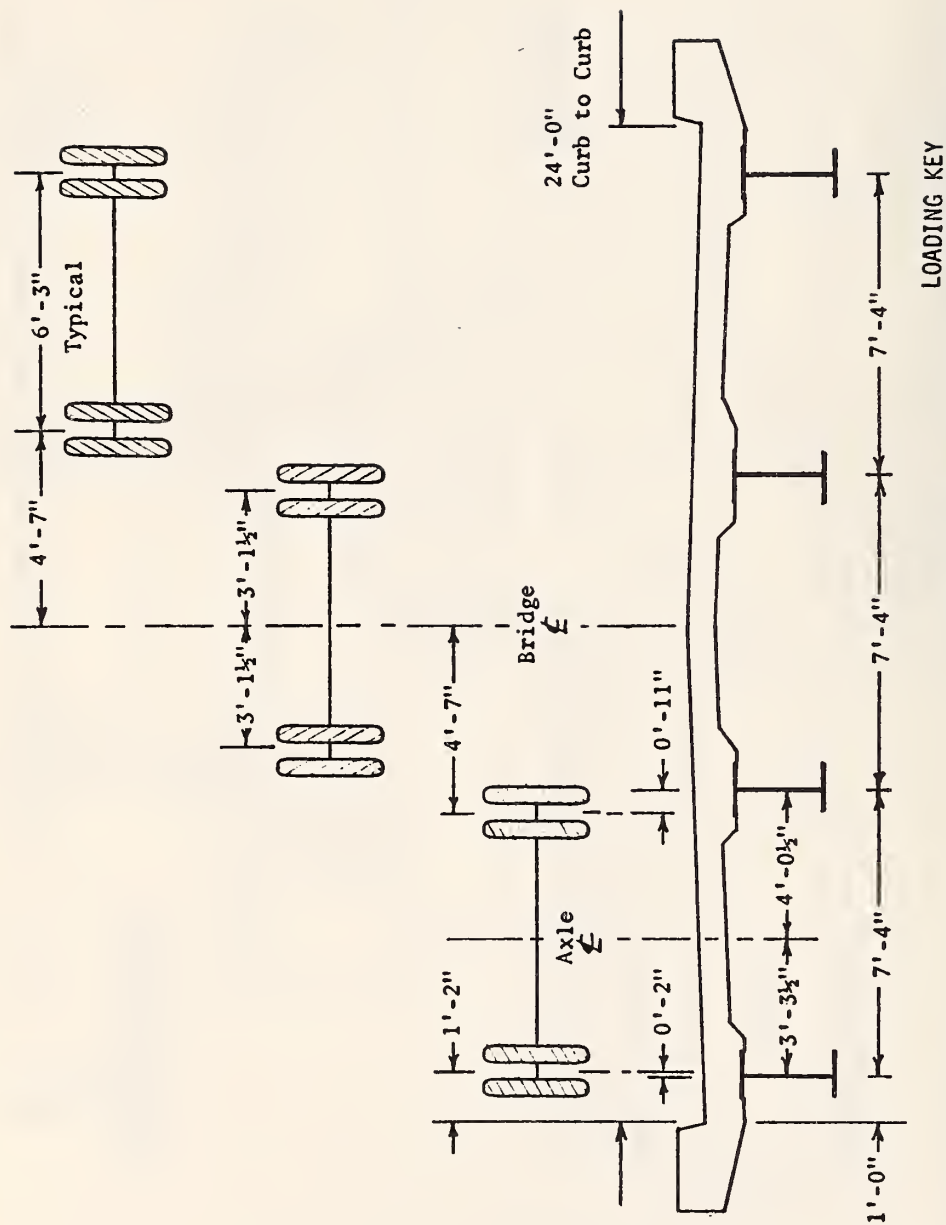
FIG. 6 - LOADING KEY FOR ALL TEST VEHICLES IN THEIR RESPECTIVE LANE LOCATION FOR BRIDGE NO. 3

- Surface Gages (Concrete Surface Strain)
- Lower Gages (Steel Strain)
- ↕ Deflection Gages



Not to Scale

FIG. 7 - STRAIN GAGE AND DEFLECTION GAGE LOCATIONS FOR BRIDGE NO. 3



STEEL "I" BEAM
BRIDGE #4

FIG. 8 - LANE LOCATION OF VEHICLES FOR BRIDGE NO. 4

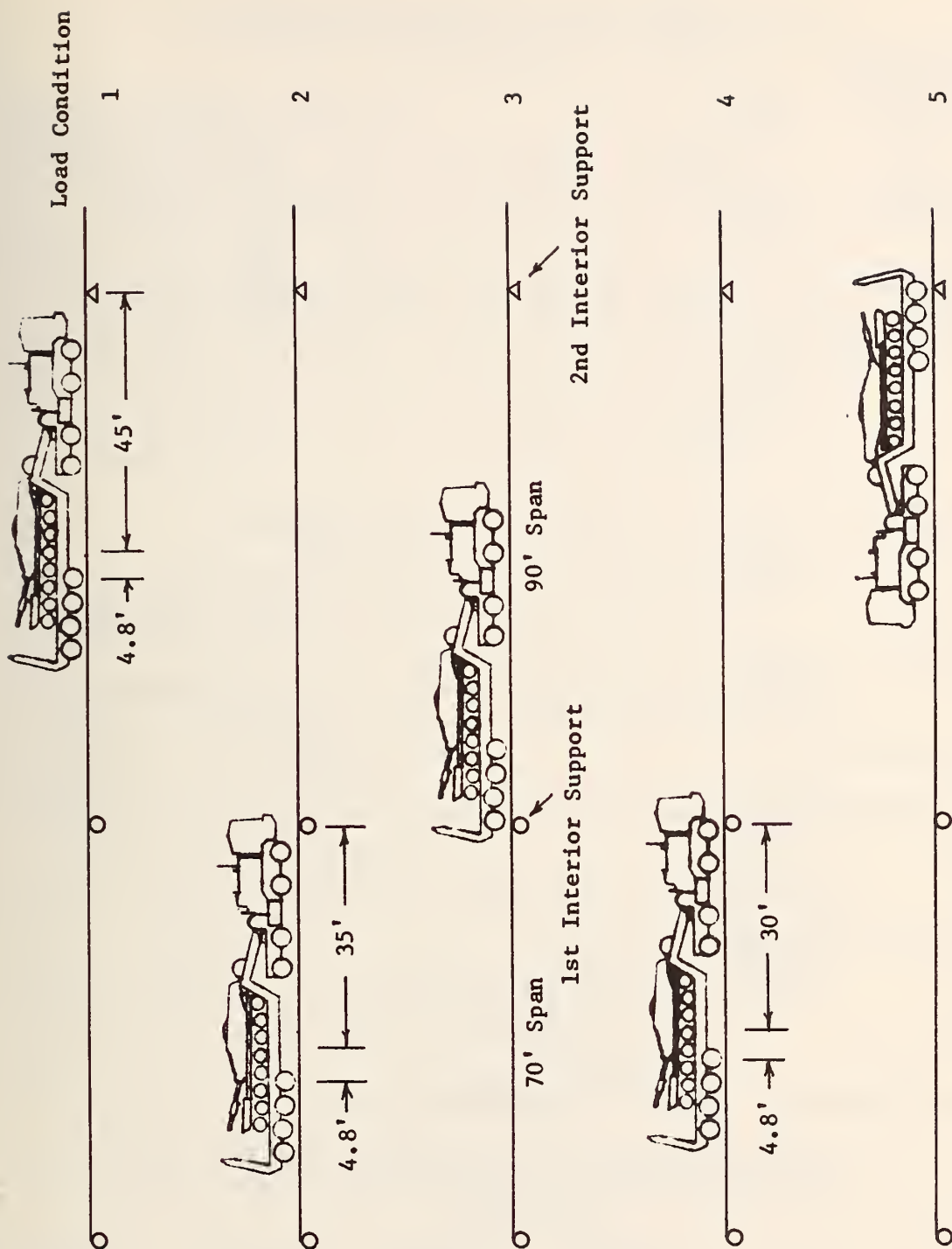


FIG. 9 - POSITION OF HET-70 TANK TRANSPORTER ALONG
BRIDGE NO. 1 FOR DIFFERENT LOAD CASES

BRIDGE #1 - Load Condition 1
c.g. of wheel loads 4.8' to left of centerline
of interior span

$$\begin{aligned} .5075(4.75) &= 2.41 \\ .8061(4.17) &= \underline{3.36} \\ &5.77 \end{aligned}$$

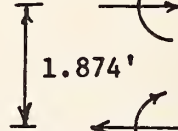
$$\begin{aligned} 13.74(4.75) &= 65.27 \\ 15.69(4.17) &= \underline{65.43} \end{aligned}$$

M (including slab)

$$\begin{aligned} 94.82(1.874) &= 177.69 \\ &112.9 \\ &\underline{5.77} \\ &296.36^k \end{aligned}$$

$$P = 130.7$$

$$M = 5.77$$



$$P = 94.82^k$$

$$M = 112.9^k$$

Sh 67,68

Bm 45

$$\begin{aligned} .8061(4.17) &= 3.36 \\ 1.448(4.17) &= \underline{6.04} \\ &9.40 \end{aligned}$$

$$\begin{aligned} 15.69(4.17) &= 65.43 \\ 16.67(4.17) &= \underline{69.51} \\ &134.94 \end{aligned}$$

M (including slab)

$$\begin{aligned} 170.7(1.874) &= 319.89 \\ &200.9 \\ &\underline{9.40} \\ &530.19^k \end{aligned}$$

$$P = 134.94$$

$$M = 9.40$$



Sh 68,69

Bm 46

$$P = 170.7$$

$$M = 200.9$$

Sum of Forces Check

$$\begin{aligned} \text{Moment Check } 530.19 \\ \underline{296.36} \end{aligned}$$

$$826.55 \times 2 = 1653.1^k \text{ calculated}$$

1715 Preliminary Report #1

Page B-12

$$\longrightarrow 265.64$$

$$\longleftarrow 265.52$$

per half section

$$\text{Percent Difference} = (100) \frac{(1715 - 1653.1)}{1715} = 3.6\%$$

RATIO IN PERCENT OF TOTAL RESISTING MOMENT
PROVIDED BY

	Exterior Girder	Interior Girder	Interior Girder	Exterior Girder
Girder & Slab	17.93	32.07	32.07	17.93
Girder Alone	17.99	32.01	32.01	17.99
Experimental (Page B-26)	22	29	28	21

FIG. 10 - CORRELATIONS BETWEEN COMPUTER AND EXPERIMENTAL
DATA FOR BRIDGE #1

COMPARISON OF DEFLECTIONS IN FOOT UNITS

	Node	Computer	Experimental Page B-54
Midspan - 90' Span			
Load Condition 1			
Exterior Girder	163	.0482	.045
Interior Girder	165	.0590	.0592
.4 Point - 70' Span*			
Load Condition 2			
Exterior Girder	44	.0238	.0233
Interior Girder	46	.0366	.0425
.4 Point - 70' Span*			
Load Condition 4			
Exterior Girder	44	.0242	-----
Interior Girder	46	.0368	-----

COMPARISON OF MAXIMUM STRESSES IN PSI UNITS

Computer maximum stringer stress based on positive stringer moment - beam 46 - 90' span (see pages 16 and E-4).	7884
Maximum measured stringer stress (see page B-19).	7050
Computer maximum stringer stress based on negative stringer moment at 1st interior support - beam 28 (see page E-7 for details of calculation).	7396
AASHO (3) allowable live load plus impact stress based on 20,000 psi allowable total stress for A-36 steel (see page E-4 for further explanation).	11200
Maximum computer longitudinal concrete deck stringer stress.	360
AASHO allowable concrete stress for measured $f'_c = 6870$ psi	2748
for Class A concrete $f'_c = 3000$ psi	1200
Maximum computer predicted stringer shear stress.	2511
AASHO allowable shear stress A-36 steel.	12000
See page E-7 for further comparison calculations concerning stud shear connectors.	
Also see page E-8 for calculations regarding transverse stresses in concrete deck versus allowable AASHO stresses.	

* Nodes are at 30' point, whereas experimental values are at 28' point along span.

FIG. 10 (Continued)

Also compared in Figure 10 are the deflections at the node points. For load condition 1 the deflections at the centerline of the 90' span are .0482' for node 163 and .0590' for node 165 (for location of these nodes, see page C-4). The measured deflection at these same node points (preliminary report no. 3, page B-54) show values of .045' and .0592' respectively. For the middle of the end span the computer deflection under load condition 2 is .0238' at node 44 and .0366' at node 46. This is compared with the experimental data of .0233' for node 44 and .0425' for node 46 as listed on page B-54.*

In the analysis of single simply supported spans, one can usually predict the position of the loads for the absolute maximum moment in a span through a simple well-known criteria.** For a continuous beam no such simple criteria is available. However, through the use of the computer program one can insert multiple loading conditions at closely spaced intervals along the bridge to ascertain the maximum loading position by trial and error. Multiple loading conditions are an economical computer calculation by the finite element method since only one vector column need be replaced in the solution of the matrix equations. Load conditions 2 and 4 were chosen five feet apart, and show practically identical results for deflections at the .4 point of the end span.

Load conditions 3 and 5 were also included in the analysis for the purpose of determining the maximum vertical shear stress in the girders. From a review of the printout, a maximum shear of 65,150 lbs. occurs in beam element 64 under loading condition 5.*** On the basis that the web-shear area of the W 36 x 170 steel beam is 25.95 sq. in. the resulting shear stress is only 2,511 psi.

Figure C-12 shows the proration of the static loads described in Volume I to the nearest node point on a five foot grid spacing along the bridge. This load condition was included only for the convenience of the author to compare deflection readings between Volume I which modeled the entire bridge and Volume II which models only half the bridge. The results were practically identical.

Appendix E contains further correlations between computer predicted, measured, and AASHO allowable stresses for Bridges #1-#4.

3. Bridge #2

Figure 11 shows the location of the HET-70 tank transporter on bridge #2 for three loading conditions. Load condition 1 represents the loading from which the section moment was calculated on page B-12; preliminary report 1. Figure 12 compares the computer

* Divide values in inches on page B-54 by 12 to get values in feet shown above.

** The maximum moment in a beam loaded with a moving series of concentrated loads will occur at the load nearest the center of gravity of the loads on the beam when the centerline of the beam splits the distance between the c.g. of the loading system and the load at the point of maximum moment.

*** See page C-8.

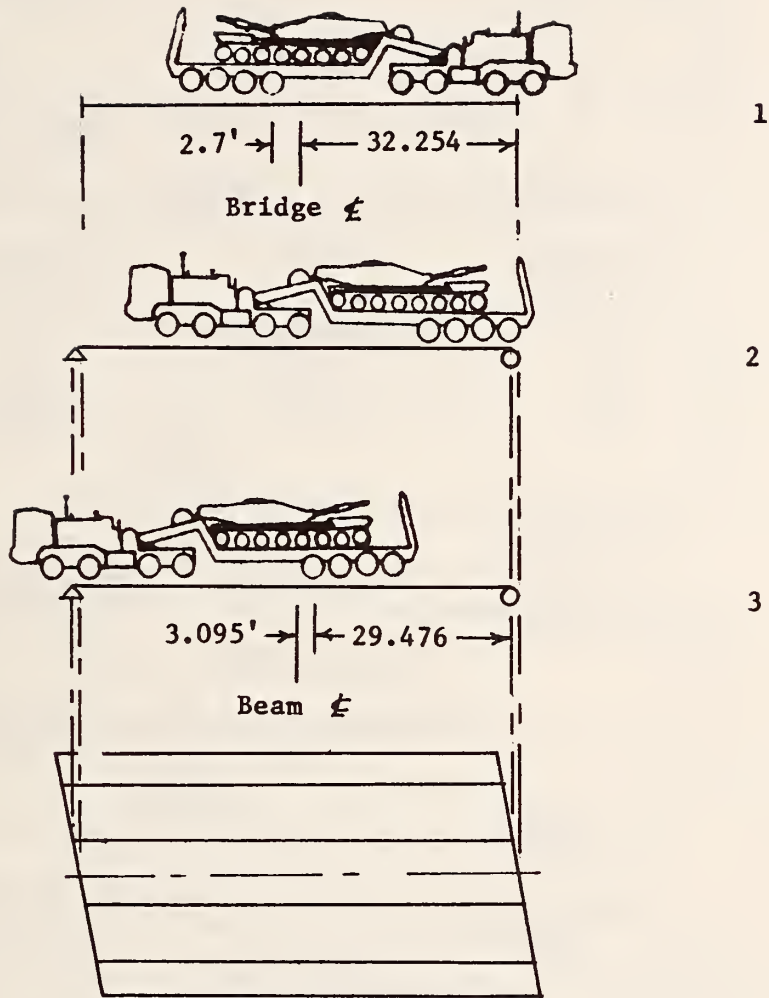


FIG. 11 - LOCATION OF HET-70 TANK TRANSPORTER ON
BRIDGE NO. 2 FOR VARIOUS LOAD CASES

BRIDGE #2 - Load Condition 1
Skew section near centerline of bridge as indicated by
beams 25-28

Sh 49,50		P = 94.16	10.18(4.35) = 44.283
		M = 1.634	11.60(4.30) = 49.880
Bm 25		M (including slab)	94.163
		37.73(2.478) = 93.49	.1000(4.35) = .4350
		1.63	.2788(4.3) = 1.1988
		P = 37.73 ^k	
		M = 86.12 ^k	1.6338
		86.12	
		181.24	
Sh 51,52		P = 119.37	13.55(4.3) = 58.265
		M = 6.410	14.21(4.3) = 61.103
Bm 26		M (including slab)	119.368
		187.60(2.478) = 464.87	.7427(4.3) = 3.194
		6.41	.7479(4.3) = 3.216
		194.40	6.410
		665.68	
		P = 187.60	
		M = 194.40	
Sh 53,54		P = 130.12	15.83(4.3) = 68.069
		M = 5.685	14.43(4.3) = 62.049
Bm 27		M (including slab)	130.118
		170.30(2.478) = 422.00	.7595(4.3) = 3.266
		5.69	.5626(4.3) = 2.419
		232.50	5.685
		660.19	
		P = 170.30	
		M = 232.50	
Sh 55,56		P = 91.68	10.83(4.3) = 46.569
		M = .9249	10.37(4.35) = 45.110
Bm 28		M (including slab)	91.679
		42.46(2.478) = 105.22	.1825(4.3) = .7848
		.92	.0322(4.35) = .1401
		87.04	.9249
		193.18	
		P = 42.46	
		M = 87.04	

Moment Check	181.24	Sum of Forces Check	
	665.68		
	660.19		435.33
	193.18		438.09
	1700.29 ^k		
	1735	Calculated	
Percent Difference		Preliminary Report #1	
		Page B-12	
(100) $\frac{(1735 - 1700)}{1735} = 2.0\%$			

FIG. 12 - CORRELATION BETWEEN COMPUTER AND EXPERIMENTAL DATA
FOR BRIDGE #2

RATIO IN PERCENT OF TOTAL RESISTING MOMENT
PROVIDED BY

	Exterior Girder (High Side)	Interior Girder	Interior Girder	Exterior Girder
Girder & Slab	10.66	39.15	38.83	11.36
Girder Alone	14.35	32.40	38.75	14.50
Experimental (Page B-30)	14	31	36	19

COMPARISON OF DEFLECTIONS AT SKEWED CENTER SECTION OF BRIDGE

Node	Computer	Experimental Page B-55
93	.007967	.0108
96	.01838	.0233
99	.01809	.0233
102	.007995	.0108

COMPARISON OF MAXIMUM STRESSES IN PSI UNITS

Computer maximum girder compression stress based on positive girder moment - beam 26 (see pages 20 and E-18).	1476
AASHTO allowable concrete girder stress.	2000
Computer maximum longitudinal compression stress in the concrete slab.	466
AASHTO allowable concrete compression slab stress.	1200
Computer predicted maximum live load and impact stress at the bottom of the girder for HET-70 loading.	804
Maximum actual girder stress recorded, based on 8700 psi concrete (see pages B-21, B-58, and E-17).	570
See pages E-16, E-18, and E-20 for discussion of prestressing steel stresses, diagonal tension reinforcement, and transverse slab analysis.	

FIG. 12 (Continued)

results with preliminary report 1, and shows excellent agreement for calculating the moment along the skew section in accordance with the criteria described on page 18. When preliminary report 1 was written, the bridge moment was calculated according to this criteria for a non-skew bridge. Fortunately, in the section considered by Figure 12 the wheel loads on the bridge were on the same side of the section for a skew bridge as they would be for the non-skew bridge. Therefore, for a symmetrical loading pattern about the center path of the bridge, the resulting moment for the non-skew and skew bridges are the same.

When we look at the ratio of total resisting moment carried by each of the girders across the skew section as shown in Figure 12, we note that there is considerable difference between the distribution pattern taken by the girder and slab versus the moments taken by the girder alone. In comparing these results with the experimental data, there seems to be an inconsistency in the interpretation of the statement, "moment taken by each girder." Reason would seem to dictate that the slab must interact with the prestressed girder to carry the bending moment, yet there is much better correlation by comparing the girder moments alone with the experimental values rather than comparing the girder and slab moments to the experimental values. The author has no explanation for this. It probably has something to do with the fact that the experimental values were determined by considering a non-superelevated bridge, and prorating the width of the concrete slab to act with the girder proper. On this basis, from the computer data, the author has been able to proceed by statics calculation to balance top and bottom axial loads for each girder, but the results are rather confusing because the width of the slab section would seem to change at every five foot interval along the bridge. Apparently there is an interaction between the torsional moments and the bending moments in the skew bridge that changes the picture considerably from section to section. The number of strain gage points in the experimental tests were not enough to shed any further light on the problem. It is suggested that this might be a fruitful area for exploration experimentally -- namely, to correlate the slab width necessary to balance the girder moments along the various sections of the bridge by computer analysis and further experimentation.

Prior to making the runs published in this report, the author did input bridge 2 into the computer without superelevation and curvature, and found that there was a considerable difference between the girder moments of that analysis and the results published herein. Of course, refining the bridge input to provide superelevation and curvature provides a more realistic model.

During the first few computer runs the author provided a moment resistance about the longitudinal axis at the support points of the girders for skew bridges #2 and #3. Unfortunately, this produced exceptionally high end moments at the supports which were difficult to explain in terms of the simply supported conditions. He, thereupon, removed all rotational restraints; and the new computer runs from which the results of this report are taken did give zero end moments about the y axis of the bridge.

It should be noted that the composite girder moments as shown in Figure 12 are an equivalent moment computed from a beam element slaved to shell elements. In design, these equivalent moments would then be applied to design of a true shear connected composite section. There is still considerable hand calculation involved in evaluating the equivalent section moment for each girder. It may be possible to augment the SSAP2 program to compute these equivalent moments directly.

As a matter of interest, load condition 1 does not give the maximum moment situation for the interior girders. Somewhat higher moments were developed for load condition 3, which placed the individual wheel loads on girder two to satisfy the simple girder maximum moment criteria.

4. Bridge #3

Figure 13 shows the position of the HET-70 tank transporter on bridge #3 for the various load cases which are similar to bridge #2. Calculations for moments and deflections, load condition 1, for this bridge are given in Figure 14. In bridge #3 it was necessary to recalculate the simple beam bridge moments from that presented on page B-12. The reason for recalculating these moments was because some of the loads for the non-skew bridge were on opposite sides of the moment section after they would be placed for the skew bridge, resulting in an error of approximately 11%. Therefore, each girder was treated as a simple beam carrying the loads shown in Figure C-23. The new calculations showed a skewed section moment of 1147 foot kips, while the old section moment presented on page B-12 was 1235 kips. Figure 14 shows a comparison of the moment calculated on the basis of each girder acting as a simple beam versus the final computer results after redistribution of the moments to the girders. Notice the considerable change that has occurred through the interaction of the various pieces of the bridge. The data shown by Figure 14 is self-explanatory.

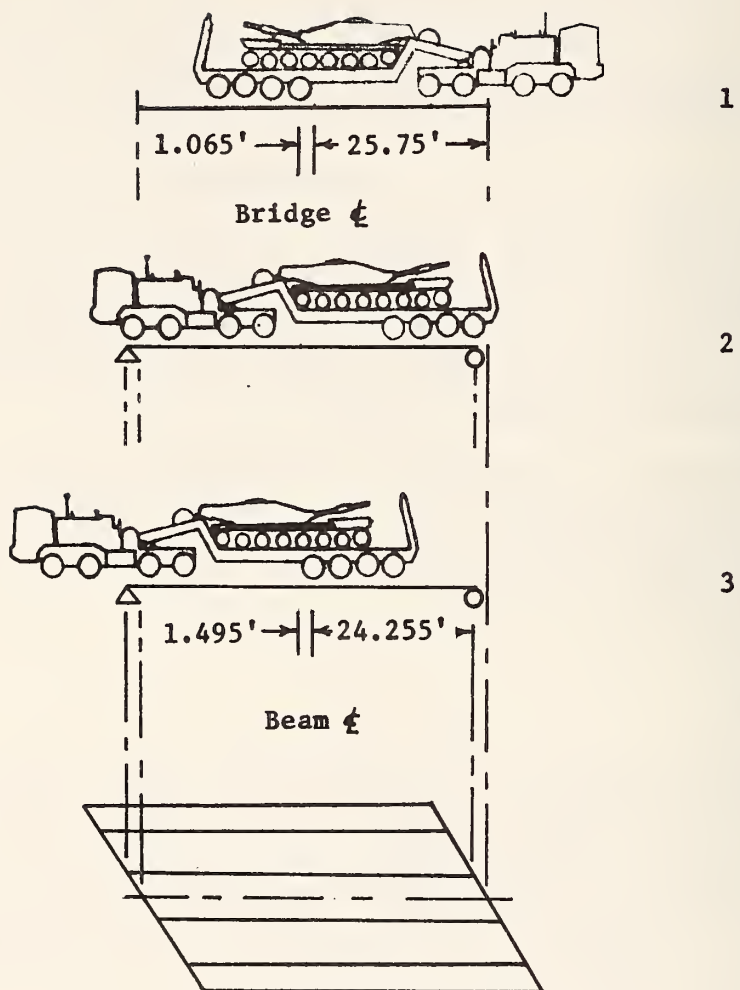










FIG. 13 - POSITION OF HET-70 TANK TRANSPORTER ON BRIDGE NO. 3 FOR VARIOUS LOAD CASES

BRIDGE #3 - Load Condition 1
Skew section near centerline of bridge as indicated by
beams 17-20

Sh 33,34		P = 80.20 M = 2.70		.3247(3.42) = 1.111 .4657(3.42) = <u>1.593</u> 2.704
			M (including slab)	
Bm 17			66.08(1.98) = 130.83 2.70 <u>73.60</u> 207.13	11.04(3.42) = 37.757 12.41(3.42) = <u>42.442</u> 80.199
		P = 66.08 ^k M = 73.60 ^k		
Sh 35,36		P = 101.44 M = 6.85		.9563(3.42) = 3.271 1.046(3.42) = <u>3.577</u> 6.848
			M (including slab)	
Bm 18			127.10(1.98) = 251.66 6.85 <u>108.20</u> 366.71	14.35(3.42) = 49.077 15.31(3.42) = <u>52.360</u> 101.437
		P = 127.10 M = 108.20		
Sh 37,38		P = 101.64 M = 6.61		1.052(3.42) = 3.598 .8796(3.42) = <u>3.008</u> 6.606
			M (including slab)	
Bm 19			123.00(1.98) = 243.54 6.61 <u>89.96</u> 340.11	15.20(3.42) = 51.984 14.52(3.42) = <u>49.658</u> 101.642
		P = 123.00 M = 89.96		
Sh 39,40		P = 89.30 M = 2.86		.4361(3.42) = 1.491 .3987(3.42) = <u>1.364</u> 2.855
			M (including slab)	
Bm 20			63.27(1.98) = 125.21 2.86 <u>65.48</u> 193.55	13.29(3.42) = 45.452 12.82(3.42) = <u>43.844</u> 89.296
		P = 63.27 M = 65.48		

Moment Check

Computer

Simple Beam Calculation

207.13
366.71
340.11
193.55
1107.50^k

48.04
474.97
518.25
107.83
1147.09^k

Percentage Difference

Sum of Forces Check

$$(100) \frac{(1147.09 - 1107.5)}{1147.09} = 3.5\%$$

→ 379.45
← 372.58

FIG. 14 - CORRELATION BETWEEN COMPUTER AND EXPERIMENTAL RESULTS FOR BRIDGE #3

RATIO IN PERCENT OF TOTAL RESISTING MOMENT
PROVIDED BY

	Exterior Girder (High Side)	Interior Girder	Interior Girder	Exterior Girder
Girder & Slab	18.70	33.11	30.71	17.48
Girder Alone	21.82	32.08	26.68	19.42
Experimental (Page B-28)	20	30	30	20

COMPARISON OF DEFLECTIONS AT SKEWED CENTER SECTION OF BRIDGE

Average of Nodes	Computer	Experimental Page B-55
67 and 80	.0065	.0058
70 and 83	.0093	.0100
73 and 86	.0092	.0100
76 and 89	.0065	.0058

COMPARISON OF MAXIMUM STRESSES IN PSI UNITS

Computer maximum beam steel tensile predicted stress based on live load and impact positive moment in beam 18 (see pages 25 and E-26).	6055
Maximum measured HET-70 stress (see page B-20)	3450
AASHTO 1935 allowable live load plus impact steel stress; 16000 - 10072.	5928
Also see page B-12 for design loading stress.	5900
Computer maximum shear stress (see page E-26).	81
AASHTO allowable web shear stress.	90
Computer maximum bond stress (see page E-26).	27
AASHTO allowable bond stress.	120
See page E-27 for discussion concerning transverse slab stresses.	

FIG. 14 (Continued)

5. Bridge #4

Figure 15 shows the location of the HET-70 tank transporter on bridge #4 for four load cases. Only the moment distribution for load condition 1 is presented in Figure 16. There were no experimental values for this bridge with the HET-70 loading. However, the Tennessee report does show ratios of 23% to exterior girders and 27% to interior girders for an HS-40 center-path loading at crawl speed which is in agreement with the data shown in Figure 16, although for a different type of vehicle.

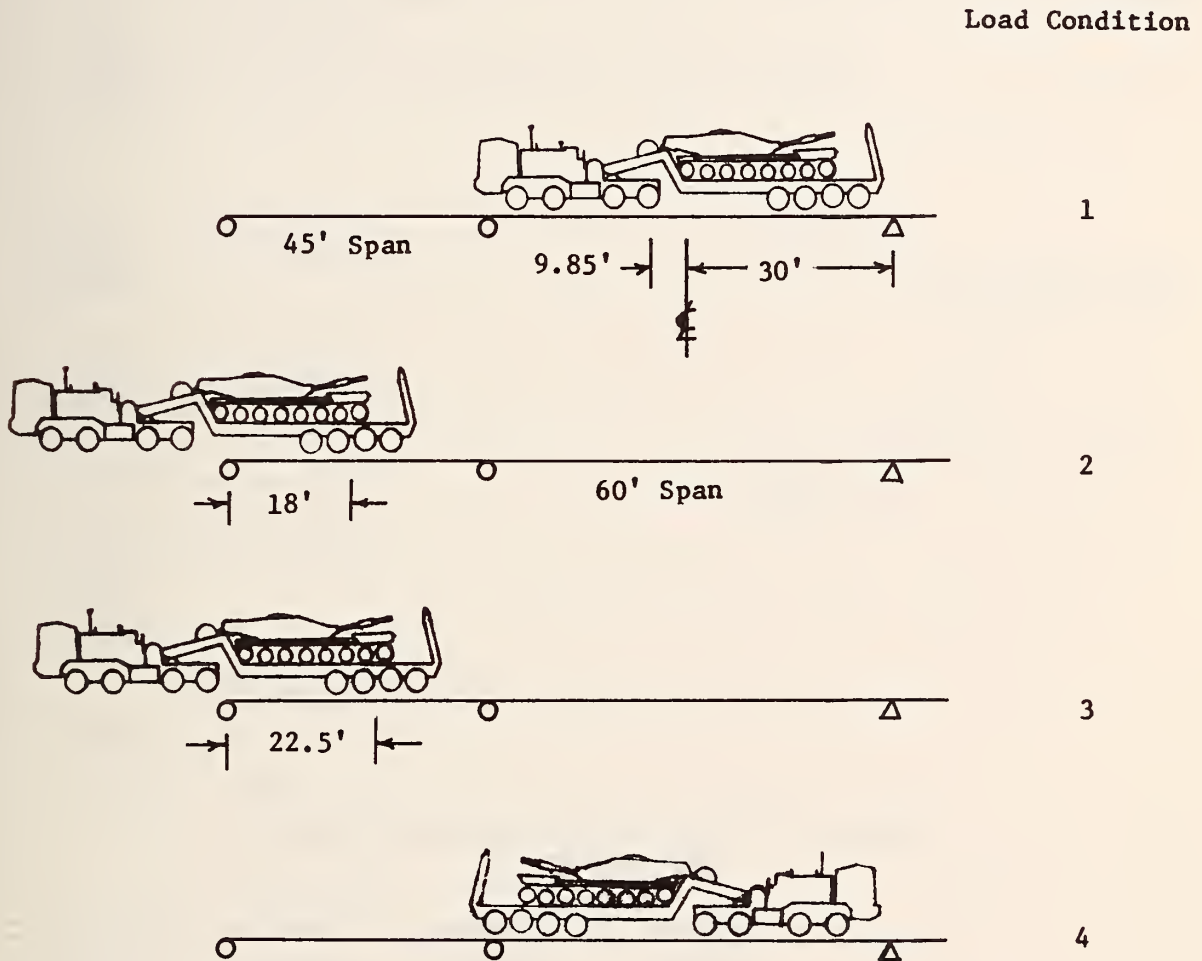
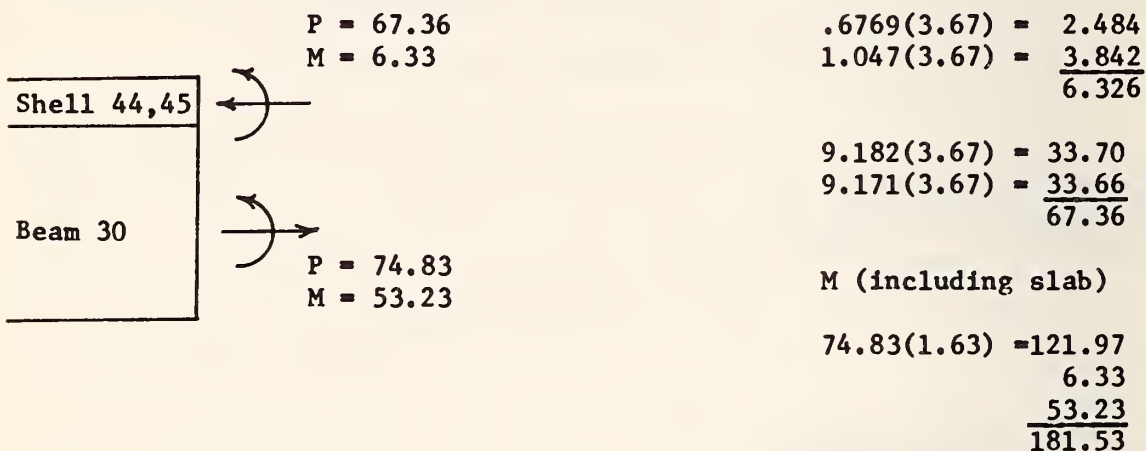
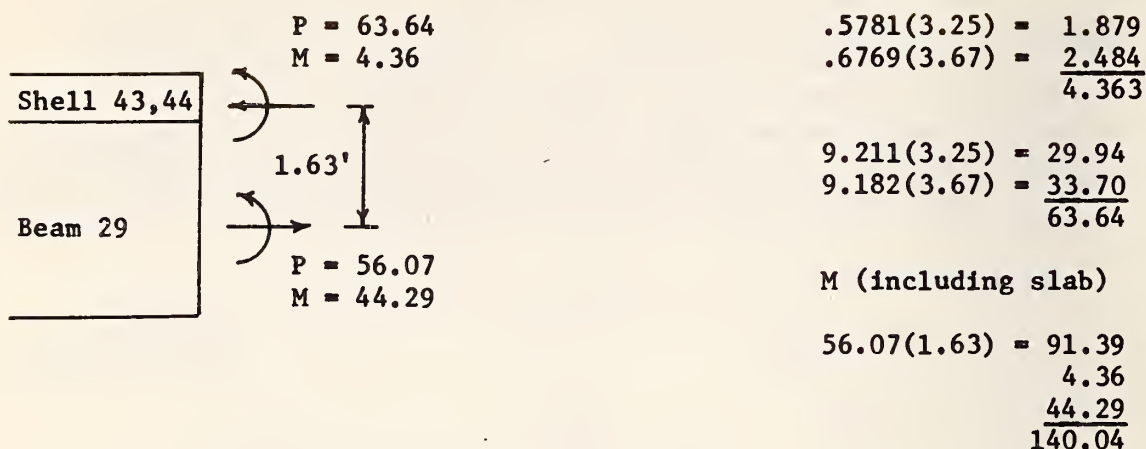


FIG 15 - LOCATION OF HET-70 TANK TRANSPORTER ON BRIDGE NO. 4 FOR VARIOUS LOAD CASES

BRIDGE #4 - Load Condition 1



Sum of Forces Check

→	130.90
←	131.00

RATIO IN PERCENT OF TOTAL RESISTING MOMENT PROVIDED BY

	Exterior Girder	Interior Girder	Interior Girder	Exterior Girder
Girder & Slab	21.77	28.23	28.23	21.77
Girder Alone	22.71	27.29	27.29	22.71

FIG. 16 - COMPUTER PREDICTIONS FOR LOAD DISTRIBUTION AND DEFLECTION FOR BRIDGE #4

COMPARISON OF MAXIMUM STRESSES IN PSI UNITS

Compression stress in steel girder for maximum positive live load plus dead load moment.	12,399
Allowable flexural stress.	18,000
Computer predicted maximum stress for negative live and dead load moment.	10,887
Maximum shear stress.	5,590
Allowable shear stress.	11,000
See page E-30 for a discussion of the transverse slab stresses.	

FIG. 16 (Continued)

III. CONCLUSIONS AND LIMITATIONS

1. The results of this research show excellent correlation between computer analysis and experimental results for straight, continuous, composite steel girder concrete deck bridges and for skew, simple span composite concrete girder and concrete deck bridges when the skew is under 30° .
2. Computer methodology presented herein will allow the direct determination of actual wheel loads (military or non-military) to the longitudinal load carrying members of the above bridges without the restrictive simplifying assumptions associated with empirical methods.
3. The computer methodology presented herein can safely be used to determine stresses and deflections of the above bridges for any heavy military traffic, subject to the provisions that the traffic is slow enough (crawl speed, less than 5 mph) so that the loading can be considered a static loading condition.
4. In the case of the HET-70, the path of travel should be a centerline path along the bridge; with no other traffic on the bridge.
5. With respect to widened bridges the computer program can be used to determine the most favorable path of travel for the HET-70. Care must be taken to examine the continuity provisions between old and new construction.
6. This research is limited to a linear analysis program, the SSAP2 program; therefore, the computer program, as it now stands, can only be used when the response of the bridge is known to be in a linear range.

IV. RECOMMENDATIONS

1. It is recommended that other types of bridges, such as box girder bridges, curved girder bridges, and long span structures (suspension bridges and arches) be investigated with the SSAP2 program to determine its reliability in predicting stresses and deflections of these bridge types.
2. A curved beam element should be investigated for its correlation in the SSAP2 program with expected data on curved girder bridges.
3. Using the computer program, it is possible to input different design parameters on selected bridge types to develop simplified stress charts for rapidly determining the load carrying capability of these types of bridge structures on an emergency basis. It is recommended that further research be done to prepare these charts for decision aids for field personnel for various classes of heavy military vehicles.
4. The capabilities of non-linear programs should be investigated for correlation of stress prediction in the non-elastic behavior of these bridge structures.

APPENDIX A

**Background Correspondence Pertaining to Establishment
of Project**

OMITTED

APPENDIX B

Preliminary Research Reports

PRELIMINARY RESEARCH REPORT
OF A
HIGHWAY BRIDGE LOADING STUDY
WITH THE
HET-70 MAIN BATTLE TANK TRANSPORTER

by

Robert F. Varney
Structural Research Engineer
Structures and Applied Mechanics Division
Office of Research and Development
Bureau of Public Roads
Washington, D. C.

June, 1969

ACKNOWLEDGMENTS

The research reported herein was carried out as a cooperative effort of the Bureau of Public Roads, Tennessee Department of Highways, Department of the Army and the University of Tennessee. The study was conducted in the Winchester, Tennessee area between April 18 and May 8, 1969.

The assistance of the many Tennessee Department of Highway personnel and in particular Mr. Henry W. Derthick, Bridge Engineer, prior to and during the study in promptly furnishing logistic support to the Bureau of Public Roads research team when and as needed is gratefully acknowledged. The assistance provided by Dr. E. G. Burdette of the University of Tennessee is also appreciated.

The loadings of the bridges with the HET-70 tank transporter and the M-60 combat tank were performed competently and diligently by the Department of the Army armored equipment task group from Fort Knox, Kentucky, under the leadership of Lt. Wayne G. Kerkhoff.

The Bureau of Public Roads field bridge research task group consisting of the author and Mr. Harry Laatz was ably assisted in the field by Mr. Richard Richter and Mr. Harry Shutz of the Washington Office Bridge Division, by Mr. Anton Urbas, Junior Engineer, and by - Mr. George Crum who performed the photographic work.

Last but not least, Mr. Leon Heidebrecht of the Department of the Army provided invaluable assistance as an observer, advisor and assistant during the field study.

1. INTRODUCTION

Three bridges formerly on the Tennessee State highway system became available for research study early in 1969 when replacement bridges were ready for service. It became necessary to abandon the three serviceable bridges since they are to be inundated by a new TVA reservoir in late 1970. The approaches to the bridges remain connected to the relocated highway permitting easy access to the bridges by test vehicles with the advantage of freedom from interference with regular traffic.

At the same time that the bridges became available for research there arose a pressing need to resolve the problem of determining the effect of the new Department of the Army HET-70 Main Battle Tank Transporter loading (195,000 pounds) on typical highway bridges, particularly those of lighter load ratings. A cooperative research study by the Bureau of Public Roads, Department of the Army, Tennessee Department of Highways and University of Tennessee was therefore initiated to take advantage of the opportunity to utilize these bridge specimens for a program of controlled loadings involving the fully-loaded HET-70 tank transporter.

The primary objective of this study is to determine the actual live load bending moment distribution of various moving live loads to the main load-carrying members of typical highway bridges for correlations with empirical design distributions and with the distributions predicted by analytical methods. The measured strains and deflections under controlled loading obtained from gages located at critical sections on each bridge

provide an immediate comparison of the relative effects on each bridge of each of the various loadings. Data obtained from additional gages at other points will subsequently reveal information on live load deflections, deck slab stresses and stresses developed in cantilevered pier caps. As a corollary to the principal objective, dynamic stress amplifications at various speeds will be determined for the HET-70 tank transporter loading. Finally, fundamental information on the vibration frequencies and damping characteristics of each bridge will be developed and analyzed.

The Bridges

The three bridges used for this study are described as follows:

1. A four-span (70'-90'-90'-70') continuous steel beam structure:
the excellent approaches permitted unrestricted test vehicle speeds. Four rows of 36-inch wide-flange beams spaced at 100-inch centers support the 7-inch composite slab forming the 28-foot roadway. The beams have both top and bottom flange cover plates over the piers. The bridge is an H20-S16-44 design structure built in 1963. (Fig. B-1).
2. A 53-foot span skewed (30° right) simple span reinforced concrete T-beam bridge: the poor approaches severely restricted test vehicle speeds. Four 18-inch wide T-beam flanges spaced at 82-inch centers with an 8½-inch slab form the 24-foot roadway bridge which is an H-15 design structure built about 1938. (Fig. B-2)
3. A 65-foot span skewed (20° right) simple span prestressed concrete beam structure: the vertical and horizontal curvature and super-elevation of the approaches restricted the test vehicle speeds somewhat. Four rows of AASHO Type III prestressed I-beams at

approximately 104-inch centers support a 7-inch slab which forms the 28-foot roadway. The bridge is an H20-S16-44 design structure built in 1962. (Fig. B-3).

The Loadings

The vehicles used to load the bridge included the Department of the Army HET-70 tank transporter seen in Fig. B-1, the Bureau of Public Roads Bridge Research Test Vehicle seen in Fig. B-2 and an M-60 track-laying combat tank seen in Fig. B-3. The HET-70 tank transporter is an 8-axle pneumatic-tired vehicle with fully-loaded gross load and axle loads as indicated in Fig. B-4. The HET-70 load indicated is the load which results when the transporter is carrying an MBT-70 battle tank and was obtained by loading the transporter with an M-60 combat tank and a surcharge of armor plate strapped to the gun barrel on the tank. The HET-70 has an overall width of 12 feet and the dual wheels of the four rear axles are at 102-inch centers. The pressure in each of the 24 tires was 90 psi.

The M-60 track-laying combat tank weight of approximately 105,000 pounds is carried on two 22-inch wide rubber-cleated tracks at $9\frac{1}{2}$ -foot centers. The tracks contact the roadway over a 14-foot length.

The Bureau of Public Roads Bridge Research Test Vehicle, hereafter referred to as the BPR test vehicle, is a tractor and semitrailer combination which when loaded to 74,000 pounds closely simulates the H20-S16-44 three-axle design vehicle loading used for two of the test bridges. The two 32,000-pound dual-tired axles on the BPR test vehicle are spaced 20.4 feet apart and the 10,000-pound front axle is 13.0 feet ahead of

the first 32,000-pound axle. The pressure in each of the 10 tires was 90 psi. The dual wheels of the two heavy axles are at 75-inch centers.

2. DESCRIPTION OF TEST PROGRAM

The field study of the three bridges included the measurement of maximum bending moment strains at critical sections in each of the three different types of bridges involved. Each of the bridges required a particular selection of strain gage locations to bring out these responses most effectively. The geometry and approach conditions of each bridge as related to the dimensions of the test vehicles also required slightly different test loading patterns for each. The gage locations and loading patterns are described in detail below. The gages described do not represent all the gages installed. The responses in the additional gages will be covered in the more comprehensive final report.

Four-Span Continuous Steel Beam Bridge

The maximum measured stresses in this bridge as reported herein are the average responses from two gages located near each edge of the underside of the bottom flange of each beam at a section 4.8 feet from midspan of one of the 90-foot spans. Gages on four additional sections of two adjacent exterior and interior beams at and near midspan of the same span provided supplemental data.

Reinforced Concrete T-Beam Bridge

The concrete cover over the second bar of the four reinforcing bars in the bottom row in each T-beam flange was partially removed at the critical sections to permit installing strain gages along the lower

surface of the $1\frac{1}{4}$ -inch square bar without destroying the bond on the other three sides. Two of the sections represented the theoretical maximum moment sections on this span for the BPR test vehicle and for the HET-70 loading. Because of the skew of the bridge, the corresponding gaged sections on each beam were offset from each other. Strains and stresses computed from strains reported herein represent the maximum values measured at any of the sections on each beam for each particular loading sequence.

Prestressed Concrete Beam Bridge

The measured responses for this bridge represent the average responses from two gages located near each edge of the underside of the bottom flange of each of the four beams. Five cross-sections at or near the theoretical maximum moment sections for the BPR test vehicle and for the HET-70 loading were gaged on this span.

As this simple span was also a skewed bridge the corresponding gaged sections were offset from one another on each beam and the measured strains reported herein are the maximum measured at any gaged section on each beam for each particular loading.

Test Loading Pattern

Each of the three vehicles used in the study (BPR test vehicle, HET-70, and M-60 tank) was driven across each bridge in one direction on a prescribed set of paths at various speeds. The theoretical maximum moment sections for each loading were determined and gaged with regard to the planned direction of approach of the vehicles. On the steel bridge one set of runs was made from each direction with the BPR test vehicle for supplementary data. The findings reported herein

represent only the "crawl" speed runs (about 4 mph) made with each of the three vehicular loadings in the same direction on identical paths. The prescribed paths included one path with the vehicle centered along the centerline of each bridge. The other paths included two in which each vehicle followed a line 7 feet on either side of centerline for the 28-foot roadway bridges and 6 feet on either side of centerline for the 24-foot roadway bridge. In addition, the BPR test vehicle traversed two paths on which the vehicle was centered 9 feet on either side of centerline for the two 28-foot roadway bridges. These vehicle paths are designated 1 to 5 from left to right (as seen by the driver) on the 28-foot roadways and 1 to 3 from left to right on the 24-foot roadways. The prescribed paths were closely adhered to by the vehicles on all runs except that during crossings on paths 1 and 3 on the 24-foot roadway the narrower roadway forced the HET-70 transporter and the M-60 tank to follow paths averaging 5 feet from centerline rather than the 6 feet offset followed by the BPR test vehicle.

3. PRESENTATION OF RESULTS

In this preliminary report, maximum live load bending moment stresses and strains at selected critical sections have been shown for each of the three vehicles moving across each of the three bridges at crawl speed. The strains measured on the steel beams and on the reinforcing bars have been converted to stress using an assumed elastic modulus of 30×10^6 psi. The reported values represent the maximum extreme fiber stress at the bottom flange (or lowest reinforcing bar) measured during the vehicle passage on various paths. The comparable responses for the prestressed

concrete beam bridge are reported as measured strains (microinches per inch). Fig. B-5 shows a typical cross-section of the four-span continuous steel bridge and Figs. B-6, B-7, B-8 show the maximum measured stresses at a section 4.8 feet from midspan of one 90-foot span. Comparable stresses measured on adjacent exterior and interior beams at four other sections at and near midspan in the same span indicated a 5 to 10 percent higher maximum live load stress was developed at the precise midspan section for the BPR test vehicle and M-60 tank loadings. The plotted stresses are shown for the BPR test vehicle on paths 1 to 5 and for the HET-70 and M-60 loadings on paths 2, 3, and 4, all traveling at crawl speed.

For the reinforced concrete bridge and for the prestressed concrete beam bridge, both of which are skewed, the tabulated responses are the maximum stresses or strains measured at any of the five gaged sections at or near midspan during a particular vehicle passage on one prescribed path. (Fig. B-9 and Fig. B-10). Since the effect of skewness could be determined more readily on the prestressed concrete beam bridge, only two beams were instrumented on the reinforced concrete bridge where it was necessary to remove concrete cover from the reinforcing bars. The measured strains for the skew bridges cannot be used to obtain distribution in these bridges as for the steel bridge since the tabulated maximum values do not necessarily occur simultaneously or at the same section. A more comprehensive study of the load distribution in skew bridges will be part of the final report.

The combined effects of the roadway superelevation, skew and curvature on the relative beam strains of the prestressed bridge is quite noticeable even though the maximum values tabulated again do not necessarily occur simultaneously or at the same section. It is readily apparent that relatively greater strains are induced in the two lower beams of the bridge.

4. DISCUSSION OF RESULTS

The findings presented herein represent a presentation of the digitized and tabulated measured strains which may be subject to additional refinement as the remaining supplementary data is analyzed for the final report.

For the BPR test vehicle centerline crawl run loading of the four-span continuous steel bridge (the only non-skewed structure of the three tested), 62.5 percent of the sum of the maximum measured stresses for all four beams is carried by the two interior beams. For the comparable HET-70 loading the two interior beams carried 60.6 percent; for the M-60 tank loading 64.0 percent. On this basis the relative distribution of maximum stresses among the main load-carrying members on this bridge for the wider HET-70 and M-60 loadings on bridge centerline is not significantly different from that for the BPR test vehicle.

When assessing the relative magnitudes of the responses of the three bridges studied, consideration must be given to the magnitudes of the actual applied bending moment to the design bending moment in each case. The total bridge design moment is a function of the number and spacing of beams, span length and assumed design live load in accordance with

the AASHO Standard Specifications for Highway Bridges. The total bridge applied moment is calculated from a consideration of the bridge span length and the load vehicle axle spacing and load distribution. Table 1 shows the computed applied and design bending moments for the test bridges. Values of design dead load stresses and live load plus impact stresses are also shown. For these calculations the M-60 tank load was assumed to be uniformly distributed over the 14-foot length of the roadway track contact.

5. SUMMARY

The findings to date on this study permit an indication of the maximum measured live load responses to be presented at this time. The measured responses give no indication that any distress in main load-carrying members of any of the three specimen bridges due to bending moments was induced by any of the three vehicles moving at crawl speed on normal traffic lanes. The crossings of the vehicles on the bridge centerline provided an even more favorable situation with regard to the stresses and strains developed.

6. FUTURE FINDINGS

The final report will include the dynamic response amplifications induced at various speeds, the relationships of the total indicated bending moments to static computed moments, live load deflections, stresses measured in deck reinforcing steel and in cantilevered pier caps and a correlation with a computerized theoretical analysis.

TABLE 1 COMPUTED BENDING MOMENTS AND STRESSES

DESIGN

Type of Bridge	Allowable Bending Moments and Stresses		Applied Live Load Bending Moments		
	Dead Load	Live Load & Impact	(74.4 kip) BPR Test Vehicle	(105.0 kip) M-60Tank	(195.4 kip) HET-70 Transporter
Four-span continuous steel beam (H20-S16-44)	1710 ft-kip/8900 psi*	2940 ft-kip/11200 psi*	790 ft-kip*	1455 ft-kip*	1715 ft-kip*
Reinforced concrete T-beam (H-15)	2440 ft-kip/10100 psi	1400 ft-kip/5900 psi	575 ft-kip	1205 ft-kip	1235 ft-kip**
Prestressed concrete beam (H20-S16-44)	3050 ft-kip/1490 psi	3600 ft-kip/990 psi	835 ft-kip	1515 ft-kip	1735 ft-kip

* 90-foot span

** Six axles, 157.6 kips

For these calculations, any effect of skew is disregarded; the tank loading is assumed to be uniformly distributed over the 14-foot tread contact length; the moments shown represent the total moment for the whole bridge cross section in each case.



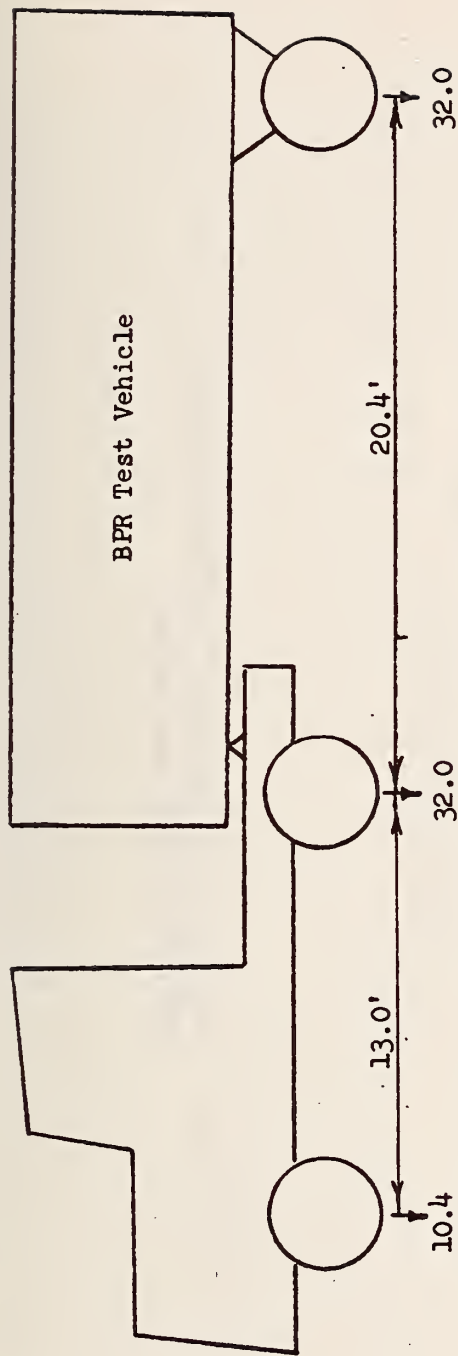
FIG. B-1 - HET-70 TANK TRANSPORTER ON FOUR SPAN
CONTINUOUS STEEL BEAM BRIDGE



FIG. B-2 - BPR TEST VEHICLE ON REINFORCED CONCRETE T-BEAM BRIDGE



FIG. B-3 - M-60 TANK ON PRESTRESSED CONCRETE BEAM BRIDGE



BPR Test Vehicle Axle Loads in Kips, Fully Loaded (74.4 Kips total)

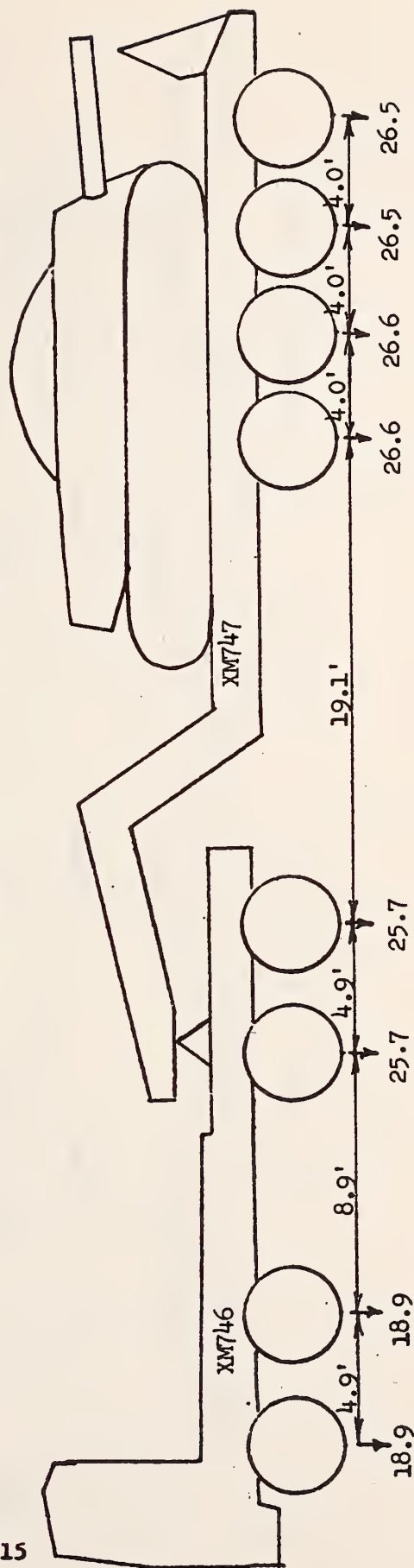


FIG. B-4 - HET-70 Axle Loads in Kips, Fully Loaded (195.4 Kips total)

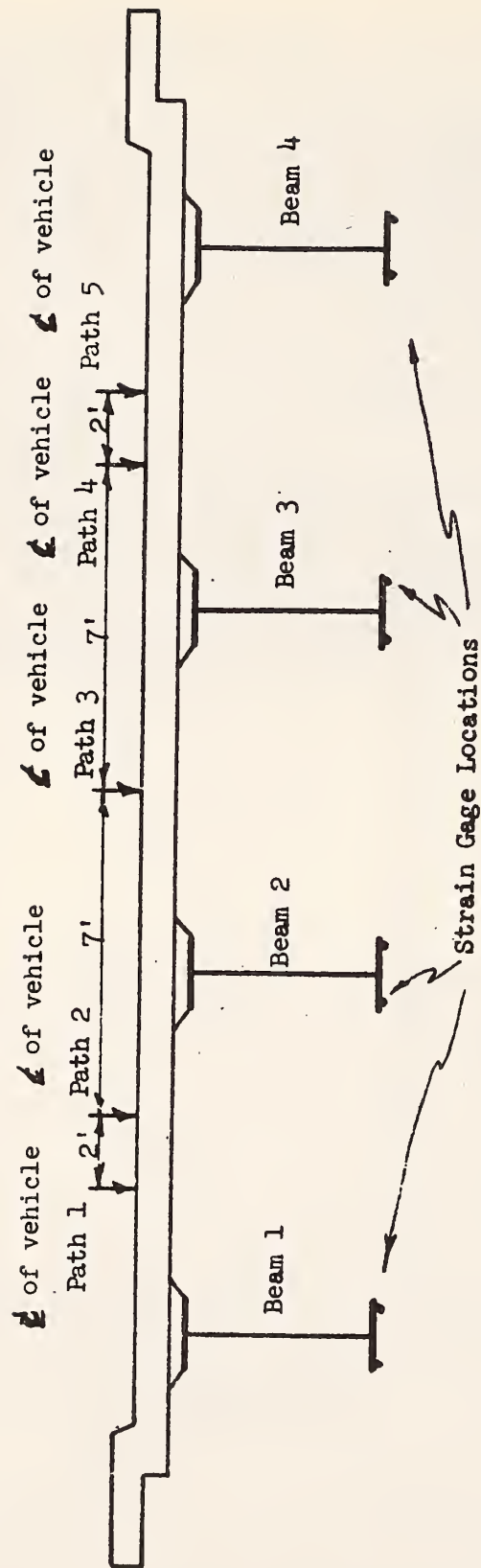


FIG. B-5 - VEHICLE PATHS AND STRAIN GAGE LOCATIONS FOR
CONTINUOUS STEEL BEAM BRIDGE

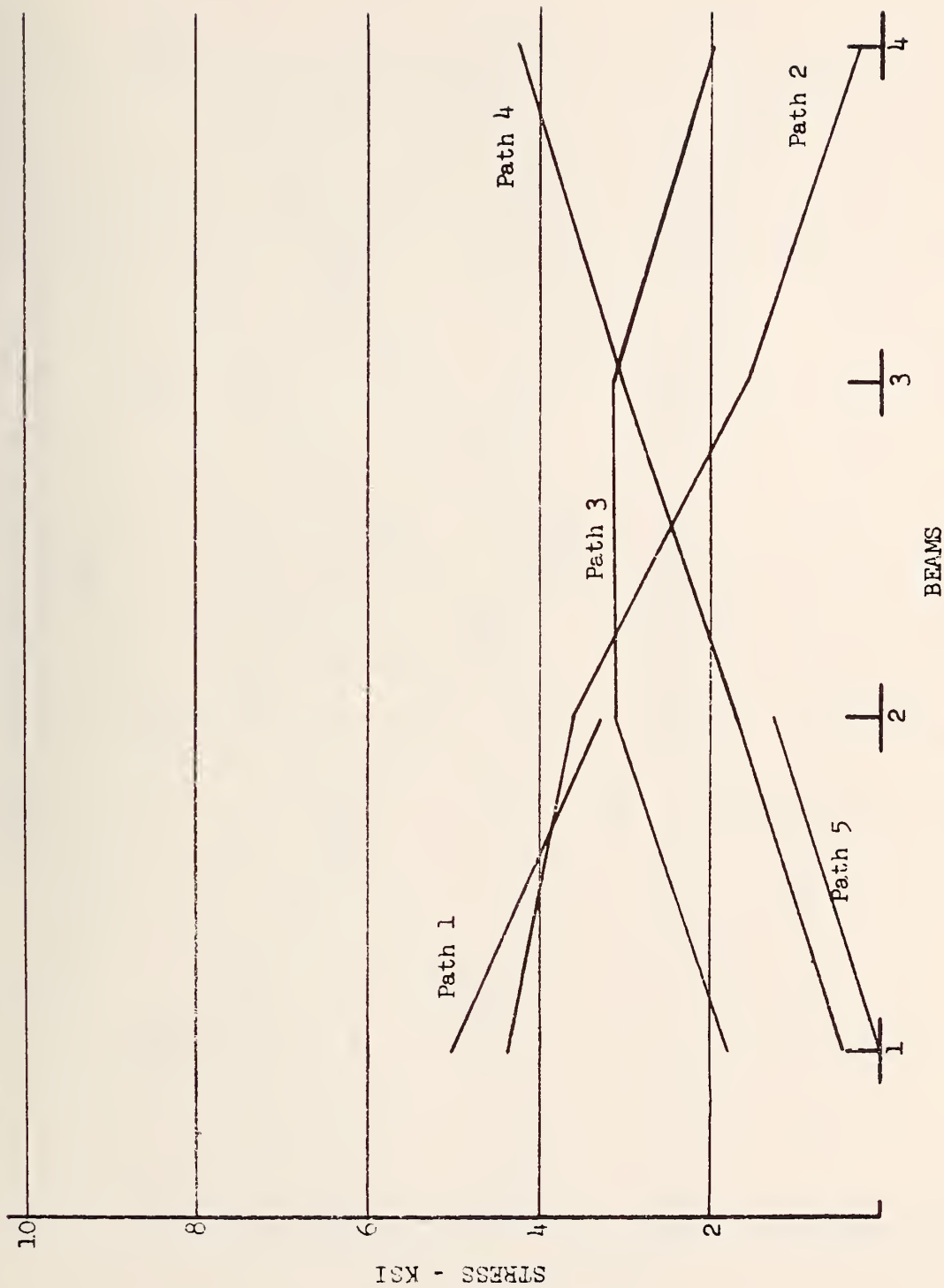


FIG. B-6 - MAXIMUM BENDING STRESSES IN CONTINUOUS STEEL BEAM
BRIDGE FOR VARIOUS PATHS OF BPR VEHICLE

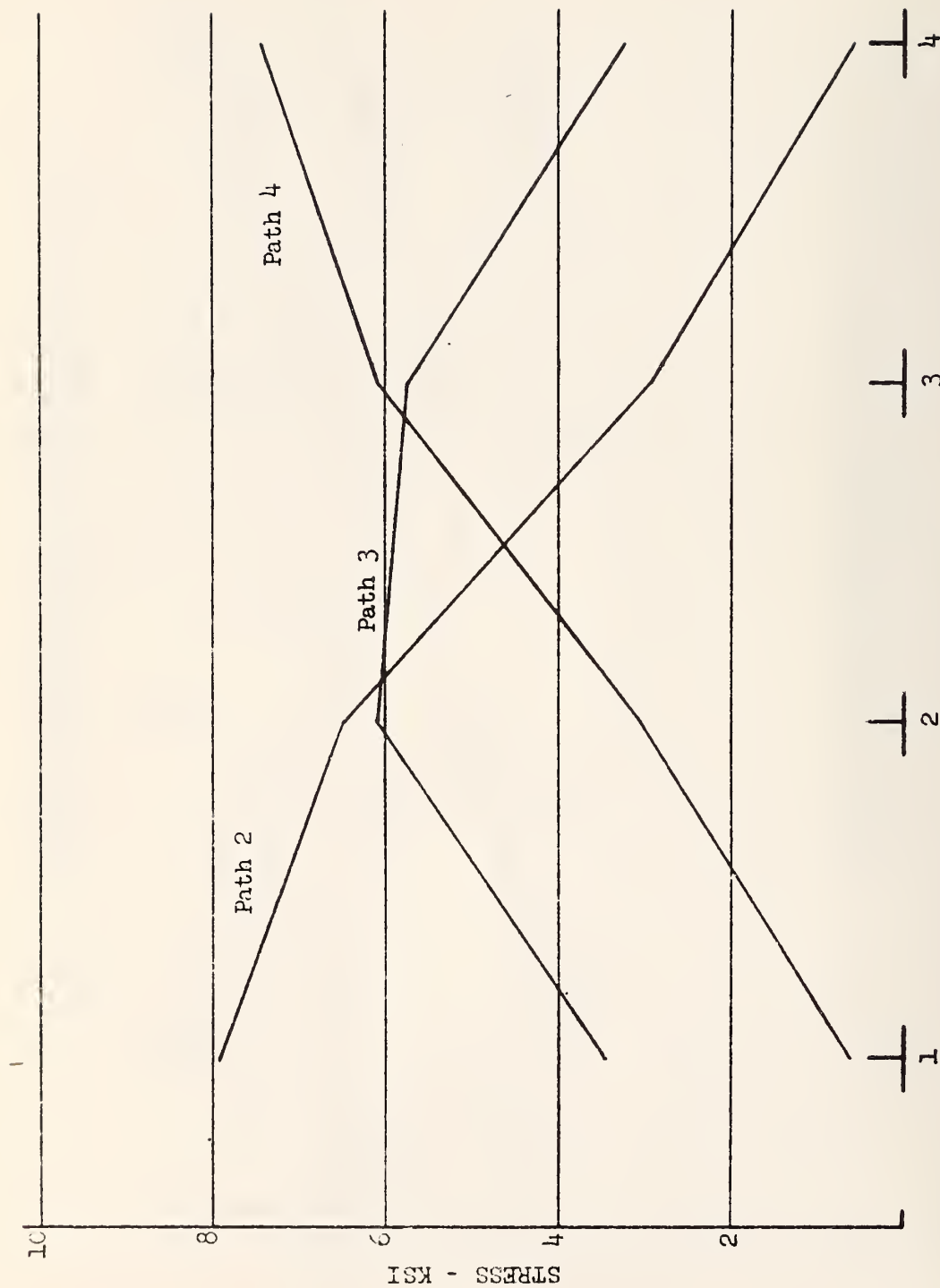


FIG. B-7 - MAXIMUM BENDING STRESSES IN CONTINUOUS STEEL BEAM
BRIDGE FOR VARIOUS PATHS OF M-60 TANK

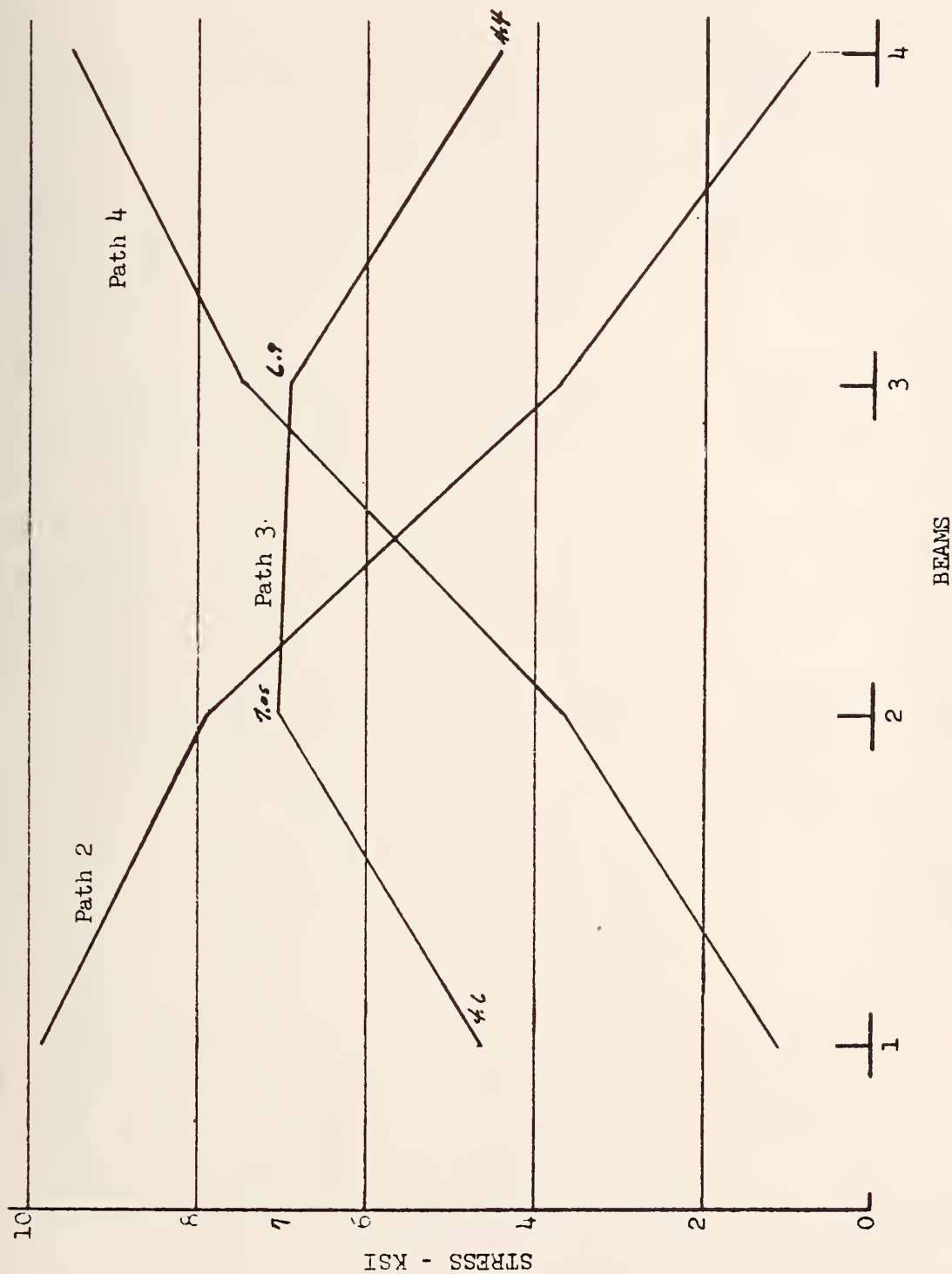
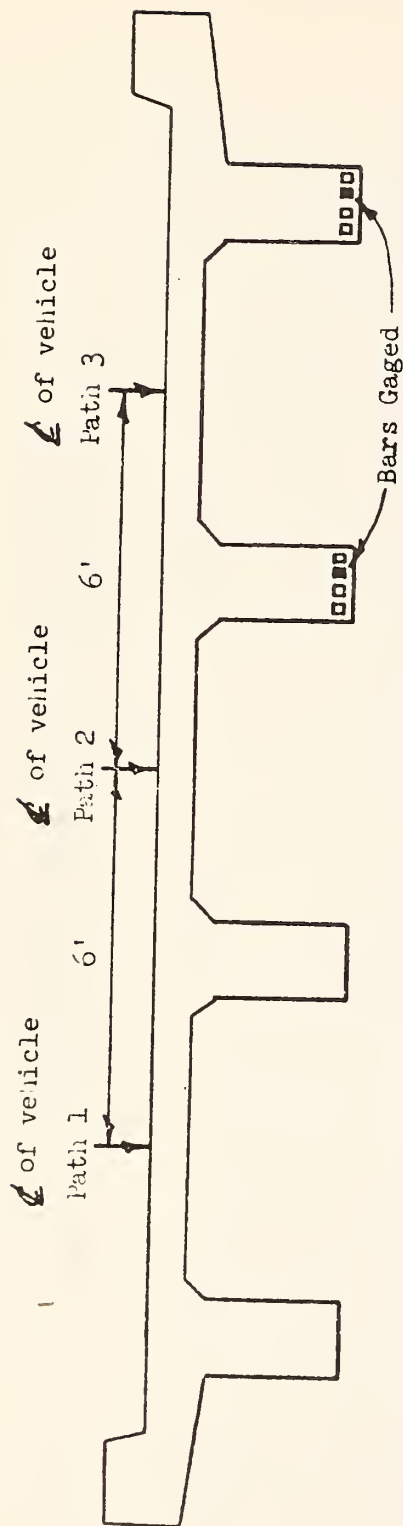


FIG. B-8 - MAXIMUM BENDING STRESSES IN CONTINUOUS STEEL BEAM
BRIDGE FOR VARIOUS PATHS OF HET-70 VEHICLE



Path 1		
BPR VEHICLE	980 psi	400 psi
M-60 TANK	2570	1040
HET-70 VEHICLE	2420	1100
Path 2		
BPR VEHICLE	1820	940
M-60 TANK	3260	2090
HET-70 VEHICLE	3450	2100
Path 3		
BPR VEHICLE	1770	2050
M-60 TANK	3040	3780
HET-70 VEHICLE	3750	3840

FIG. B-9 - MAXIMUM BENDING STRESS FOR REINFORCED CONCRETE SIMPLE SPAN BRIDGE FOR VARIOUS VEHICLES AND VARIOUS PATHS

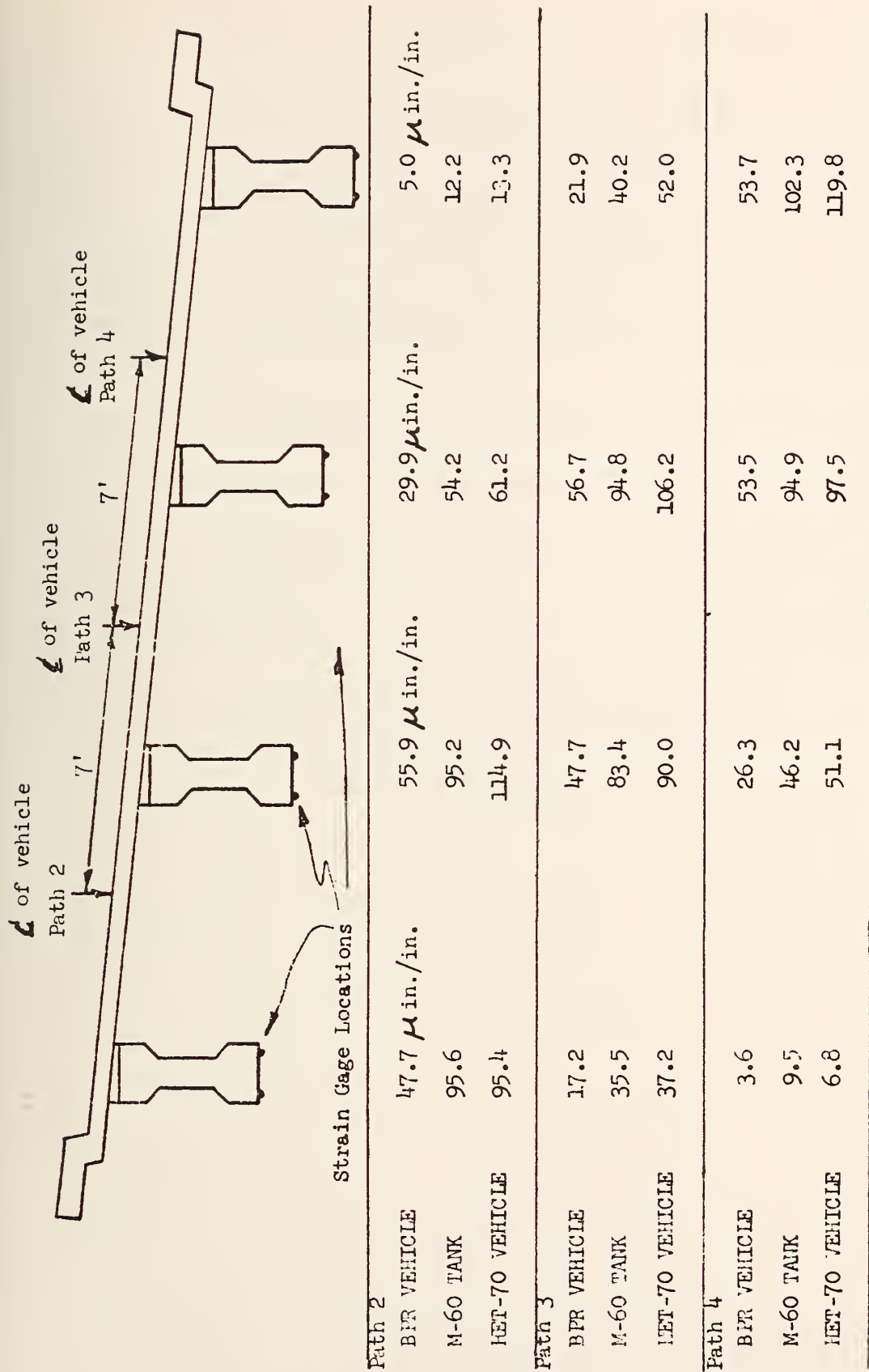


FIG. B-10 MAXIMUM BENDING STRESS FOR PRESTRESSED CONCRETE
SIMPLE SPAN BRIDGE FOR VARIOUS VEHICLES AND VARIOUS
PATHS

PHASE 2
OF
A PRELIMINARY RESEARCH REPORT
ON
AN EXPERIMENTAL LOADING STUDY
OF
THREE HIGHWAY BRIDGES IN TENNESSEE
WITH THE
U. S. ARMY HET-70 MAIN BATTLE TANK TRANSPORTER

by

Robert F. Varney
Structural Research Engineer
Structures and Applied Mechanics Division
Office of Research and Development
Bureau of Public Roads
Washington, D.C.

October 1969

FOREWORD

The first preliminary research report of the field loading study of three highway bridges with the U. S. Army HET-70 Main Battle Tank Transporter was issued in June 1969. A review of that report is recommended as a prerequisite to the assimilation of the material in this report since the former report described the specimen bridges and the test procedures in detail.

This second preliminary report is being issued in order to provide current information on the findings to date. The final comprehensive report on the study will include additional findings, a correlation with a computerized theoretical analysis of the responses of the structures, and an accompanying color film of the field test which is in the preparation stage.

1. LIVE LOAD BENDING MOMENT DISTRIBUTION

Calculations have been made by others of the total bending moment induced by the HET-70 loading (using AASHO design allowance for impact) on a typical 60-foot span steel girder and concrete slab bridge designed in accordance with the AASHO H-15-44 loading. When the proportion of the HET-70 moment assigned to the most heavily loaded girder was varied between 35 and 40 percent for a range of beam spacings between 66 and 90 inches and the results compared with design moments, a significant degree of overloading was indicated. One of the purposes of the research described herein is to determine whether actual responses of typical highway bridges under the HET-70 loading support the assumptions made in the above described calculations concerning (1) the percentage of the total HET-70 loading carried by the most heavily loaded beam and (2) the appropriate allowance for impact to be added in calculating the effect of the HET-70 loading.

The measured live load strains on the girder flanges and webs, and on the T-beam reinforcing bars and concrete surfaces were evaluated to establish the actual neutral axis locations in the various main load carrying members of the three test bridges. Typical neutral axis determinations are shown for the 90-foot span of the four-span continuous steel girder bridge in Fig. B-11 and Fig. B-12. The characteristic upward trend of the neutral axis—as the magnitude of the load on the instrumented girder increased was common to all three bridges. This has been noted by others^{1/} and advanced as an argument in favor of using the Guyon-Massonet orthotropic plate theory for load distribution in composite bridge structures in lieu of the beam

^{1/} Cassaro, M. A., Investigation of Structural Performance of the Suwannee River Bridge; Presented at the 54th Annual Meeting of AASHO, December 1968.

theory presently used for design. For the purpose of the present study the neutral axis location measured for a particular bridge and vehicle loading combination was used in the subsequent calculations of the resisting moments.

a) Four-Span Continuous H20-S16-44 Steel Girder Bridge

Using the experimentally determined neutral axis locations indicated for the centerline loadings and assigning a 100-inch wide portion of the slab to each interior girder and half the remaining slab plus curb to each exterior girder, calculations of the centroidal moments of each composite girder section were made with a number of trial values for n , the ratio of the elastic modulus of steel to that of the concrete. When a theoretical neutral axis location was obtained which provided a close comparison with the experimentally determined location, that value of n was used in calculating the actual section modulus of each girder section. The resisting moments were then obtained by combining the maximum measured bottom flange stresses with these section moduli. A good comparison was obtained with the theoretical applied moments.

The resulting distribution of the resisting moments from this analysis for the three vehicle loadings on centerline and on a normal traffic path are as follows:

RATIO OF TOTAL RESISTING MOMENT PROVIDED BY

	Exterior Girder	Interior Girder	Interior Girder	Exterior Girder
Test Vehicle Runs on Bridge Centerline				
HET-70	0.22	0.29	0.28	0.21
Tank	0.21	0.31	0.29	0.19
BPR	0.20	0.29	0.29	0.22
Test Vehicle Runs on Normal Traffic Path				
HET-70	0.04	0.15	0.32	0.49
Tank	0.03	0.16	0.32	0.49
BPR	0.03	0.16	0.32	0.49

The assignment of 35 to 40 percent of the HET-70 applied moment to the most heavily loaded girder for calculating the effect of the passage of such a vehicle in cases of beam spacing up to 90 inches appears valid from the data obtained on this bridge provided there is to be no control of the path of the vehicle on the bridge. Even higher percentages appear warranted for wider beam spacings. If the HET-70 vehicle is to be restricted to a centerline crossing, however, a lower percentage of the total applied moment might be assigned in accordance with the above tabulation of resisting moments.

b) Reinforced Concrete H-15 T-Beam Bridge

For the skewed single span reinforced concrete T-beam bridge, the stresses measured in the bottom steel reinforcing bars in the stems seemed low at first glance. The evaluation of the experimental data to account for this phenomenon proceeded as follows.

The location of the neutral axis was derived from the simultaneous strain responses of gages on the bottom reinforcing steel, on the top slab surface and on the side surfaces of the stem at a single cross section on both an interior and an exterior beam. The effect of compression reinforcement was neglected and the extent of existing concrete cracking in the stem was assumed to be less than the cracking which might result from the application of the HET-70 loading. The cracking stress for concrete in the stem was assumed to be 450 psi.

The curb section was considered to be acting compositely with the exterior stem. Calculations were made of the centroidal moments about the experimentally determined neutral axis for each T-beam section using trial values of n and trial proportions of the available deck slab width. In addition an appropriate area of concrete below the neutral axis was considered to be effective in tension to a point where the measured stresses in the section indicated a stress level of 450 psi. A balanced section consistent with the measured neutral axis locations was found to occur when a value for n of 6.5 was used and when 102 inches of slab width was assigned to the interior T-beam section and 62 inches of slab width to the exterior section.

The section modulus for each T-beam composite section was then calculated using these values. Assuming the bridge to be symmetrical in response, the calculated section moduli were combined with the maximum measured live load stresses to obtain the following distribution of resisting moments, the sum of which correlated very well with the respective applied moments.

RATIO OF TOTAL RESISTING MOMENT PROVIDED BY

	Exterior T-Beam	Interior T-Beam	Interior T-Beam	Exterior T-Beam
Test Vehicle Runs on Bridge Centerline				
HET-70	0.20	0.30	0.30	0.20
Tank	0.21	0.29	0.29	0.21
BPR	0.18	0.32	0.32	0.18
Test Vehicle Runs on Normal Traffic Path				
HET-70	0.10	0.21	0.32	0.37
Tank	0.11	0.23	0.28	0.38
BPR	0.08	0.18	0.33	0.41

Thus in spite of the 30-degree skew of this bridge the resisting moment distribution for centerline runs is essentially the same as for the non-skewed steel bridge. For the normal traffic path runs the distribution is more uniform; whether due to skewness or to some other factor is not known.

c) Prestressed Concrete H20-S16-44 Bridge

The calculation of the resisting moments for the composite girder sections of the skewed single span prestressed concrete bridge required that numerical values be assigned to the moduli of elasticity of the concrete in the deck slab and in the girders. The first step was to establish the ratio of the two moduli.

Trial values of the ratio of the moduli and trial proportions of the available deck slab width were used to calculate centroidal moments about the measured neutral axis locations. The curb section was considered to be fully composite with the exterior girder. The effect of superelevation and variation of overhang was neglected and the bridge was considered

to have symmetrical section properties. When a correlation of the measured and theoretical neutral axis locations was achieved, the ratio of the modulus of the deck slab concrete to the girder concrete was found to be 0.83 and the effective slab widths required for the interior and exterior girders were 122 inches and 60 inches respectively.

Next the apparent modulus of the girder concrete was determined by equating the calculated test vehicle applied moment to the measured resisting moments in accordance with the following equation.

$$\frac{\text{Applied Moment}}{E_c} = 2 \left[\frac{\text{Interior Girder Resisting Moment}}{E_c} \right] + 2 \left[\frac{\text{Exterior Girder Resisting Moment}}{E_c} \right]$$

The terms in brackets are known since $\left[\frac{\text{Resisting Moment}}{E_c} \right] = S e$ where S is the calculated section modulus based on the experimentally determined neutral axis and e is the measured bottom flange live load tensile strain.

When the expression equating the applied and resisting moments was solved, an apparent modulus of elasticity, E_c , for the girder concrete of 6.9×10^6 psi was obtained. This value compares well with values obtained in like manner by other researchers.^{2/} The reasons for the higher values obtained for apparent moduli in this way compared with values from laboratory tests are thought to be due to the higher rate of loading and the small strains measured. These factors tend to make the calculated apparent modulus more nearly resemble the higher tangent modulus than the normally measured secant modulus. In addition the modulus of elasticity of concrete is known to increase with age.

^{2/} Douglas and VanHorn, Lateral Distribution of Static Loads in a Prestressed Concrete Box Beam Bridge, Lehigh University FEL Report No. 315.1, 1966.

When the resisting moments were calculated a good comparison was obtained with the theoretical applied moments and the following distribution resulted.

RATIO OF TOTAL RESISTING MOMENT PROVIDED BY

	Exterior Girder	Interior Girder	Interior Girder	Exterior Girder
Test Vehicle Runs on Bridge Centerline				
HET-70	0.14	0.31	0.36	0.19
Tank	0.15	0.32	0.36	0.17
BPR	0.13	0.32	0.38	0.17

The right hand columns in which the higher ratios appear represent the low side of the superelevated roadway.

Test Vehicle Runs on Normal Traffic Path

	Exterior Girder	Interior Girder	Interior Girder	Exterior Girder
HET-70	0.02	0.18	0.34	0.46
Tank	0.03	0.18	0.37	0.42
BPR	0.04	0.17	0.36	0.43

The right hand side columns again represent the low side of the roadway.

For the centerline loadings it is evident that a greater proportion of the total resisting moment is provided by the interior girders than for the other two bridges. For the normal traffic path loadings, a lesser proportion of the total resisting moment is provided by the more heavily loaded exterior girder than was the case for the steel bridge.

2. DYNAMIC AMPLIFICATIONS OF STRESS

Dynamic amplification of stress results when a vehicle crosses a structure at a speed sufficient to induce a random vibration (which may be more or less harmonic) that results in an increase of measured stress over that measured under the crawl speed crossing by the same vehicle. The crawl speed stress corresponds to the static live loading of the structure. The stress amplification due to moving load is a transient effect and one not amenable to precise repetition or definition. The individual maximum measured values of all responses measured will therefore be utilized in this instance to describe dynamic amplifications in the three test bridges under the three vehicle loadings. The only dynamic amplifications of stress which are of concern are those which occur in the presence of a high level of static live load stress. Lightly loaded members often exhibit a large dynamic amplification percentage which are of no concern since the resultant stress level is still relatively low.

a) Four-Span Continuous Girder Bridge

It was planned that the test vehicles would cross this bridge at nominal speeds of 15 mph, 30 mph and the maximum speed attainable in addition to the crawl speed runs of about 3 mph. The site conditions and vehicle characteristics limited the maximum speeds to 29.2 mph for the tank, 38.7 mph for the HET-70 and 43.0 mph for the BPR test vehicle. The maximum speed (for the HET-70) under the best roadway conditions is reported to be about 40 mph. Maximum speed runs were generally attempted only on centerline paths across the bridge.

The maximum dynamic stress amplification under the HET-70 vehicle moving on centerline in the 90-foot span was an 18.7 percent increase to 8,350 psi in the interior girder bottom flange on a maximum speed run. A slightly higher stress level was reached on a normal traffic path run at 15 mph but this represented only a 5.1 percent increase to 9,300 psi in the exterior girder bottom flange. On the same vehicle runs, the dynamic stress amplifications in the end span were even lower, reaching 12.3 percent and 9.0 percent for centerline and normal traffic path runs respectively.

For the BPR test vehicle crossings the maximum stress amplifications occurred in the end span for both centerline and normal traffic paths. The maximum amplification for a centerline run was a 16.7 percent increase of the interior girder bottom flange stress to 3,920 psi at 15 mph. The maximum comparable normal traffic path amplification was a 36.2 percent increase to 5,550 psi in the exterior girder also at 15 mph. The maximum stress amplifications observed in the 90-foot span for the BPR test vehicle were 5.1 and 6.8 percent for centerline and normal traffic path runs respectively.

For the tank crossings all dynamic stress amplifications of heavily loaded members were less than 5.0 percent.

The preceding stress amplifications are summarized below for reference.

	MAXIMUM PERCENTAGE OF STRESS AMPLIFICATION			
	End Span		90-Foot Span	
	Centerline	Normal Path	Centerline	Normal Path
HET-70	12.3	9.0	18.7	5.1
Tank	<5.0	<5.0	<5.0	<5.0
BPR	16.7	36.2	5.1	6.8

It is apparent that the dynamic stress amplifications observed in this bridge over the full range of speed of the HET-70 vehicle on both centerline and normal traffic paths is quite moderate compared to the allowance for impact in design. While the dynamic stress amplification under the BPR test vehicle exceeded the design impact allowance in one instance, the total live load stress for this loading level was well below the design level.

b) Reinforced Concrete T-Beam Bridge

The approach roadway for this bridge had been obliterated during construction of the replacement roadway and bridge. The temporary approach roadway constructed to allow the test vehicles to get on the bridge for the purpose of this study was of light construction and limited the test vehicle speeds to about 10 mph except that the tank was able to reach 20.1 mph. At this speed there was virtually no dynamic amplification of stress in the bridge under the passage of the HET-70 vehicle. Under the BPR test vehicle the dynamic stress amplification in one heavily loaded member reached a surprising 24 percent at 10.3 mph. The maximum amplification for the tank at 20.1 mph was 13.5 percent. Due to the limited speeds attained on this bridge, no further comment on these results is warranted.

c) Prestressed Concrete Bridge

The maximum speeds attained on this bridge for the HET-70 vehicle, the BPR vehicle and the tank were 36.9 mph, 32.5 mph and 15.0 mph respectively. The tank speed was limited by the difficulty of steering the tracked vehicle on the curved roadway alignment.

As was observed on the steel bridge, the BPR test vehicle induced the highest dynamic stress amplifications (25 percent) and the tank induced the lowest (about 5 percent). The maximum amplifications under

the HET-70 vehicle passages were of the order of 15 percent. The dynamic stress amplifications are obviously not a function of the ratio of vehicle length to bridge length since the tank and the HET-70 vehicle represent two extremes of vehicle length and yet induce smaller dynamic amplifications than the BPR test vehicle whose length falls between that of the tank and the HET-70. Undoubtedly the vehicle suspensions have a greater influence on dynamic stress amplification than any other single factor.

On this bridge an attempt was made to stimulate greater dynamic amplification under the passage of the HET-70 vehicle by driving the vehicle at 15 mph several times over a 2-inch thick plank placed at various locations on the bridge deck. No significant difference in the dynamic stress amplification resulted.

3. OTHER BRIDGE MEMBER RESPONSES

Grouped in this section but discussed separately are the initial findings deduced from special gages installed on the structure or from general observations made during the conduct of the field test or during the reduction of the data.

a) Measured Deck Slab Stresses

A single strain gage was installed on a transverse No. 5 reinforcing bar of the bottom layer of bars located at 5-inch centers in the deck slab on the prestressed concrete bridge. The bar was exposed by removing the concrete cover on the underside of the slab with a chipping hammer at a point midway between the interior girders and 10 feet from the line of girder bearings at the abutment. The responses of this gage were monitored during crossings of the bridge with each of the three test vehicles on centerline and normal traffic paths and during two special runs in which

the BPR test vehicle and HET-70 tank transporter were driven across the bridge with one line of wheels directly over the location of the subject gage. Only in the latter two instances were significant stresses recorded. The maximum stress recorded for the BPR test vehicle loading was 2,860 psi and for the HET-70 tank transporter loading was 3,440 psi. It is evident from the low magnitudes of these steel stresses that neither of these loadings represented a severe transverse positive bending moment condition for the 7-inch concrete deck slab in this bridge.

b) Measured Pier Cap Bending Stresses

The instrumented prestressed concrete bridge span was one of a series of simple spans with intermediate supports on concrete hammerhead piers. The cantilevered caps of the piers supported the exterior lines of bridge girders while the two interior lines of girders were located over the center monolithic portion of each pier. In order to measure the live load effect transmitted to caps through the exterior girder bearings, a horizontal reinforcing bar near the cap top surface comprising part of the tensile reinforcement resisting the exterior girder bearing reactions on the cantilevered pier cap was exposed by removing the concrete cover with a chipping hammer, and a strain gage was installed on the bar (Fig. B-13). The maximum live load stress recorded in this bar under the HET-70 loading was 3,740 psi. The calculated dead load stress for this member was 7,300 psi. It is evident that the maximum influence of the HET-70 vehicle on this member imposed no severe loading condition.

4. CONTINUING WORK

Additional findings are being extracted from the field test data in the following subject areas:

1. Bridge deflections under live loading.
2. Maximum moment sections in skewed bridges.
3. The dynamic characteristics of the test bridges.

A brief motion picture film is being prepared by the Federal Highway Administration Publication and Visual Aids Branch to supplement the published findings. The film will depict the conduct of the field study and will illustrate some typical findings drawn from the research.

A computerized routine for the theoretical analysis of the responses of highway bridges under any given live loading is currently being debugged and is expected to be ready for inclusion in the final report.

5. SUMMARY

This study affirms that it would be difficult to predict live load resisting moment distributions generally in highway bridges for specific loadings due to the many variables which influence such distributions. This study does, however, demonstrate the degree to which resisting moment distribution can be controlled by restrictions on the path and speed of crossing of a particular vehicle on a given bridge. It is further demonstrated that a considerable reserve capacity may exist in a bridge for safely carrying greater live loads than design calculations would indicate.

With regard to the effect of the speed of the vehicle while crossing a bridge, the HET-70 vehicle crossed two widely different bridge types at the maximum speed attainable without inducing dynamic amplifications

of live load stress greater than 18.7 percent. By contrast the BPR test vehicle which more nearly resembles a typical highway truck induced much higher live load dynamic amplifications. It is apparent that some characteristic of the HET-70 vehicle, perhaps the overall load distribution or the particular suspension system may tend to reduce the impact of this vehicle on highway bridges compared to more typical highway vehicles.

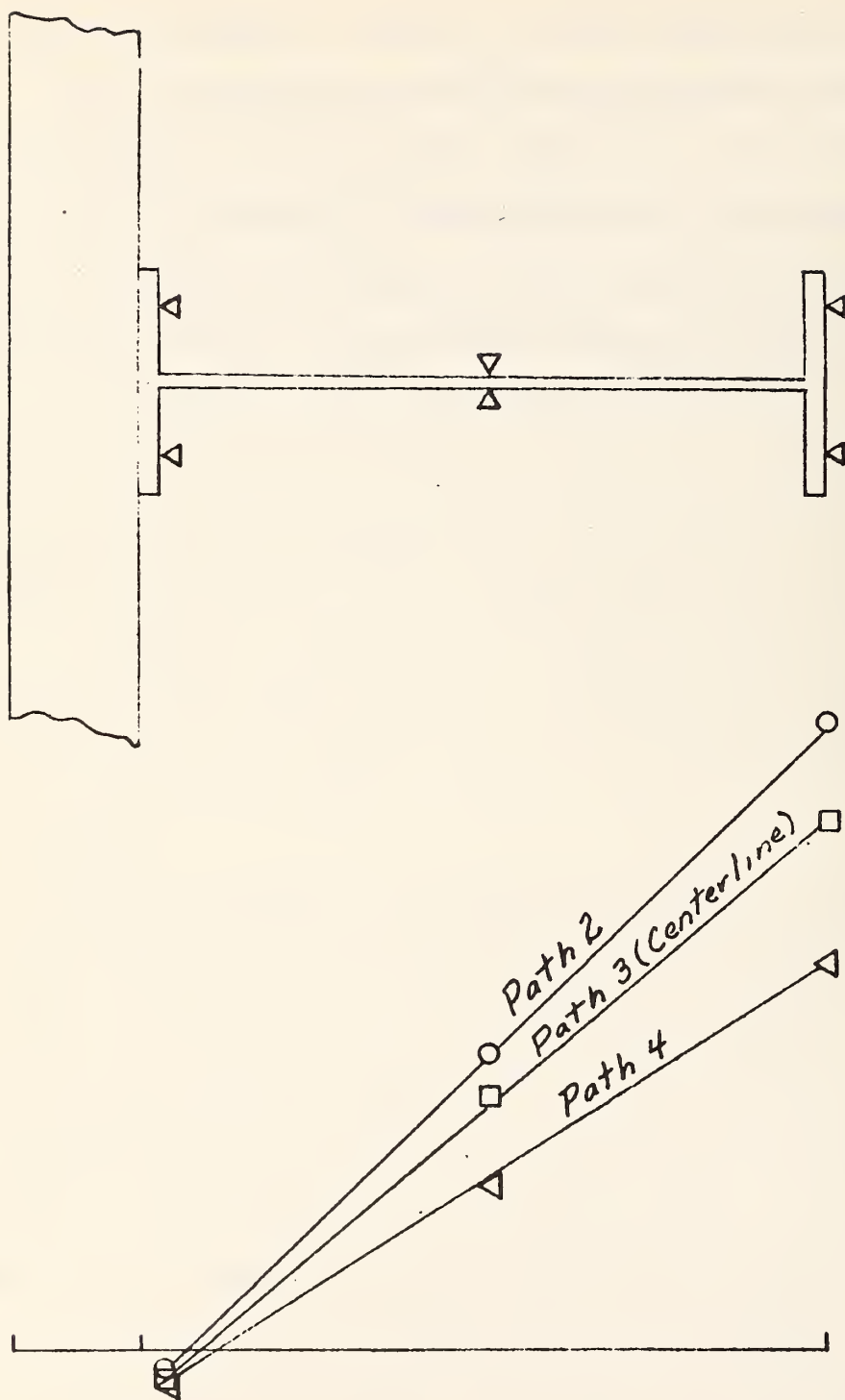


FIG. B-11 - NEUTRAL AXIS LOCATION FROM MEASURED STRAINS WITH HET-70 LOADING, INTERIOR GIRDER NEAR MID-SPAN OF 90' SPAN, FOUR SPAN CONTINUOUS STEEL GIRDER BRIDGE.

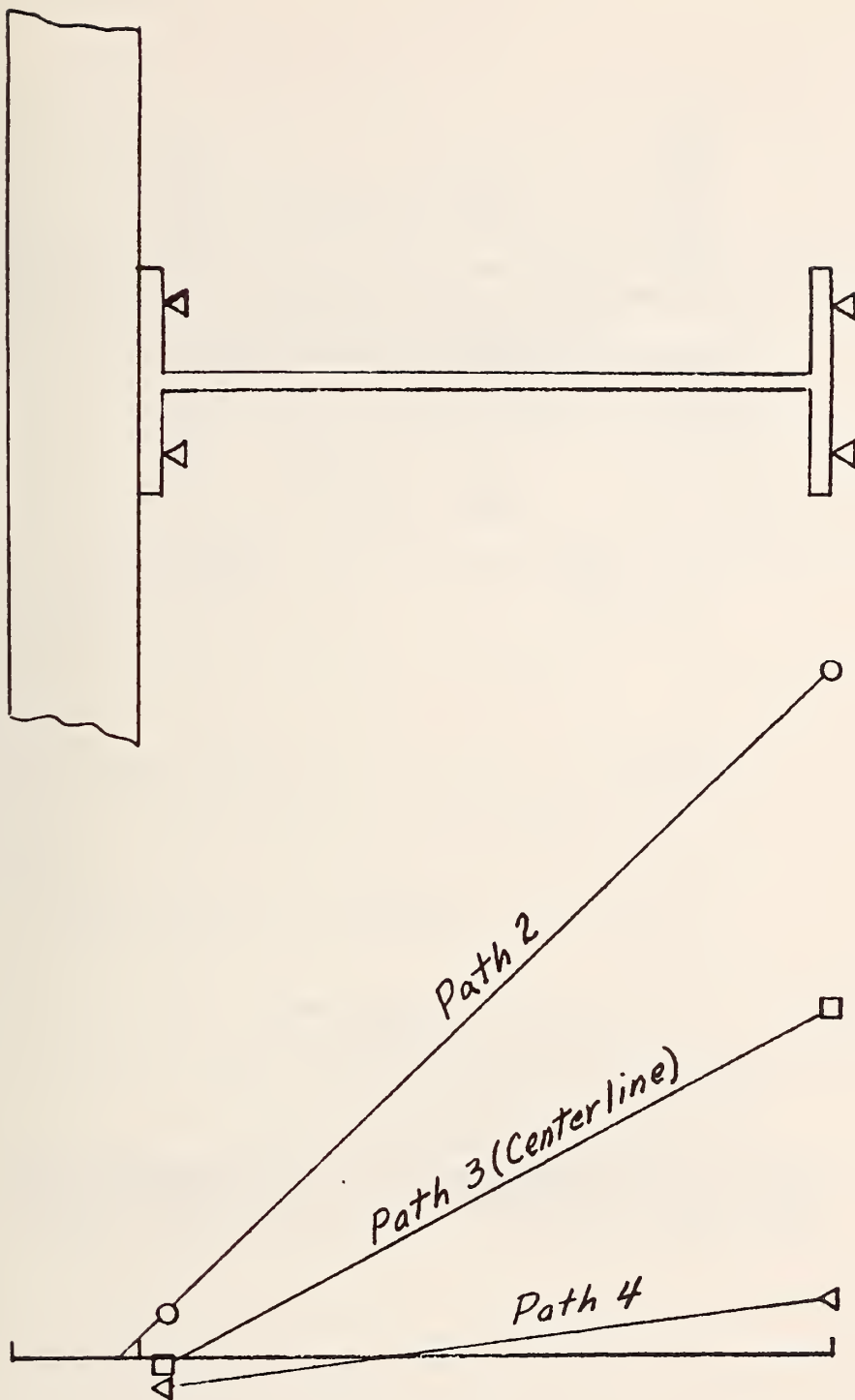


FIG. B-12 - NEUTRAL AXIS LOCATION FROM MEASURED STRAINS WITH HET-70 LOADING, EXTERIOR GIRDER NEAR MID-SPAN OF 90' SPAN, FOUR SPAN CONTINUOUS STEEL GIRDER BRIDGE.

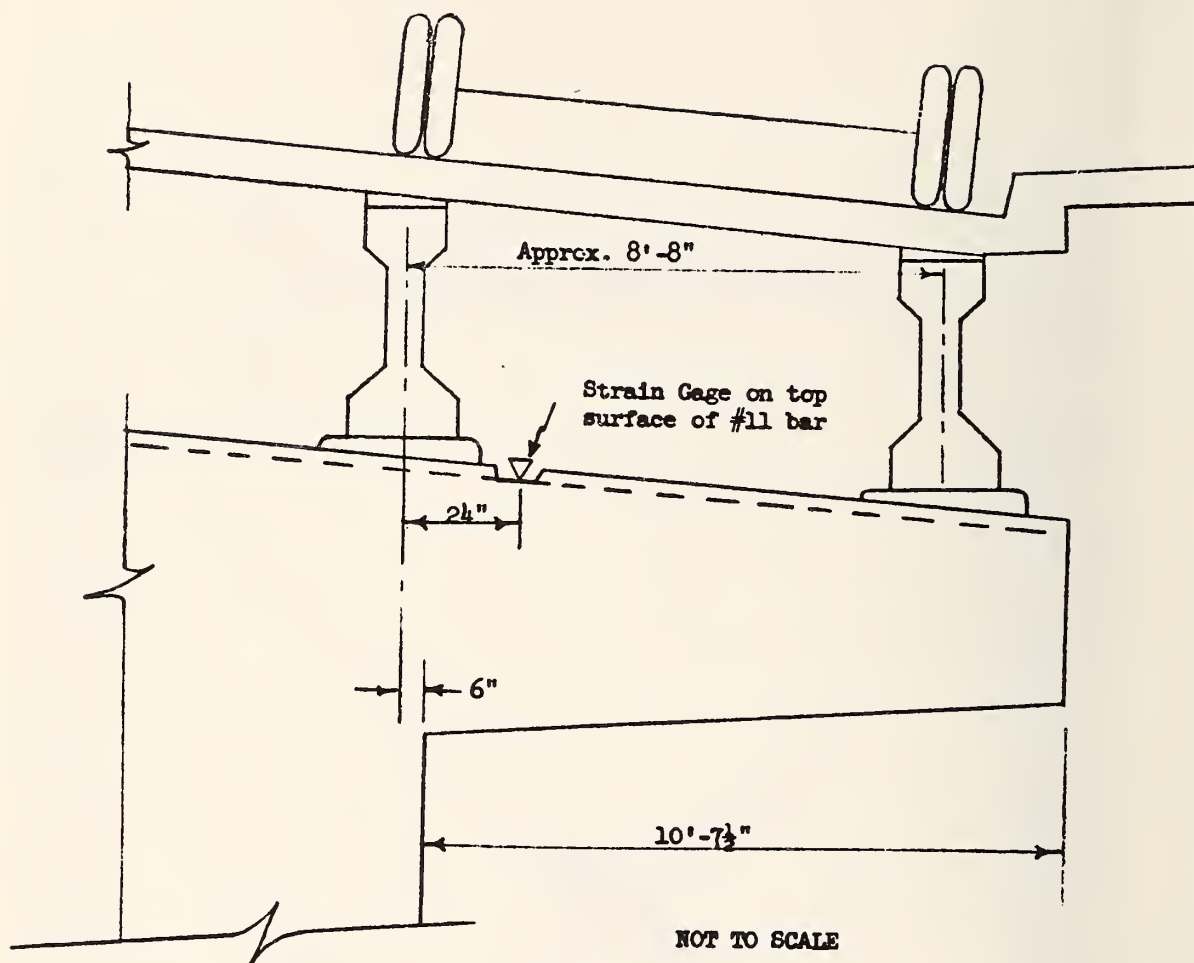


FIG. B-13 - STRAIN GAGE LOCATION IN PIER CAP FOR MEASURING LIVE LOAD EFFECTS TRANSMITTED BY EXTERIOR GIRDER BEARINGS.

PHASE 3
of
A Preliminary Research Report
on
An Experimental Loading Study
of
Three Highway Bridges in Tennessee
with the
U. S. Army HET-70 Main Battle Tank Transporter

by
Robert F. Varney
Structural Research Engineer
Structures and Applied Mechanics Division
Office of Research and Development
Bureau of Public Roads
Washington, D.C.
May, 1970

FOREWORD

This is the third research report on the field loading studies of three highway bridges in Tennessee with the U. S. Army HET-70 Main Battle Tank Transporter. The two previous reports were issued in June, 1969 and October, 1969. A review of those reports is recommended as a prerequisite to the reading of this report in order to provide background material for the better understanding of the material presented herein. This report completes the presentation of the field study findings. A summary final report will be issued in the near future to consolidate the material presented in the three preliminary reports. Additional information on a computerized theoretical analysis of the bridge loadings will also be provided in the final report.

An 18-minute narrated color film describing the conduct of the field study and presenting some preliminary findings has been prepared by the Bureau of Public Roads. Loan of the film which is entitled "Tennessee Bridge Test" may be had upon request to:

U. S. Department of Transportation
Federal Highway Administration
Photographic Section
Washington, D. C. 20591

1. INTRODUCTION

This report presents findings resulting from the analysis of the measured live load responses of the following highway bridges described in detail in the first preliminary report of this research:

1. A four-span (70'-90'-90'-70') continuous steel rolled beam bridge.
2. A 53-foot span skewed (30° right) simple span reinforced concrete T-beam bridge.
3. A 65-foot span skewed (20° right) simple span prestressed concrete I-beam bridge.

Each of these bridges were loaded in turn with the following test vehicles also described in detail in the first report:

1. A three-axle tractor and semi-trailer combination which closely simulated an HS-20-44 design vehicle (called BPR herein).
2. A 105,000 pound U. S. Army track-laying combat tank.
3. A 195,400 pound 8 axle pneumatic-tired U. S. Army HET-70 tank transporter.

In this report the effect of skew on the two concrete bridges is contrasted with the behavior of the unskewed steel bridge. In other sections of the report the live load deflections and vibration responses of the bridges are discussed in detail. Finally, a procedure for evaluating the capability of simple span bridges to carry the HET-70 Main Battle Tank Transporter loading is described.

2. BRIDGE DEFLECTIONS

A summary presentation of the maximum measured live load deflection responses of the longitudinal girders for the four-span continuous steel bridge is contained in Table 2. The deflection responses of the main load-carrying member of the two concrete bridges are summarized in Table 3.

A comparison of the live load deflections in these tables shows that the two concrete bridges are considerably less flexible than the steel bridge as would be expected. Of the two concrete bridges, the prestressed bridge with the wide beam spacing and thinner slab exhibits the less uniform distribution of deflection to the four main load-carry members with the HET-70 loading on the bridge centerline. This behavior parallels the less favorable distribution of resisting moments noted in the Phase 2 report. The deflection responses of the steel bridge indicate that the interior girders are relatively more flexible than the exterior girders in the 70-foot end span compared to the 90-foot second span. Concurrent live load stress magnitudes in the end span exterior girders were generally only slightly lower than in the second span exterior girders. The maximum live load stress magnitudes in the interior girders were slightly higher in the end span than in the second span. It is not known without confirming studies on other bridges of this type whether the relatively greater flexibility of the interior girders (as compared with exterior girders) in the end span is characteristic of this particular bridge or is a hitherto unrecognized characteristic of certain types of continuous-span steel girder structures. The ratios of the interior to exterior maximum live load girder deflections and stresses are summarized in Table 4.

It is apparent that lateral distributions of deflection are also a function of vehicle dimensions. The narrower BPR test vehicle loading was not as well distributed laterally on the steel bridge as the other test vehicle loadings. Lateral distributions of loading were not evaluated for the concrete bridges. In general no significance would be expected to attach to the analysis of lateral deflection distribution for these short-span skewed concrete bridges. However, consistent with the observation in the Phase 2 report that the interior girders of the prestressed bridge provided a greater proportion of the total resisting moment, the live load deflections of the interior girders of this bridge are proportionately greater than the exterior girder deflections.

3. EFFECT OF SKEW

To determine whether the location of the section at which the maximum live load stress developed in the longitudinal load-carrying members is influenced by bridge skew, strain gages were located on the two concrete bridges at a number of closely spaced sections near midspan. Fig. B-14 shows the strain gage locations on the T-beam stem reinforcement, together with the maximum live load stresses at each gage point for the various test loadings. Figs. B-15, 16, and 17 present similar responses from strain gages located on the bottom surfaces of the prestressed concrete girders. The maximum responses at any section in each member for a particular loading condition are underscored. The theoretical maximum moment sections for simple beam loading are also indicated. Additional details on the gaging and loadings referred to in these figures are given in the first preliminary report.

Two readily apparent phenomena associated with the T-beam bridge responses are seen in Fig. B-14:

1. The maximum observed responses in the interior girders generally did not occur at the theoretical maximum moment section calculated for a simple span beam loading.
2. The maximum bending moment stress in the exterior girder occurs at or near midspan for all test vehicle crossings on all paths.

The prestressed girder bridge with thinner slab and wider girder spacing is seen to respond as follows:

1. When the interior girders are heavily loaded, (Fig. B-16) the maximum stresses occur at sections closer to midspan than in the T-beam bridge but generally not at the theoretical section calculated from simple beam loading.
2. When the exterior girders carry a significant portion of the distributed load (Figs. B-15 and B-17) the maximum stresses occur very nearly at the section at which they would be calculated to occur, based on theoretical simple beam loading.

On each skewed bridge the measured responses on the same interior member give indications that the maximum response may occur at either of two sections. Since this phenomenon was evident for loadings with all three vehicles it may be attributable to the unsymmetrical transverse distribution of wheel loads to main members in skewed bridges.

Strain gages were also located on closely spaced sections on the 70-foot end span and 90-foot second span of the unskewed continuous span steel girder bridge. In the 90-foot second span, the maximum bending moment

stresses occurred at the midspan section of both exterior and interior girders for all loadings with each test vehicle. In the 70-foot end span the maximum stresses generally occurred at the same section for loadings with each test vehicle. This is based on responses of the interior girder since no observations were made on the exterior girder. It is concluded that the variations in the locations of the maximum moment sections for the different vehicles on the different paths on the two concrete bridges may be attributable to the effect of skew. However, any generalized conclusions about the effect of skew based on observations on two bridges are not warranted. Additional research in this area leading to the more economical design of short and intermediate span skewed beams appears to be in order, however, based on indications that live load bending moments in skewed bridges may be more uniformly distributed than assumed for simple span beam loading.

4. BRIDGE VIBRATIONS

Vibration responses measured on each bridge include natural frequencies, mode shapes, amplitudes and damping. Vibration data were available from strain and deflection gages and from low-frequency-sensitive vertical accelerometers mounted on the deck of the steel girder bridge on each side of the roadway of each of the two instrumented spans during the BPR test vehicle runs. Vehicle-induced vertical accelerations measured at these four points provided good definition of the vibration mode shapes. Additional detail on this instrumentation technique will be included in the final report.

A unique opportunity was afforded in this study to evaluate the effect on bridge responses of high-frequency forced vibrations such as

were imposed by the passages of the heavy track-laying tank. The passage of this tracked vehicle is comparable to a wheeled vehicle crossing a bridge with a transversely corrugated deck. No detailed correlation was made of the various factors involved such as the cleat spacing on the tracks, the speed of the tank crossing and the response of the bridge. Nevertheless the variations in the bridge forced-vibration frequency of response obviously resulted from the interrelationship of the speed and the cleat spacing. At crawl speeds only the bridge natural frequencies of response were in evidence.

The high-frequency forced vibrations imposed by the passage of the tank at speeds from 10 to 20 mph ranged in frequency between 28 and 64 cps and were superimposed on the bridge natural frequency response (Fig. B-18). As noted above the frequency of the forced response was generally proportional to the speed of passage. The high-frequency vibration amplitudes were often of considerable magnitude as seen in Fig. B-18 even though this response is in the region above resonance where amplification factors are less than unity.

No comparable high-frequency responses were observed under the passage of the rubber-tired BPR and HET-70 vehicles. In these instances only the natural frequencies of the bridge responses and some low-frequency forced responses were in evidence. It was also evident that all responses induced by the tracked vehicle were far more harmonic in character than the responses induced by the rubber-tired vehicles.

Another unusual feature observed during the tank passage was a vibration amplitude of considerable magnitude in the prestressed concrete bridge at the bridge natural frequency (6.9 cps) during the passage of the

tank at crawl speed. It may be surmised in the absence of more positive evidence that the repetition rate of the passage of tank track cleats at crawl speed may have been close to the natural frequency of the bridge with the unexpected result of high stress amplifications at crawl speed for this vehicle. The magnitudes of natural frequency responses of the other two bridges under a similar condition was not as pronounced. In general, however, the forced excitation of bridge natural frequencies and higher frequencies by frequent passages of tracked vehicles on bridges could be a matter of concern.

The bridge responses under passages of the rubber-tired vehicles are summarized as follows:

a) Four-span continuous steel girder bridge

The principal free vibration responses observed from accelerometer responses during the passage of the BPR vehicle fell in the 3.0-3.6 cps range with two mode shapes (Fig. B-19) which could not be differentiated in frequency. For vehicle runs on centerline the fundamental vibration mode shape was apparent ("a" in Fig. B-19). When the BPR vehicle runs were made on a normal traffic path, a similar mode shape was observed except that opposite sides of the roadway were out of phase ("b" in Fig. B-19).

Vibrations induced by the passage of the HET-70 test vehicle were less pronounced and were also in the 3.0 to 3.6 cps range. Speed had little effect on the development of free vibration response. Beat frequencies were also observed on some runs.

For one brief period one higher harmonic was excited by the BPR vehicle at about 6.0 cps ("c" in Fig. B-19). Vibration frequencies from 2.4 to 5.0 cps were observed under the passage of the tank in addition to the very high forced frequencies previously described. The free

vibration double amplitude magnitudes were of the order of 0.15 inch. The observed logarithmic decrement of vibration was 0.05, evidence of a lightly damped structure.

A composite EI was calculated from the observed fundamental natural frequency and this EI value was used to calculate theoretical live load deflections for comparison with measured values. The measured deflections were somewhat lower than the values calculated in this manner.

b) Prestressed Concrete Bridge

Vibration responses of this bridge were taken from the strain and deflection dynamic variations. The free vibration natural frequency was measured at 6.9 cps. The magnitude of vibration amplitude was so low for all test vehicles that the determination of a viscous damping coefficient was impossible. During the crawl run passage by the BPR test vehicle, typical 2.7 cps forced vibration responses of considerable magnitude were observed in the bridge. These are attributed to the natural frequency vibrations of the vehicle suspension system induced by engine vibrations. The vibration responses to the tank passage are a combination of the bridge natural frequency and the forced frequencies described above. The responses to the HET-70 passage were the bridge fundamental frequency and a low-amplitude forced frequency of about 1 cps at crawl speed. The value of EI calculated from the natural frequency was used in the calculation of theoretical deflections. Contrasted to the findings for the steel bridge, the average measured live load deflections were somewhat higher than the predicted values with the interior girders deflecting much more in relation to the exterior girders than the theoretical proportions of the resisting moments would indicate.

c) Reinforced Concrete T-Beam Bridge

Vibration responses on this bridge were also obtained from strain and deflection variations. The free vibration natural frequency was measured at 8.5 cps for loadings by all test vehicles. Due to the very low vibration amplitudes under the rubber-tired vehicles no damping analysis was possible. The bridge vibration responses to the HET-70 vehicle passage were essentially no different than for the passage of the BPR test vehicle. The value of EI calculated from the observed natural frequency of 8.5 cps was used in turn to calculate the theoretical live load deflections of the structure for loading with the tank. A good correlation was obtained with the measured deflections reported previously.

5. APPLICATIONS

The findings from the field research are being utilized to develop procedures for predicting the capability of any bridge to carry the HET-70 loading. Two approaches are being prepared as follows:

a) Bridge Loading Nomograph

A type of nomograph which may be used for evaluating the capacity of simple span bridges of various lengths to tolerate passage of a heavy loading without distress is illustrated in Figs. B-20 and B-21. The nomograph shown was conceived and prepared by the Bridge Division of the Bureau of Public Roads Office of Engineering and Operations. This nomograph is based on the experimental findings presented in the first two reports of this series covering field studies of the three bridges. The user of the nomograph must select a maximum permissible stress level which in turn will equate to a live load moment capacity to be introduced

into the nomograph. A maximum permissible stress level of 75 percent of the yield point of the structural material has been suggested. The limitations of the sample nomograph are indicated. Similar nomographs can be developed to suit the various requirements of different users.

b) Computer-Programmed Analysis of Bridge Loading

A computer-programmed analytical technique for evaluating the behavior of any bridge under any imposed static live loading is now being perfected. In this program the deck slab and girder components of a bridge are modeled as members of a rectangular grid system. Values for torsional and flexural inertia and shear area are assigned to each member of the model in accordance with the requirement that the structural response of the model must simulate exactly the response of the prototype bridge. Material properties must likewise be evaluated correctly in the model.

A stiffness matrix method is used to analyze the grid. Since the program requires that all load forces be applied at the joints of the grid, distributions of the wheel loads of an assumed vehicle loading which fall between the joints of the grid must be distributed to the adjacent joints before initiating the program. The analysis provides joint displacements and element end forces (flexure, torsion and shear) for evaluating the maximum loading effects. This routine is presently programmed for the CDC 6600 computer..

6. EPILOGUE

This study was undertaken to establish a procedure for evaluating the load-carry capabilities of typical highway bridges under various heavy vehicle loadings. Other related findings resulting from the research have also been presented throughout the three preliminary reports.

While only the live load bending moments and deflections have been treated in this study, other aspects of loading are generally more amenable to precise calculation and less susceptible to experimental measurement. The maximum shear concentrations for any vehicle loading are readily calculated for evaluations of shear stresses whereas the experimental measurement of shear and bond stresses is not so easily accomplished. However, additional findings will be available from observations of the bridge response to the application of ultimate loadings to be made in a subsequent study of these specimen bridges and will provide additional insight into the various failure modes.

This final progress report will be followed by a summary final report of the material contained in the three preliminary reports and will also include the details of the computer program for analyzing bridge behavior under applied static live loading. The readers should also look forward to the reports on the subsequent study, described above, for additional information on the ultimate static live load capacity of these bridges. The subsequent study is expected to provide information on such matters as load distribution to various members in the structural material yield range, the effect of plastic yielding on the load capacity and finally the ultimate capacity of the structures in different modes of failure.

TABLE 2

MAXIMUM MEASURED LIVE-LOAD DEFLECTIONS, FOUR-SPAN
CONTINUOUS STEEL BRIDGE

LOADINGS		SPAN DEFLECTIONS (INCHES)			
Vehicle/Location	Speed	Midspan 90-foot span		0.4 point 70-foot span	
		Exterior Girder	Interior Girder	Exterior Girder	Interior Girder
One BPR each lane	crawl	0.50	0.55	0.30	0.41
HET-70 on centerline	crawl	0.54	0.71	0.28	0.51
HET-70 on centerline	Max.	0.66	0.82	0.35	0.62
HET-70 normal lane	crawl	1.09	0.81	0.59	0.55
Tank on centerline	crawl	0.35	0.49	0.19	0.38
Tank normal lane	crawl	0.71	0.53	0.41	0.42
1/800 span length		1.35	1.35	1.05	1.05

TABLE 3

MAXIMUM MEASURED LIVE LOAD DEFLECTIONS, REINFORCED
CONCRETE AND PRESTRESSED CONCRETE BRIDGE

REINFORCED CONCRETE T-BEAM BRIDGE		
Loadings	Beam Deflections (inches)	
	Exterior	Interior
One BPR each lane	0.07	0.10
HET-70 on centerline	0.07	0.12
HET-70, normal lane	0.10	0.11
Tank on centerline	0.06	0.11
Tank, normal lane	0.10	0.10

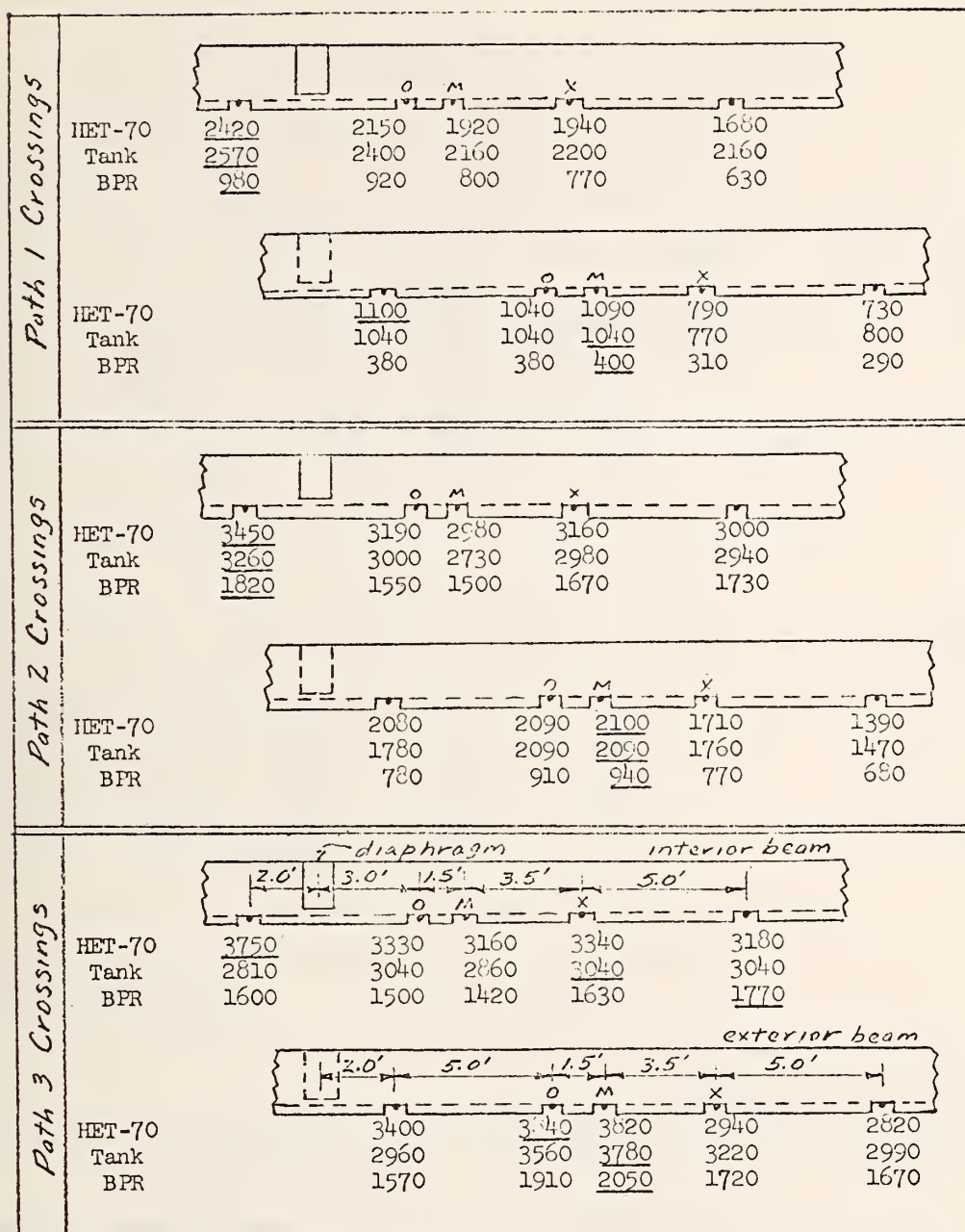
PRESTRESSED CONCRETE GIRDER BRIDGE		
Loadings	Girder Deflections (inches)	
	Exterior	Interior
One BPR each lane	0.11	0.15
HET-70 on centerline	0.13	0.28
HET-70, normal lane	0.33	0.30
Tank on centerline	0.14	0.24
Tank, normal lane	0.18	0.16

TABLE 4

GIRDER RESPONSE DISTRIBUTION FACTORS, FOUR-SPAN
CONTINUOUS STEEL BRIDGE

Loadings	0.4 point End Span		Midspan Second Span	
	Deflection	Stress	Deflection	Stress
BPR	2.08	1.93	1.43	1.70
Tank	2.01	1.85	1.38	1.66
HET-70	1.83	1.77	1.32	1.52

Tabulated factors show $\frac{\text{maximum interior girder response}}{\text{maximum exterior girder response}}$ for centerline runs of individual vehicles at crawl speeds.



Crawl Speed Runs

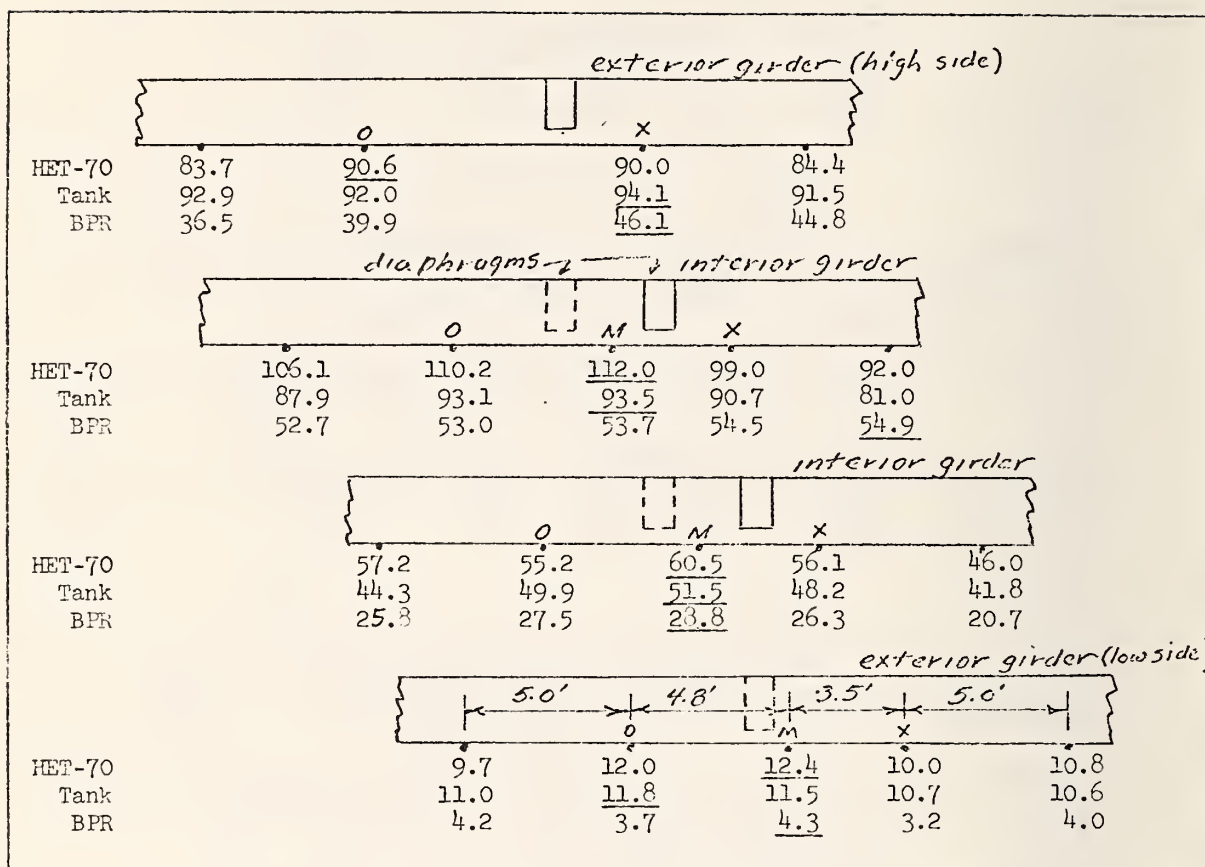
Theoretical maximum moment sections for vehicle movement from left to right on simple span beams as follows:

Tank = M (beam midspan)

BPR = X

HET-70 = O

FIG. B-14 - ELEVATIONS OF T-BEAM STEMS SHOWING MAXIMUM LIVE LOAD STRESSES AT GAGE POINTS AND BOTTOM REINFORCING BARS.



Average Values For Crawl Speed Runs

Path 2 Crossings

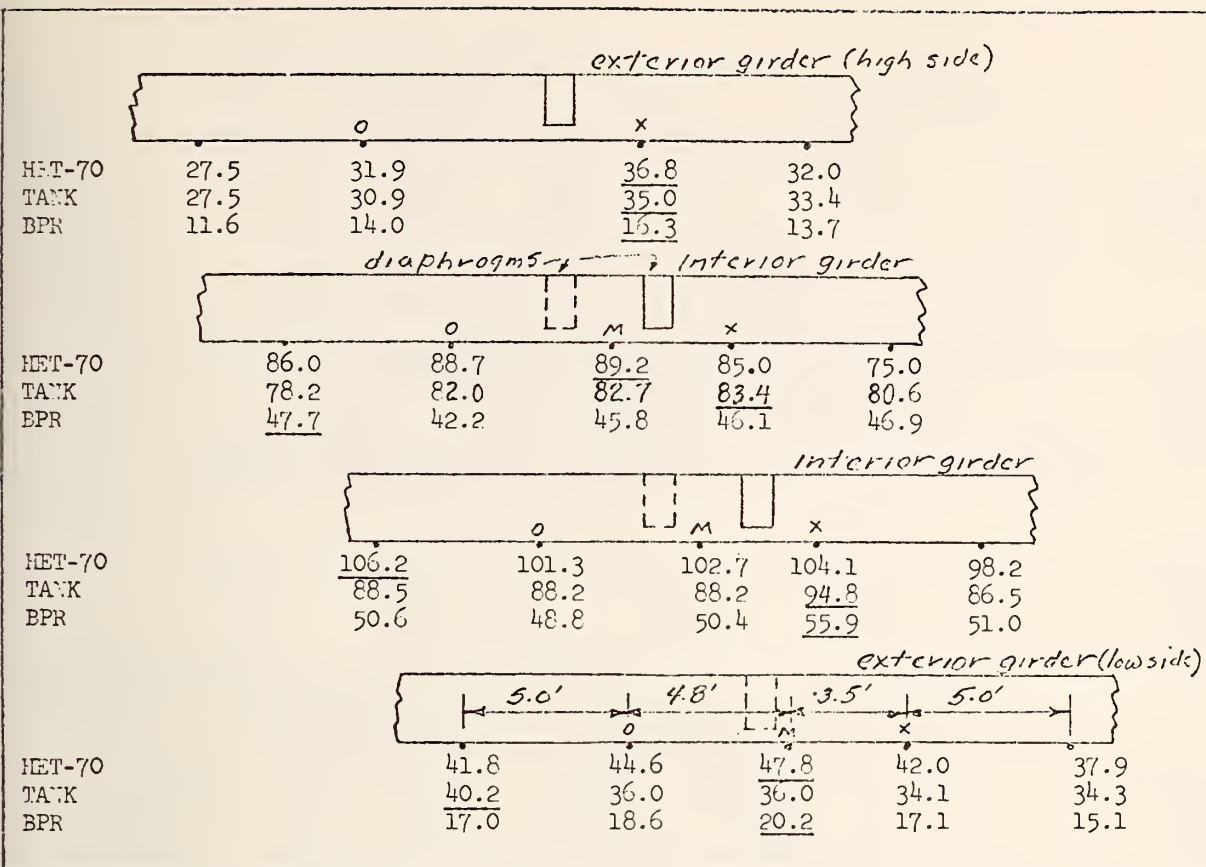
Theoretical maximum moment sections for vehicle movement from left to right on simple span beams as follows:

Tank = M (beam midspan)

BPR = X

HET-70 = 0

FIG. B-15 - ELEVATIONS OF PRESTRESSED GIRDERS SHOWING MAXIMUM LIVE LOAD STRAINS AT GAGE POINTS ON BOTTOM SURFACES FOR PATH 2 CROSSINGS.



Average Values For Crawl Speed Runs

Path 3 Crossings

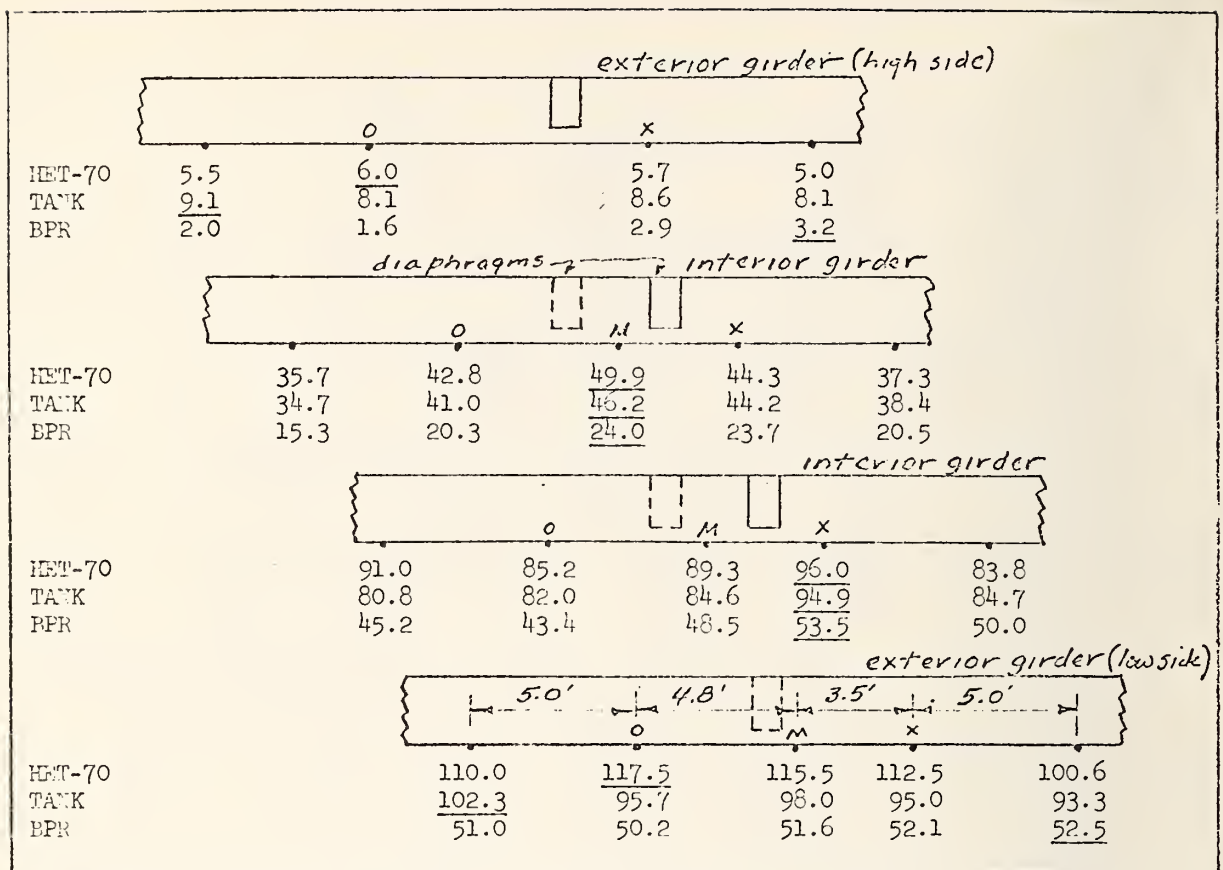
Theoretical maximum moment sections for vehicle movement from left to right on simple span beams as follows:

TANK = M (beam midspan)

BPR = X

HET-70 = 0

FIG. B-16 - ELEVATIONS OF PRESTRESSED GIRDERS SHOWING MAXIMUM LIVE LOAD STRAINS AT GAGE POINTS ON BOTTOM SURFACES PATH 3 CROSSINGS.

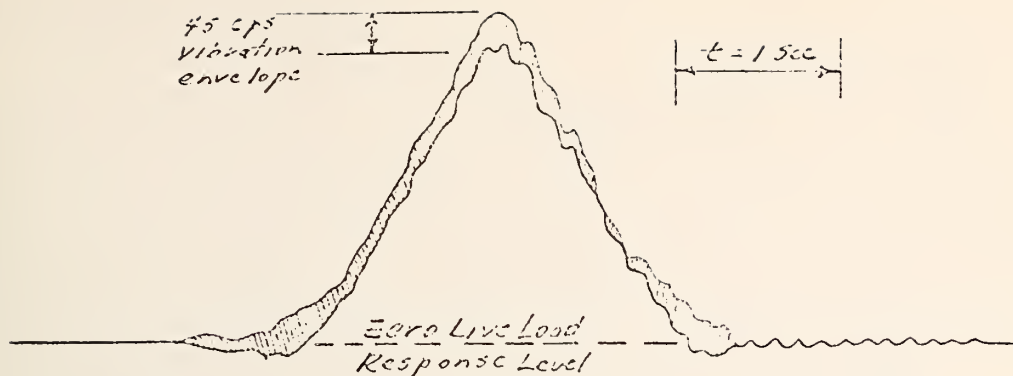


Average Values For Crawl Speed Runs
Path 4 Crossings

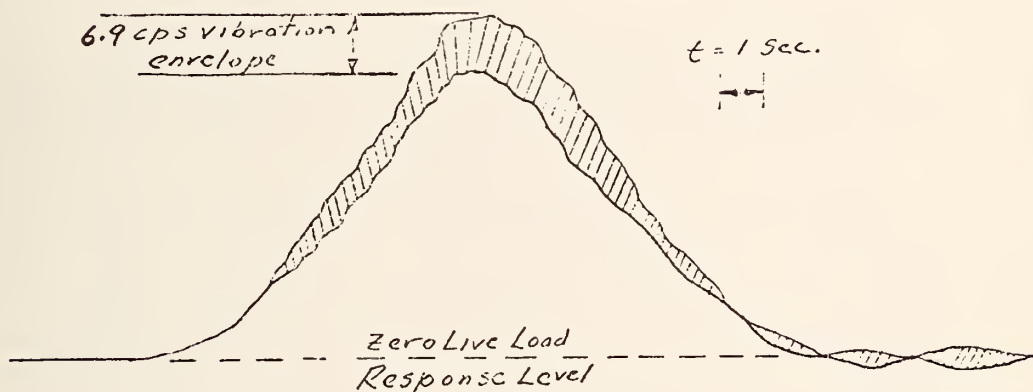
Theoretical maximum moment sections for vehicle movement from left to right on simple span beams as follows:

TANK = M (beam midspan)
BPR = X
HET-70 = 0

FIG. B-17 - ELEVATIONS OF PRESTRESSED GIRDERS SHOWING MAXIMUM LIVE LOAD STRAINS AT GAGE POINTS ON BOTTOM SURFACES PATH 4 CROSSINGS.



15 mph - 45 cps forced frequency and 6.9 cps fundamental bridge frequency responses superimposed on static live load response.



Crawl - Large amplitude 6.9 cps frequency responses superimposed on static live load response.

FIG. B-18 - TYPICAL VIBRATION RESPONSES AT MID-SPAN OF THE BRIDGE SUPERSTRUCTURE, PRESTRESSED CONCRETE GIRDER BRIDGE UNDER PASSAGE OF THE TRACK LAYING TANK.



a) 3.0 - 3.6 cps



b) 3.0 - 3.6 cps



c) 6.0 cps

**FIG. B-19 - OBSERVED NATURAL FREQUENCIES IN MODE SHAPES OF
BRIDGE SUPERSTRUCTURE VERTICAL VIBRATIONS,
FOUR SPAN CONTINUOUS STEEL GIRDER BRIDGE.**

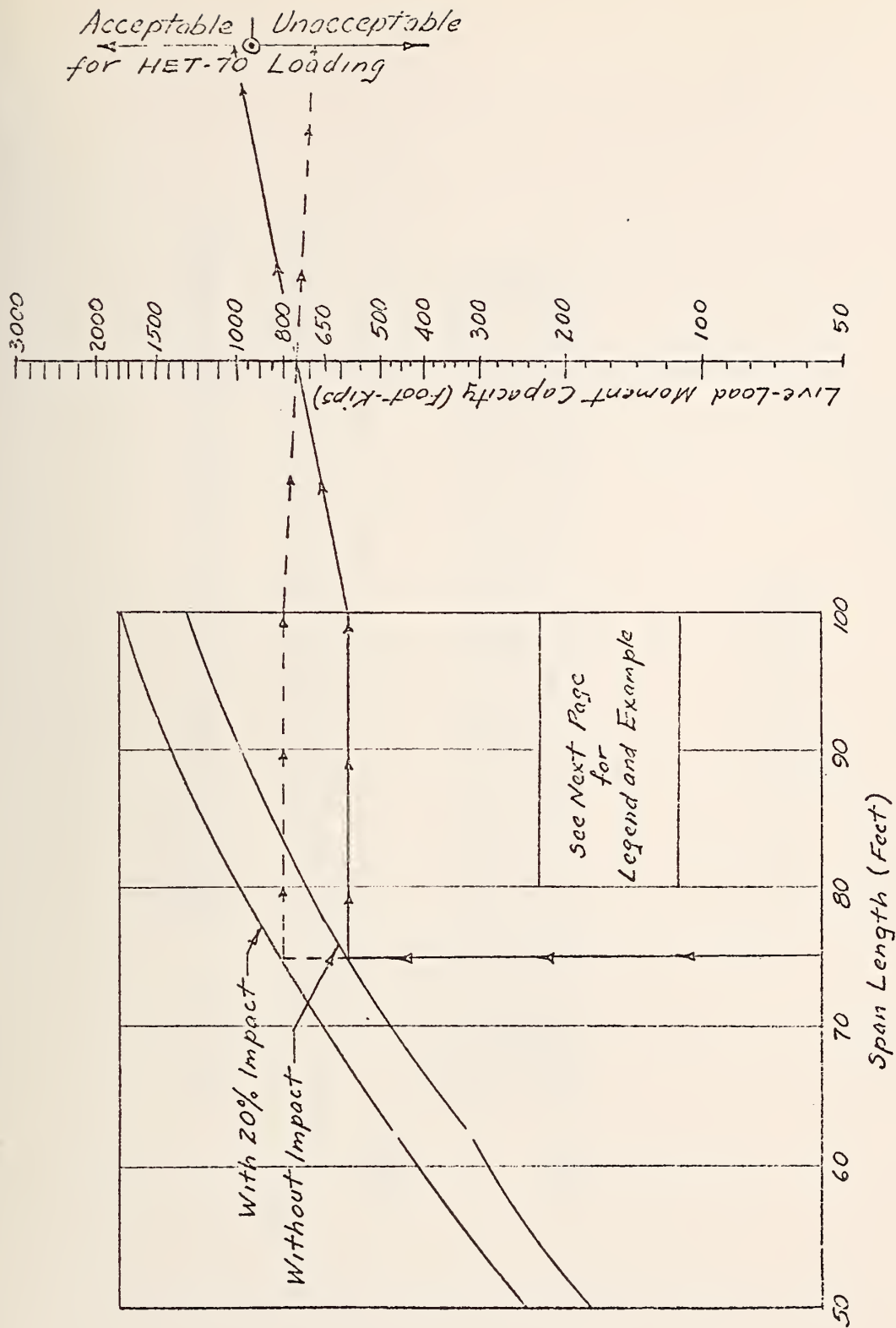
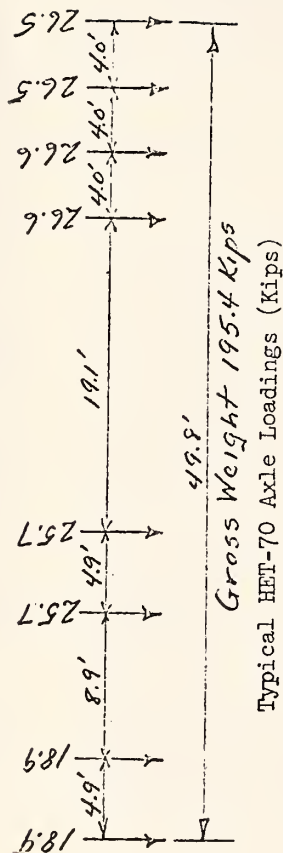


FIG. B-20 - HET-70 BRIDGE LOADING CAPACITY NOMOGRAPH



Legend Nomograph is designed for the case of the HET-70 tank transporter loaded to 195,400 pounds and travelling on centerline of a simple span bridge. The maximum moment caused by an individual stringer is taken as one-third the total moment caused by the HET-70 loading based on measured load distributions on four-girder bridges. The curve without impact is for crawl speed crossings and the curve with 20 percent impact is for normal speed crossings.

Example

Given: a 75-foot simple span slab and girder bridge with a live-load moment capacity of 750 foot-kips.

Solution: The Crossing of the HET-70 tank transporter on the centerline of the span at crawl speed is acceptable, and at normal speed is unacceptable.

FIG. B-21 - LEGEND AND EXAMPLE FOR HET-70 BRIDGE LOADING CAPACITY
NOMOGRAPH

APPENDIX C

Details of Computer Input Data and Load Conditions

APPENDIX C

Details of Computer Input Data and Load Conditions

1. General

To move the HET-70 live load along the bridge without having to reconstruct a new set of coordinates for each load condition, a five foot interval of spacing was used between nodes along bridges 1 and 4, and as close to a five foot interval of spacing as possible along skew bridges 2 and 3. The interval of spacing in bridges 2 and 3 was adjusted to accommodate the location of the intermediate diaphragms. The format for data input follows exactly the same procedures as described in Volume I. Multiple load conditions were used for each run to save computer time since only the applied load side of the equilibrium equations needs to be reset for each load condition.

2. Bridge #1

Figure C-1 shows the coordinate location of nodes used for bridge #1 for the HET-70 loading. Because of the symmetry of the bridge, and the fact that the HET-70 loading would be located along the centerline of the bridge, the input data was materially reduced by treating the bridge as one-half of a bridge with prescribed boundary conditions along the longitudinal centerline. For example, at node 6 the slope of both the deck and the diaphragm must equal zero for symmetry of loading and symmetry of bridge. This is accomplished by putting a number 1 in column 25 of the input data card prescribing the boundary conditions for these nodes. Also note that there is no physical length between node 7 and node 6; hence, these nodes are treated as ends of cantilevers that cannot rotate but can move vertically. Figure C-2 shows the cross section of the half section of the bridge. Figure C-3 shows a portion of the input data that will explain the format for the boundary condition code. Figure C-4 shows the beam numbering and diaphragm numbering for bridge #1. Notice that the diaphragms do not exist at every 5' intervals, whereas the double node numbering has been continued along the 5' intervals. This is so that an automatic grid system can be set up for the length of the bridge at the beginning of a program and the diaphragm locations changed by merely connecting the correct nodes. The nodes that are unconnected, like for example nodes 14 and 21, will not effect the computer program at all; except that in order to reduce the number of equations to be solved and hence the CPU time involved, all six boundary condition codes were fixed with a number 1 for these nodes. This

eliminates these nodes from the program as long as they are unconnected to any portion of the bridge, and no physical significance is thus attached to them. Figure C-5 shows the plate shell numbering for the slab of bridge #1.

The following 5 figures, Figure C-6 through Figure C-10, depict the loading conditions for the input data for the HET-70. Figure C-6 identifies the location of the HET-70 near the center of the interior 90' span from which the data of Table 1 was calculated. The HET-70 is traveling from left to right on the bridge.

Bridge #1 has an 8.33' c.c. distance between longitudinal girders. Since the transverse distance between the wheels of the transporter is 8.5', it was reasonable to assume that the wheels would practically ride on the interior girders. Therefore, no moment distribution was necessary to distribute the wheel loads transversely to the girders. Figure C-6 shows the actual location of the wheel points and loads on the girder. For the input data the wheel loads are distributed as simple beam reactions to the nearest node points at the 5' intervals along the girder. Figure C-11 shows the load data input for bridge #1 for all loading conditions. *Notice when inputting load data that the node points must be in node sequence. The load condition number is the second sequence to be considered when multiple loads exist at the same node for different load conditions.* The remaining HET-70 load conditions are identified in Figures C-7 through C-10, with the direction of travel indicated by the schematic of the HET-70 transporter on the diagrams. Figure C-12 is the same static load condition used for Volume I. It was merely included to observe what the difference might be in results by inputting the concentrated loads to their nearest 5' interval node points. Figure C-8 or C-10 is expected to give the load condition transferring the maximum shear to the interior girders in the 90' spans.

3. Bridge #2

Bridge #2 has an 8.6' c.c. distance between girders. This is also close enough to 8.5' so that no transverse distribution need be done to distribute a part of the wheel loads to the outside girders. For the sake of locating node points along the girders, **coordinates are printed in the background to Figures C-16 through C-19.** The only new consideration here is that it is possible to use a simple beam criteria for placing the wheel loads on one of the interior girders to produce the absolute maximum moment in that girder. The criteria is that "the centerline of the girder shall split the distance between the center of gravity

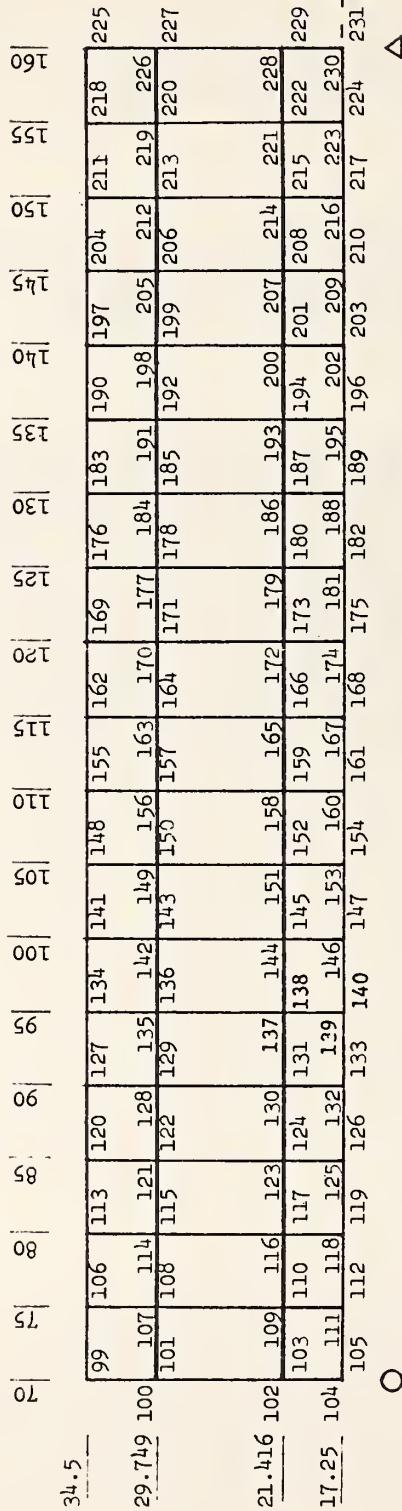
of the wheel loads actually **on** the girder and the wheel load in question that will likely be at the maximum moment position." For the load conditions shown for bridge #2 for the HET-70 loading the transporter is moving from right to left for some runs and left to right for others.

4. Bridge #3

Figures C-20 through C-26 are self-explanatory and follow the identical format for bridge #2.

5. Bridge #4

The format for bridge #4 is identical to the format of bridge #1. Because of dissymmetry of static loading it is not possible to use only half of this bridge to reduce the nodal point data input and CPU time for the static loading. Fortunately the static loading is already contained in Volume I; therefore, for convenience the bridge was reduced to a half bridge for inputting the effect of the HET-70 loading. There is no experimental data with which to correlate the results on this bridge. The information is merely to complete the report with respect to all four bridges. Figures C-27 through C-33 are self-explanatory.



NOTE: When two numbers exist at a node, the rightmost number is at the node at the center of gravity elevation of the stringers.

FIG. C-1 - COORDINATE LOCATION OF NODES USED FOR BRIDGE #1 FOR MILITARY LOADING

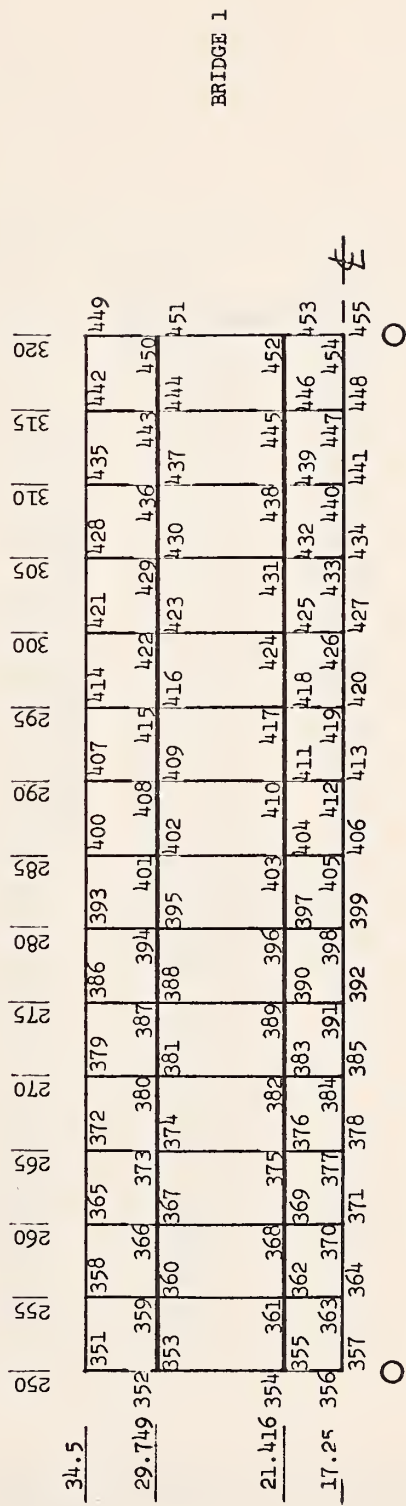
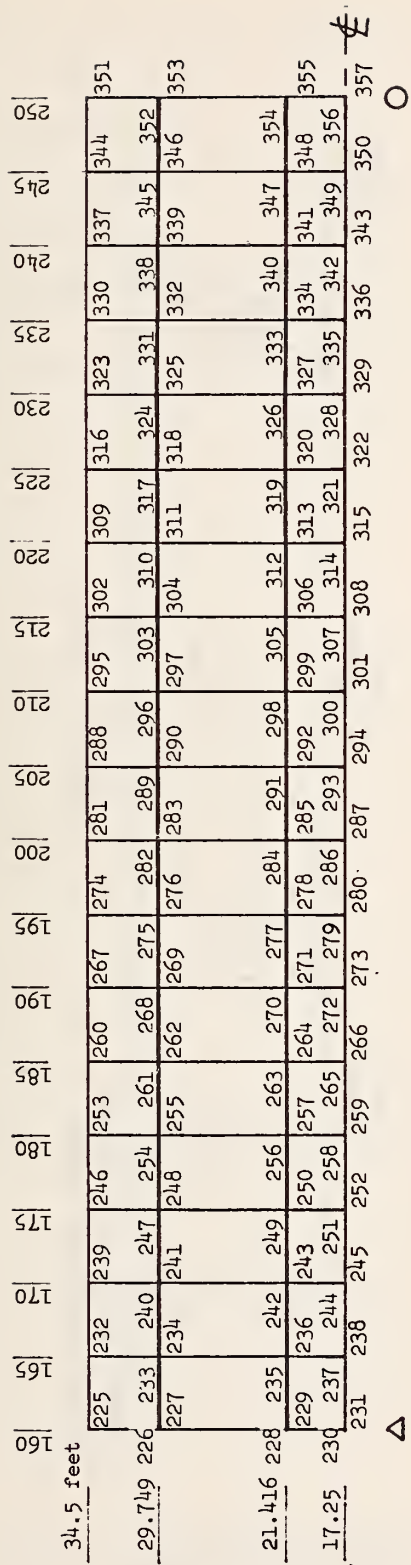
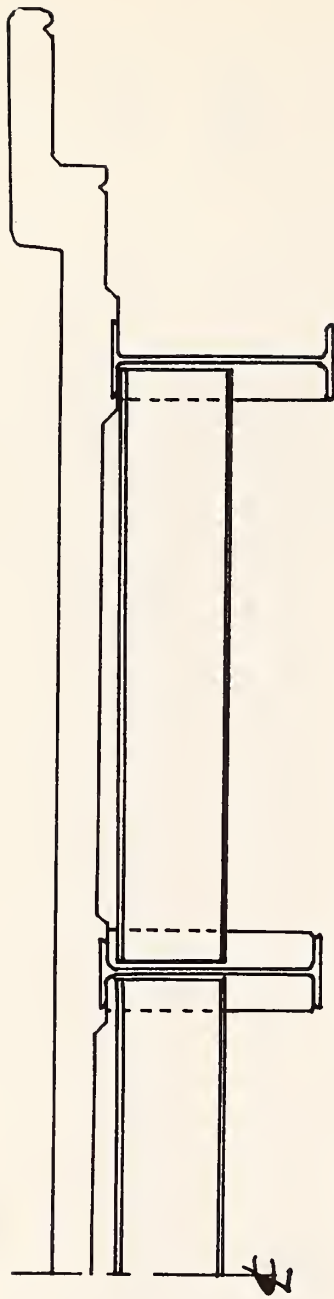
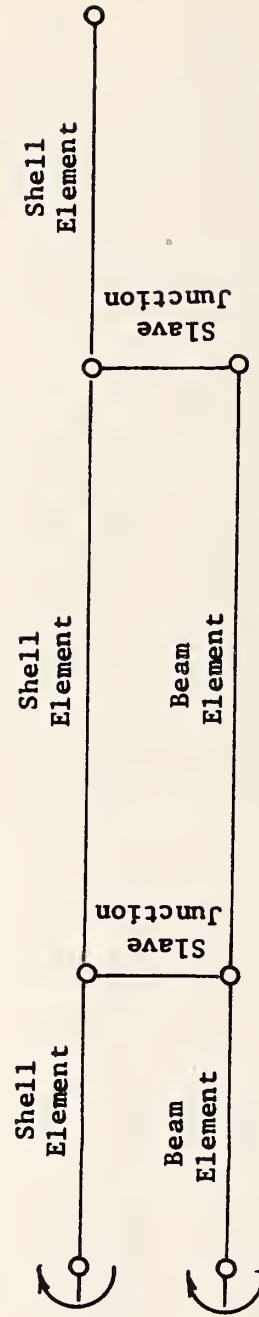


Fig. C-1 Continued.



HALF SECTION OF BRIDGE #1.



Moment restraint but no
translation restraint

COMPUTER MODEL

FIG. C-2 - HALF CROSS SECTION OF BRIDGE NO. 1 WITH
BOUNDARY CONDITIONS ALONG CENTERLINE

****BRIDGE NO. 1 WITH MILITARY LOADING HET-70**

NUMBER OF NODAL POINTS = 455

NUMBER OF ELEMENT TYPES = 2

NUMBER OF LOAD CASES = 6

NODAL POINT INPUT DATA

NODE NUMBER	BOUNDARY CONOITION CODES						NODAL POINT COORDINATES				
	X	Y	Z	XX	YY	ZZ	X	Y	Z	T	
1	0	0	0	0	0	1	0.0	34.500	1.874	0	0.0
2	0	1	1	1	0	1	0.0	29.749	1.874	0	0.0
3	2	2	2	2	2	2	0.0	29.749	0.0	0	0.0
4	0	1	1	1	0	1	0.0	21.416	1.874	0	0.0
5	4	4	4	4	4	4	0.0	21.416	0.0	0	0.0
6	0	0	0	1	0	1	0.0	17.250	1.874	0	0.0
7	0	0	0	1	0	1	0.0	17.250	0.0	0	0.0
8	0	0	0	0	0	1	5.000	34.500	1.874	0	0.0
9	0	0	0	0	0	1	5.000	29.749	1.874	0	0.0
10	9	9	9	9	9	9	5.000	29.749	0.0	0	0.0
11	0	0	0	0	0	1	5.000	21.416	1.874	0	0.0
12	11	11	11	11	11	11	5.000	21.416	0.0	0	0.0
13	0	0	0	1	0	1	5.000	17.250	1.874	0	0.0
14	1	1	1	1	1	1	5.000	17.250	0.0	0	0.0
15	0	0	0	0	0	1	10.000	34.500	1.874	0	0.0
16	0	0	0	0	0	1	10.000	29.749	1.874	0	0.0
17	16	16	16	16	16	16	10.000	29.749	0.0	0	0.0
18	0	0	0	0	0	1	10.000	21.416	1.874	0	0.0
19	18	18	18	18	18	18	10.000	21.416	0.0	0	0.0
20	0	0	0	1	0	1	10.000	17.250	1.874	0	0.0
21	1	1	1	1	1	1	10.000	17.250	0.0	0	0.0
22	0	0	0	0	0	1	15.000	34.500	1.874	0	0.0
23	0	0	0	0	0	1	15.000	29.749	1.874	0	0.0
24	23	23	23	23	23	23	15.000	29.749	0.0	0	0.0
25	0	0	0	0	0	1	15.000	21.416	1.874	0	0.0
26	25	25	25	25	25	25	15.000	21.416	0.0	0	0.0
27	0	0	0	1	0	1	15.000	17.250	1.874	0	0.0
28	1	1	1	1	1	1	15.000	17.250	0.0	0	0.0
29	0	0	0	0	0	1	20.000	34.500	1.874	0	0.0
30	0	0	0	0	0	1	20.000	29.749	1.874	0	0.0
31	30	30	30	30	30	30	20.000	29.749	0.0	0	0.0
32	0	0	0	0	0	1	20.000	21.416	1.874	0	0.0
33	32	32	32	32	32	32	20.000	21.416	0.0	0	0.0
34	0	0	0	1	0	1	20.000	17.250	1.874	0	0.0
35	1	1	1	1	1	1	20.000	17.250	0.0	0	0.0
36	0	0	0	0	0	1	25.000	34.500	1.874	0	0.0
37	0	0	0	0	0	1	25.000	29.749	1.874	0	0.0
38	37	37	37	37	37	37	25.000	29.749	0.0	0	0.0
39	0	0	0	0	0	1	25.000	21.416	1.874	0	0.0
40	39	39	39	39	39	39	25.000	21.416	0.0	0	0.0
41	0	0	0	1	0	1	25.000	17.250	1.874	0	0.0
42	0	0	0	1	0	1	25.000	17.250	0.0	0	0.0
43	0	0	0	0	0	1	30.000	34.500	1.874	0	0.0
44	0	0	0	0	0	1	30.000	29.749	1.874	0	0.0
45	44	44	44	44	44	44	30.000	29.749	0.0	0	0.0
46	0	0	0	0	0	1	30.000	21.416	1.874	0	0.0
47	46	46	46	46	46	46	30.000	21.416	0.0	0	0.0
48	0	0	0	1	0	1	30.000	17.250	1.874	0	0.0
49	1	1	1	1	1	1	30.000	17.250	0.0	0	0.0
50	0	0	0	0	0	1	35.000	34.500	1.874	0	0.0
51	0	0	0	0	0	1	35.000	29.749	1.874	0	0.0

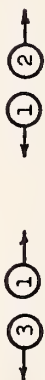
FIG C-3 - SAMPLE NODAL INPUT DATA FOR BRIDGE # 1, ILLUSTRATING BOUNDARY CONDITION CODES FOR 1/2 SECTION OF BRIDGE.

Beam Material Number



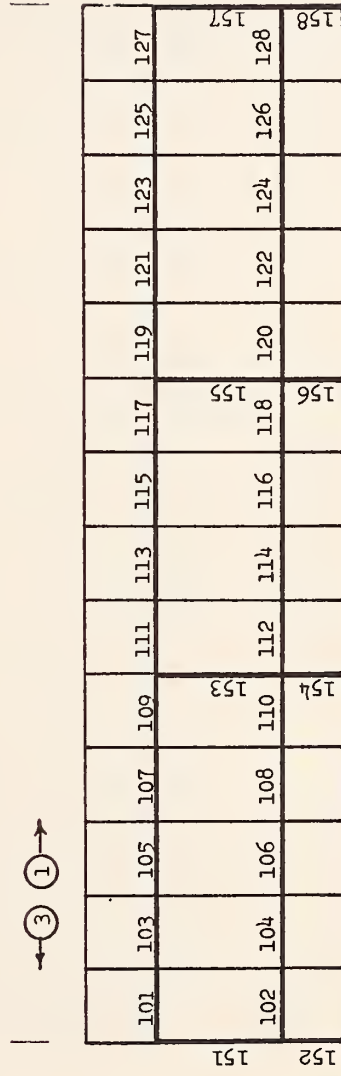
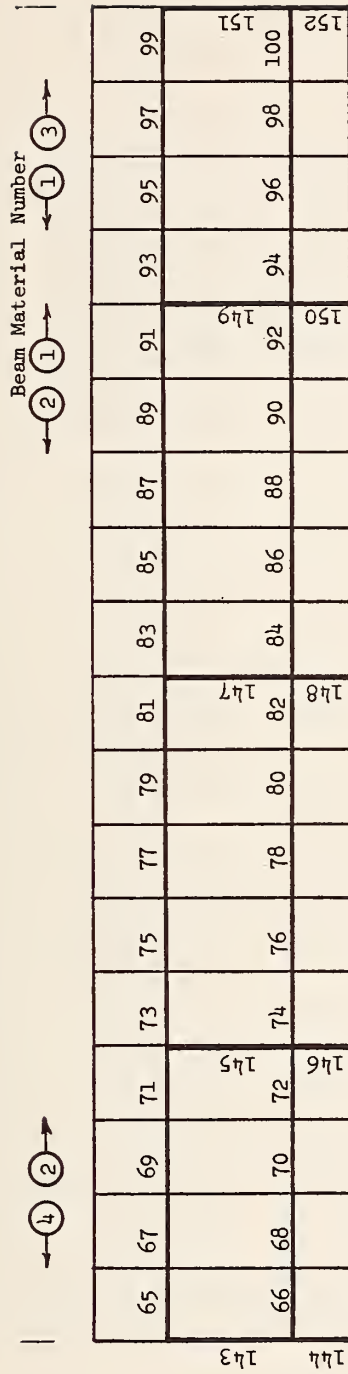
1	3	5	7	9	11	13	15	17	19	21	23	25	27	136
2	4	6	8	10	12	14	16	18	20	22	24	26	28	135
														134
														133
														132
														131
														130
														129

BRIDGE 1



29	31	33	35	37	39	41	43	45	47	49	51	53	55	57	59	61	63	147
30	32	34	36	38	40	42	44	46	48	50	52	54	56	58	60	62	64	146
																		145
																		144
																		143
																		142
																		141
																		140
																		139
																		138
																		137
																		136

FIG. C-4 - BEAM AND DIAPHRAGM NUMBERING FOR BRIDGE #1 FOR MILITARY LOADINGS



BRIDGE 1

Fig. C-4 Continued.

1	4	7	10	13	16	19	22	25	28	31	34	37	40
2	5	8	11	14	17	20	23	26	29	32	35	38	41
3	6	9	12	15	18	21	24	27	30	33	36	39	42

BRIDGE 1

43	46	49	52	55	58	61	64	67	70	73	76	79	82	85	88	91	94
44	47	50	53	56	59	62	65	68	71	74	77	80	83	86	89	92	95
45	48	51	54	57	60	63	66	69	72	75	78	81	84	87	90	93	96

FIG. C-5 - PLATE SHELL NUMBERING FOR SLAB OF BRIDGE #1 FOR MILITARY LOADING

97	100	103	106	109	112	115	118	121	124	127	130	133	136	139	142	145	148
98	101	104	107	110	113	116	119	122	125	128	131	134	137	140	143	146	149
99	102	105	108	111	114	117	120	123	126	129	132	135	138	141	144	147	150

O

Δ

C-11

151	154	157	160	163	166	169	172	175	178	181	184	187	190
152	155	158	161	164	167	170	173	176	179	182	185	188	191
153	156	159	162	165	168	171	174	177	180	183	186	189	192

BRIDGE 1

O

O

Fig. C-5 Continued.

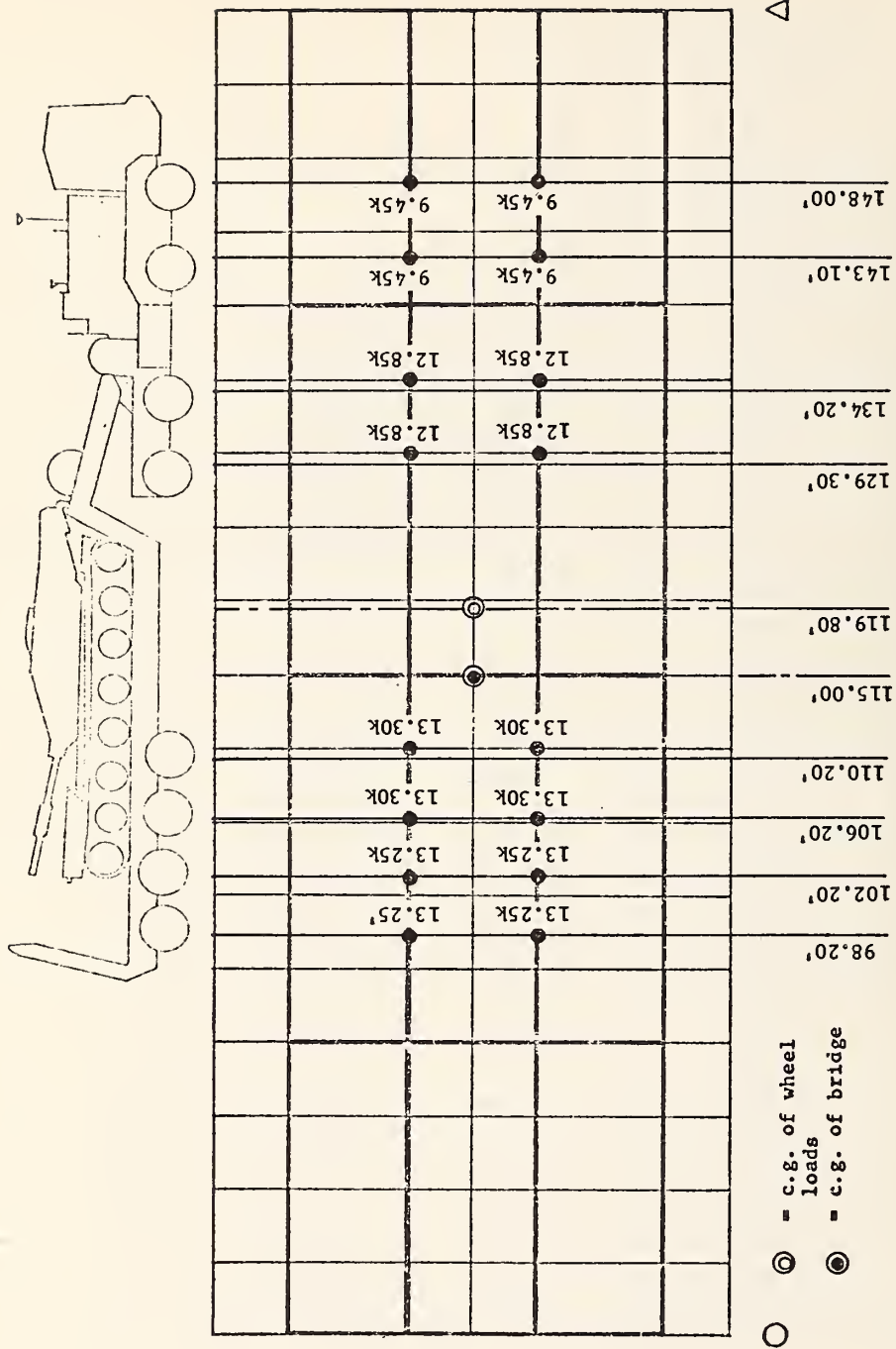


FIG. C-6 - LOAD CONDITION 1, BRIDGE 1. CENTER OF GRAVITY OF HET-70 WHEEL LOADS IN LOCATION USED TO CALCULATE THE BRIDGE MOMENT OF TABLE 1.

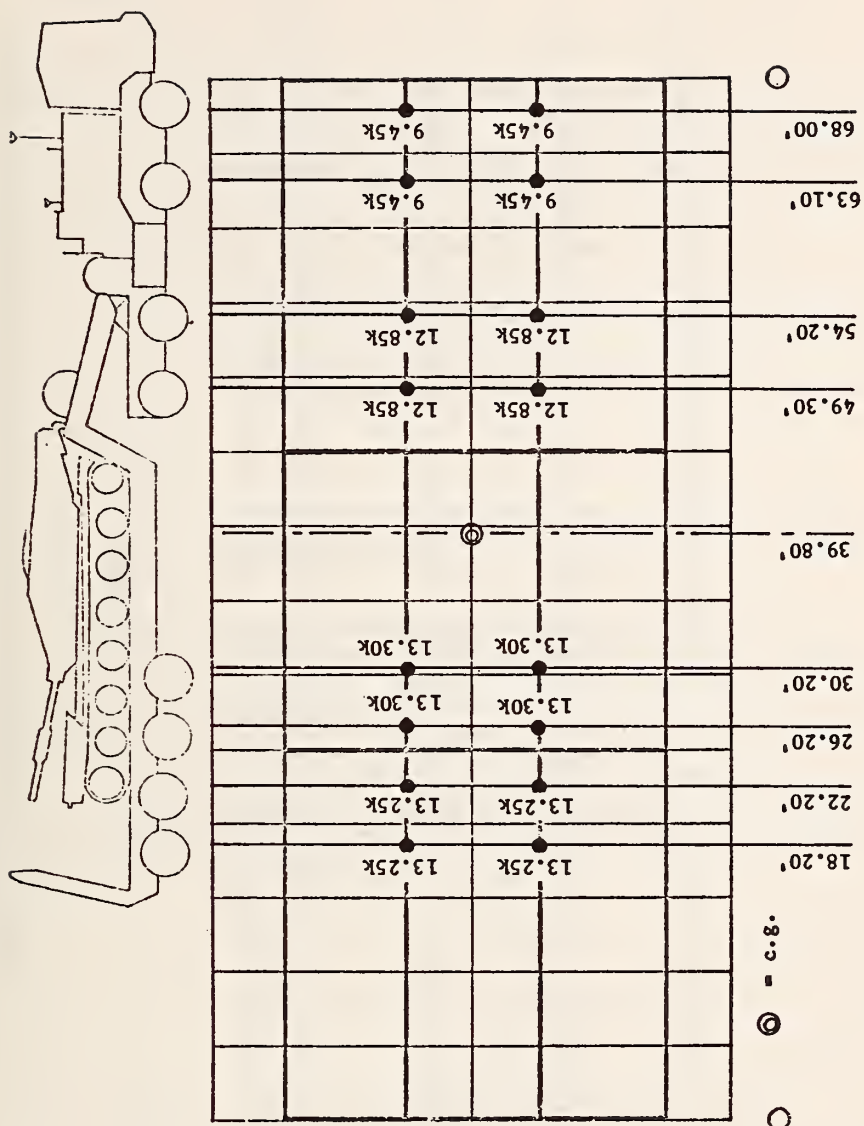


FIG. C-7 - LOAD CONDITION 2, BRIDGE 1. CENTER OF GRAVITY OF HET-70 WHEEL LOADS PLACED TO SATISFY SIMPLE BEAM CRITERIA AT CENTERLINE OF 70' SPAN.

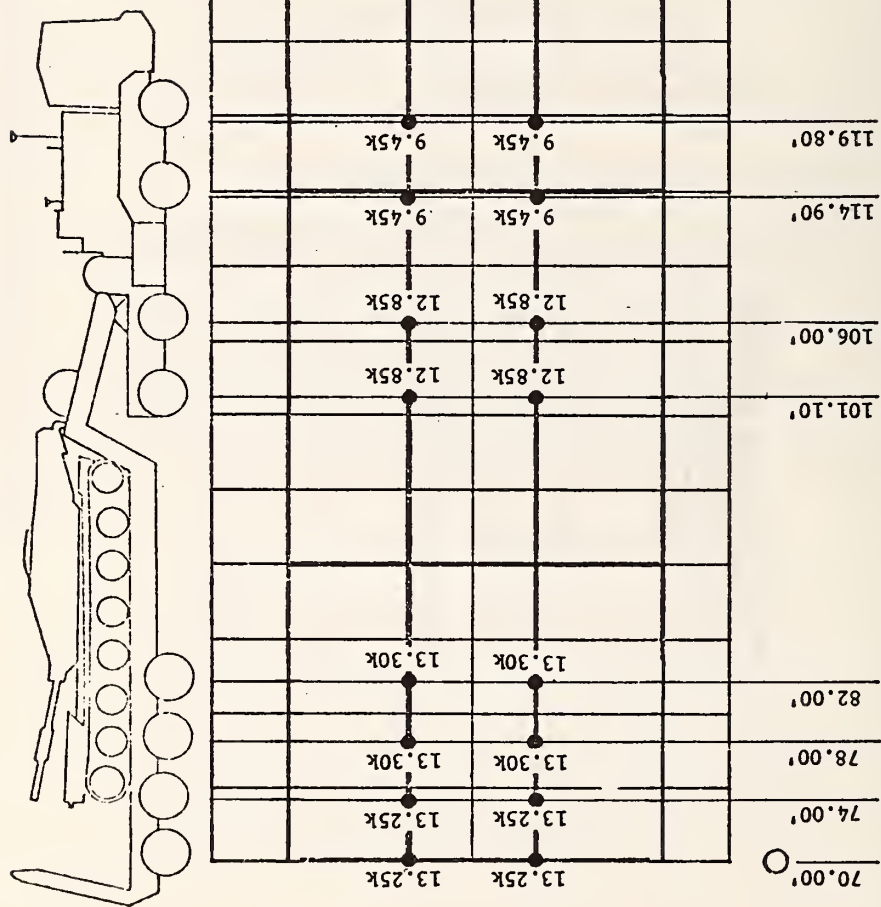


FIG. C-8. LOAD CONDITION 3, BRIDGE 1. REAR WHEEL OF TRAILER AT FIRST INTERIOR SUPPORT ON 90' SPAN.

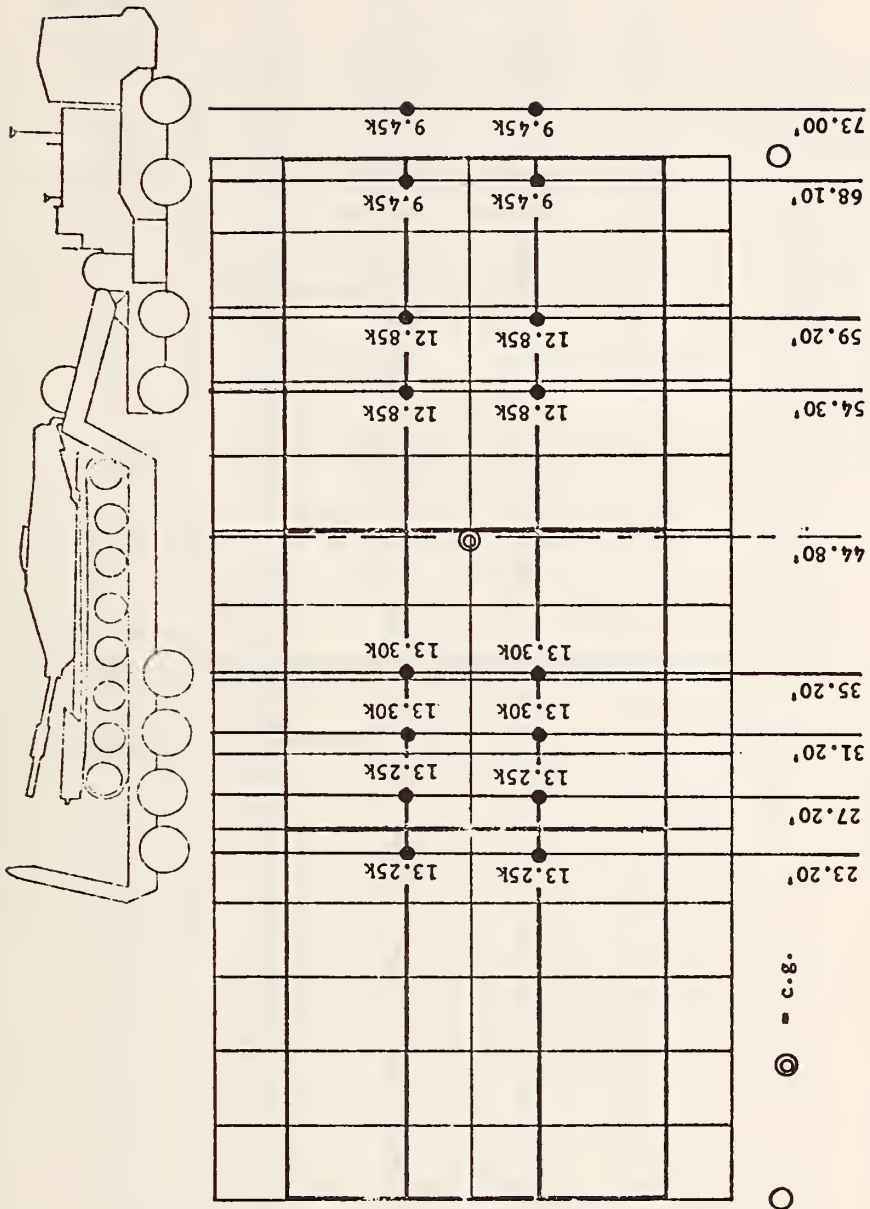


FIG. C-9 - LOAD CONDITION 4, BRIDGE 1. CENTER OF GRAVITY OF WHEEL LOADS PLACED 5' TO THE RIGHT OF LOAD CONDITION 2.

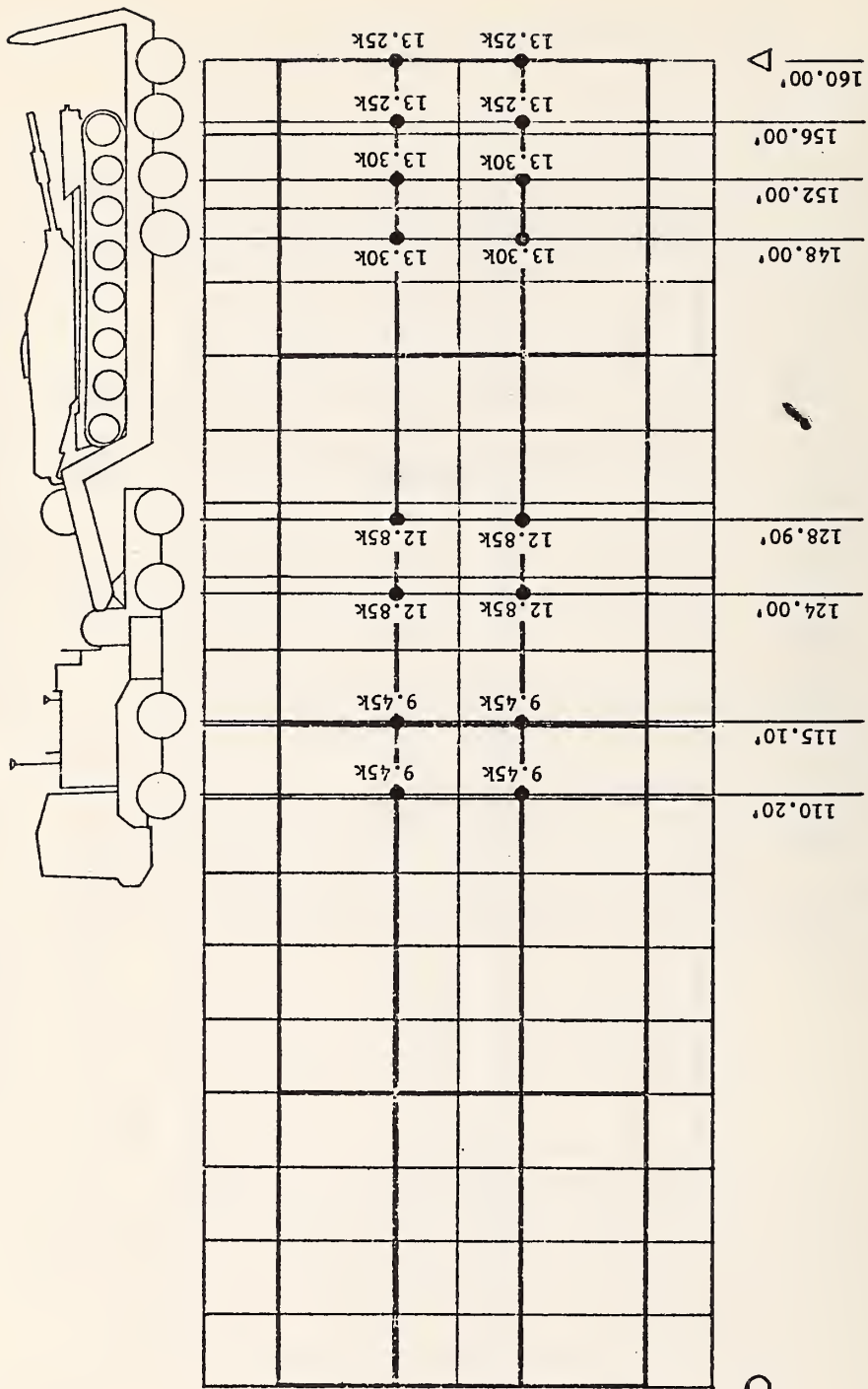


FIG. C-10. LOAD CONDITION 5, BRIDGE 1. REAR WHEEL OF TRAILER AT CENTER OF BRIDGE.

.....NODAL POINT LOADS

NODE LOAD		APPLIED LOADS					
NO.	CASE	RX	RY	RZ	MX	MY	MZ
18	2	0.0	0.0	-3.97C	0.0	0.0	0.0
25	2	0.0	0.0	-15.90C	0.0	0.0	0.0
25	4	0.0	0.0	-3.97C	0.0	0.0	0.0
32	2	0.0	0.0	-15.94C	0.0	0.0	0.0
32	4	0.0	0.0	-15.90C	0.0	0.0	0.0
39	2	0.0	0.0	-15.96C	0.0	0.0	0.0
39	4	0.0	0.0	-15.94C	0.0	0.0	0.0
46	2	0.0	0.0	-1.33C	0.0	0.0	0.0
46	4	0.0	0.0	-15.96C	0.0	0.0	0.0
53	4	0.0	0.0	-1.33C	0.0	0.0	0.0
60	2	0.0	0.0	-1.03C	0.0	0.0	0.0
67	2	0.0	0.0	-13.11C	0.0	0.0	0.0
67	4	0.0	0.0	-1.03C	0.0	0.0	0.0
74	2	0.0	0.0	-11.57C	0.0	0.0	0.0
74	4	0.0	0.0	-13.11C	0.0	0.0	0.0
81	2	0.0	0.0	-3.02C	0.0	0.0	0.0
81	4	0.0	0.0	-11.57C	0.0	0.0	0.0
88	2	0.0	0.0	-9.64C	0.0	0.0	0.0
88	4	0.0	0.0	-3.02C	0.0	0.0	0.0
95	2	0.0	0.0	-6.24C	0.0	0.0	0.0
95	4	0.0	0.0	-9.64C	0.0	0.0	0.0
102	3	0.0	0.0	-15.90C	0.0	0.0	0.0
102	4	0.0	0.0	-6.24C	0.0	0.0	0.0
109	3	0.0	0.0	-15.92C	0.0	0.0	0.0
116	3	0.0	0.0	-15.96C	0.0	0.0	0.0
123	3	0.0	0.0	-5.32C	0.0	0.0	0.0
137	1	0.0	0.0	-3.97C	0.0	0.0	0.0
142	6	0.0	0.0	-4.08C	0.0	0.0	0.0
144	1	0.0	0.0	-15.90C	0.0	0.0	0.0
144	3	0.0	0.0	-10.02C	0.0	0.0	0.0
144	6	0.0	0.0	-17.52C	0.0	0.0	0.0
149	6	0.0	0.0	-16.31C	0.0	0.0	0.0
151	1	0.0	0.0	-15.94C	0.0	0.0	0.0
151	3	0.0	0.0	-13.11C	0.0	0.0	0.0
151	6	0.0	0.0	-70.10C	0.0	0.0	0.0
158	1	0.0	0.0	-15.96C	0.0	0.0	0.0
158	3	0.0	0.0	-2.76C	0.0	0.0	0.0
158	5	0.0	0.0	-9.07C	0.0	0.0	0.0
163	6	0.0	0.0	-8.15C	0.0	0.0	0.0
165	1	0.0	0.0	-1.33C	0.0	0.0	0.0
165	3	0.0	0.0	-9.64C	0.0	0.0	0.0
165	5	0.0	0.0	-9.64C	0.0	0.0	0.0
165	6	0.0	0.0	-35.05C	0.0	0.0	0.0
170	6	0.0	0.0	-12.23C	0.0	0.0	0.0
172	3	0.0	0.0	-9.07C	0.0	0.0	0.0
172	5	0.0	0.0	-2.76C	0.0	0.0	0.0
172	6	0.0	0.0	-52.57C	0.0	0.0	0.0
179	1	0.0	0.0	-1.03C	0.0	0.0	0.0
179	5	0.0	0.0	-13.11C	0.0	0.0	0.0
186	1	0.0	0.0	-13.11C	0.0	0.0	0.0
186	5	0.0	0.0	-10.02C	0.0	0.0	0.0
193	1	0.0	0.0	-11.57C	0.0	0.0	0.0
200	1	0.0	0.0	-3.02C	0.0	0.0	0.0
207	1	0.0	0.0	-9.64C	0.0	0.0	0.0
207	5	0.0	0.0	-5.32C	0.0	0.0	0.0
214	1	0.0	0.0	-6.24C	0.0	0.0	0.0
214	5	0.0	0.0	-15.96C	0.0	0.0	0.0
221	5	0.0	0.0	-15.92C	0.0	0.0	0.0
228	5	0.0	0.0	-15.90C	0.0	0.0	0.0

STRUCTURE LOAD CASE	ELEMENT LOAD MULTIPLIERS			
	A	B	C	D
1	0.0	0.0	0.0	0.0
2	0.0	0.0	0.0	0.0
3	0.0	0.0	0.0	0.0
4	0.0	0.0	0.0	0.0
5	0.0	0.0	0.0	0.0
6	0.0	0.0	0.0	0.0

FIG. C-11 - LOAD INPUT DATA FOR BRIDGE NO. 1.

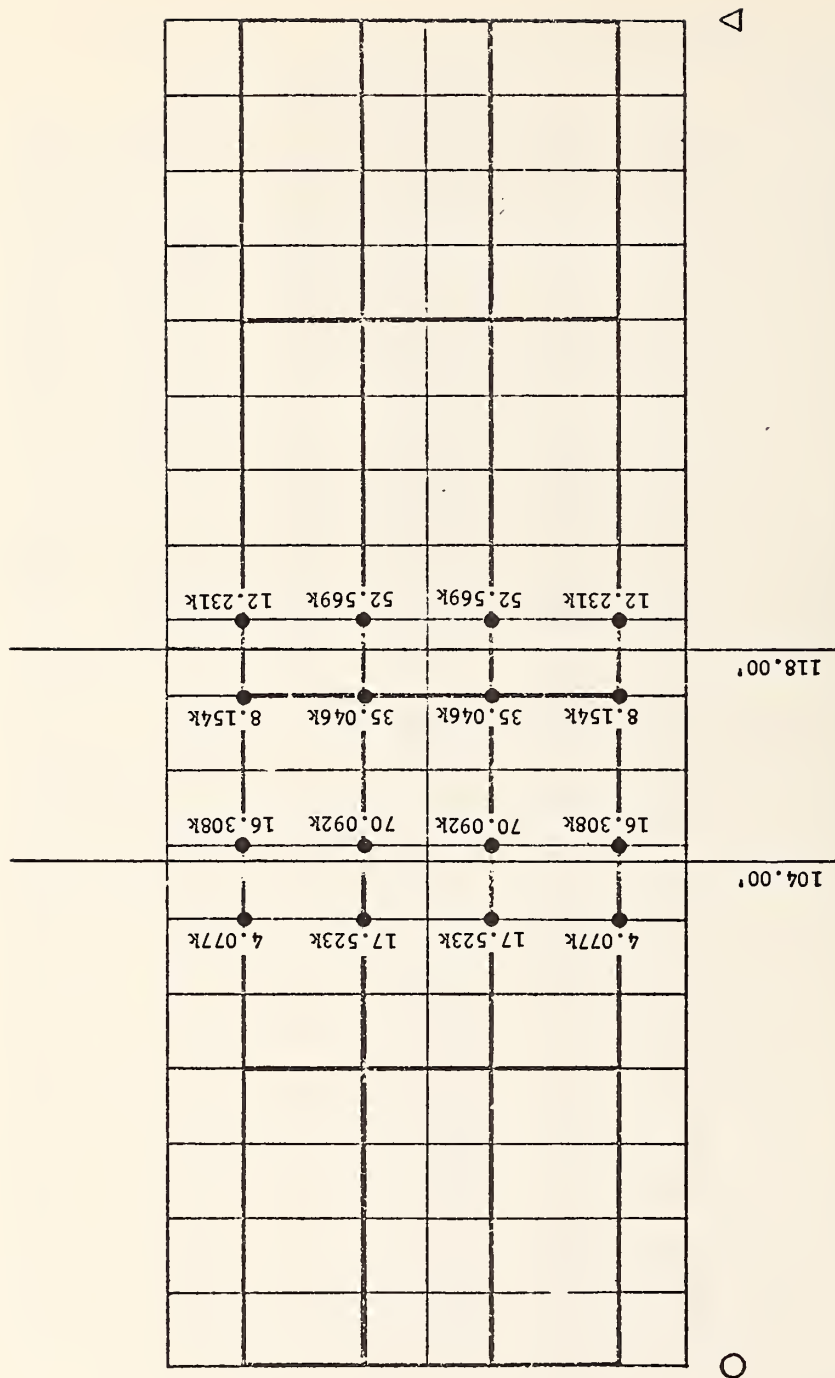


FIG. C-12. LOAD CONDITION 6, BRIDGE 1. STATIC LOADING.

FIG. C-14 - BEAM AND DIAPHRAGM NUMBERING FOR BRIDGE #2 FOR MILITARY LOADING

1	9	17	25	33	41	49	57	65	73	81	89	97	105
2	10	18	26	34	42	50	58	66	74	82	90	98	106
3	11	19	27	35	43	51	59	67	75	83	91	99	107
4	12	20	28	36	44	52	60	68	76	84	92	100	108
5	13	21	29	37	45	53	61	69	77	85	93	101	109
6	14	22	30	38	46	54	62	70	78	86	94	102	110
7	15	23	31	39	47	55	63	71	79	87	95	103	111
8	16	24	32	40	48	56	64	72	80	88	96	104	112

O

△

FIG. C-15 - PLATE SHELL NUMBERING FOR SLAB OF BRIDGE #2 FOR MILITARY LOADING

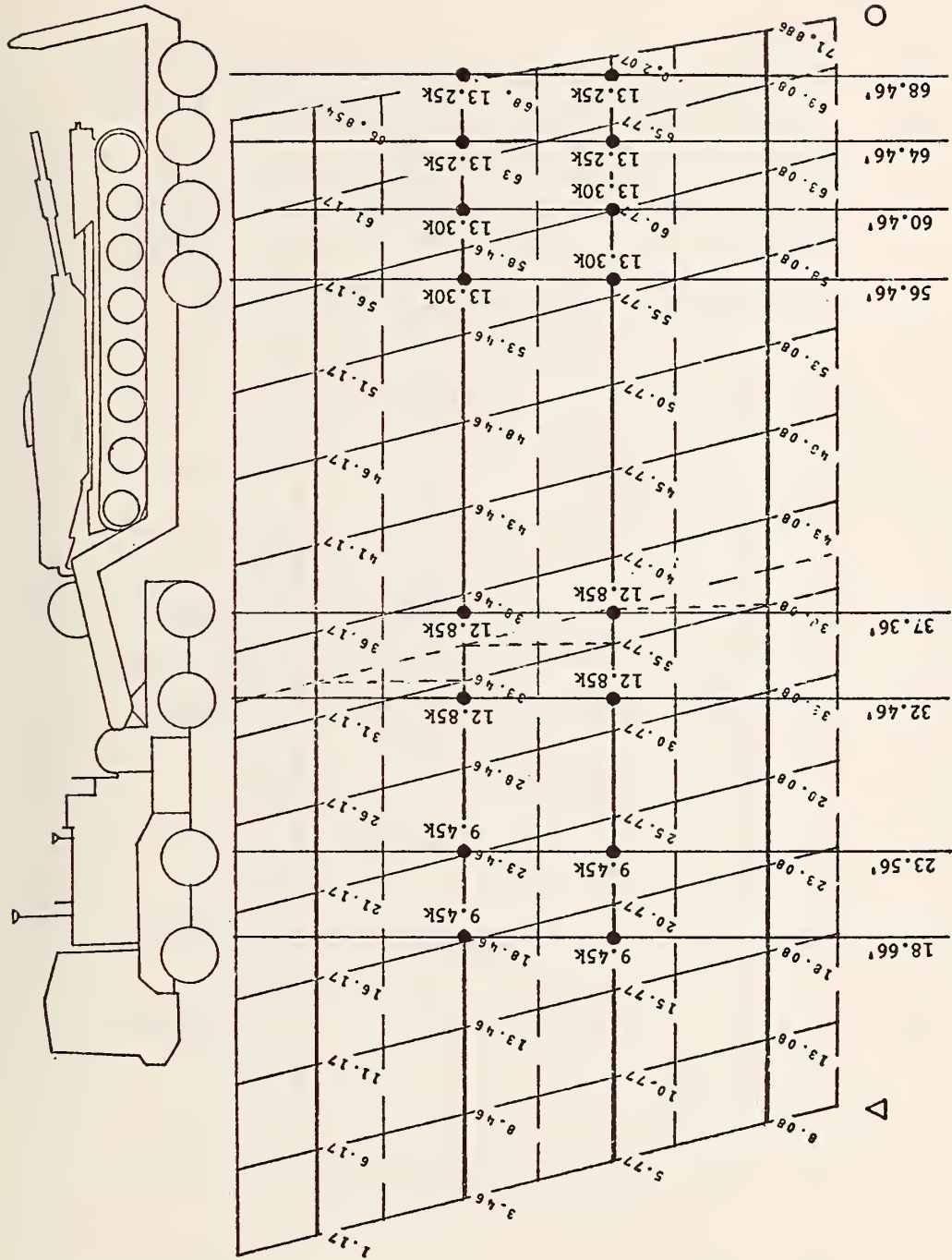
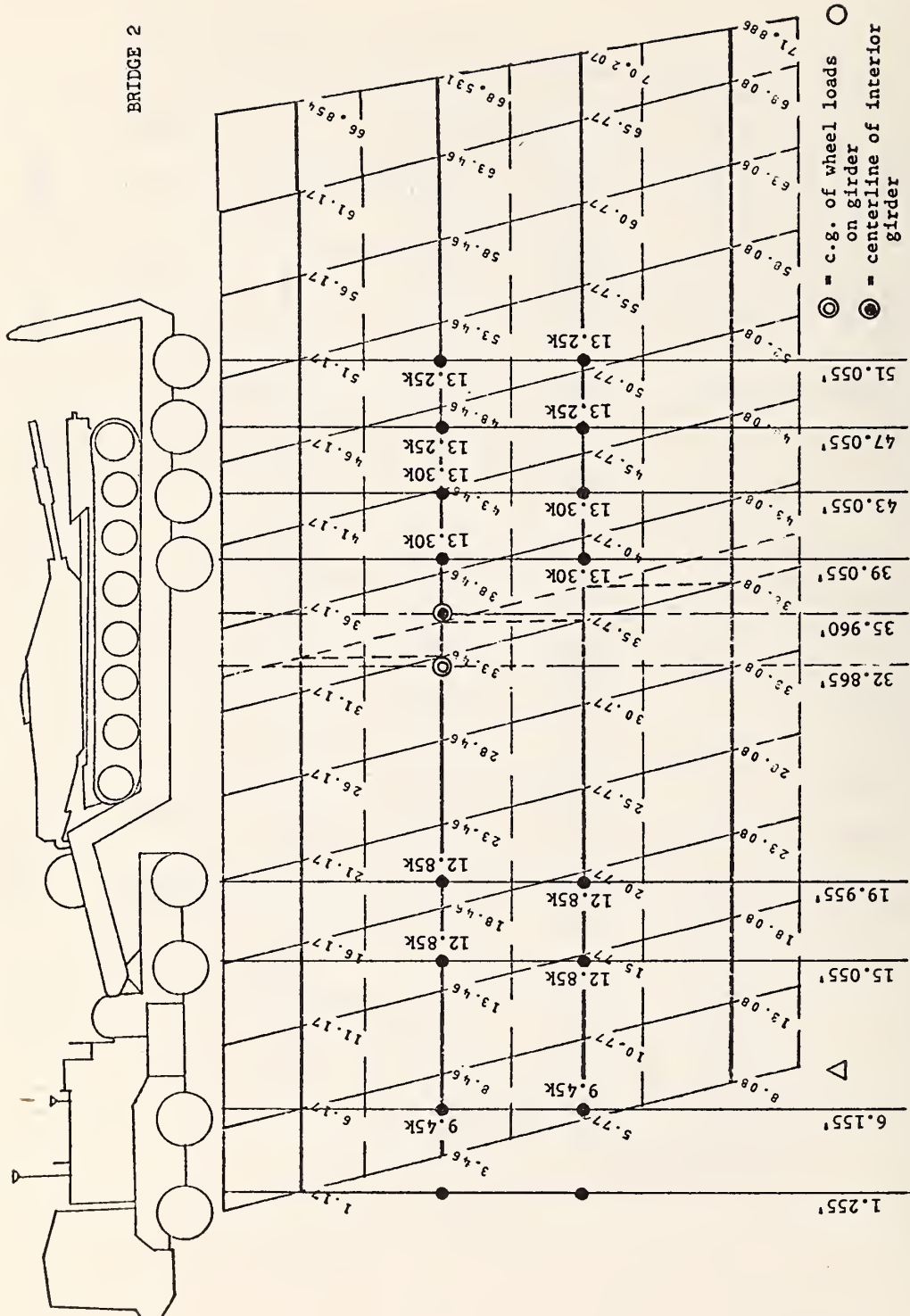


FIG. C-17. LOAD CONDITION 2, BRIDGE 2. REAR WHEEL OF TRAILER AT END OF INTERIOR GIRDER.



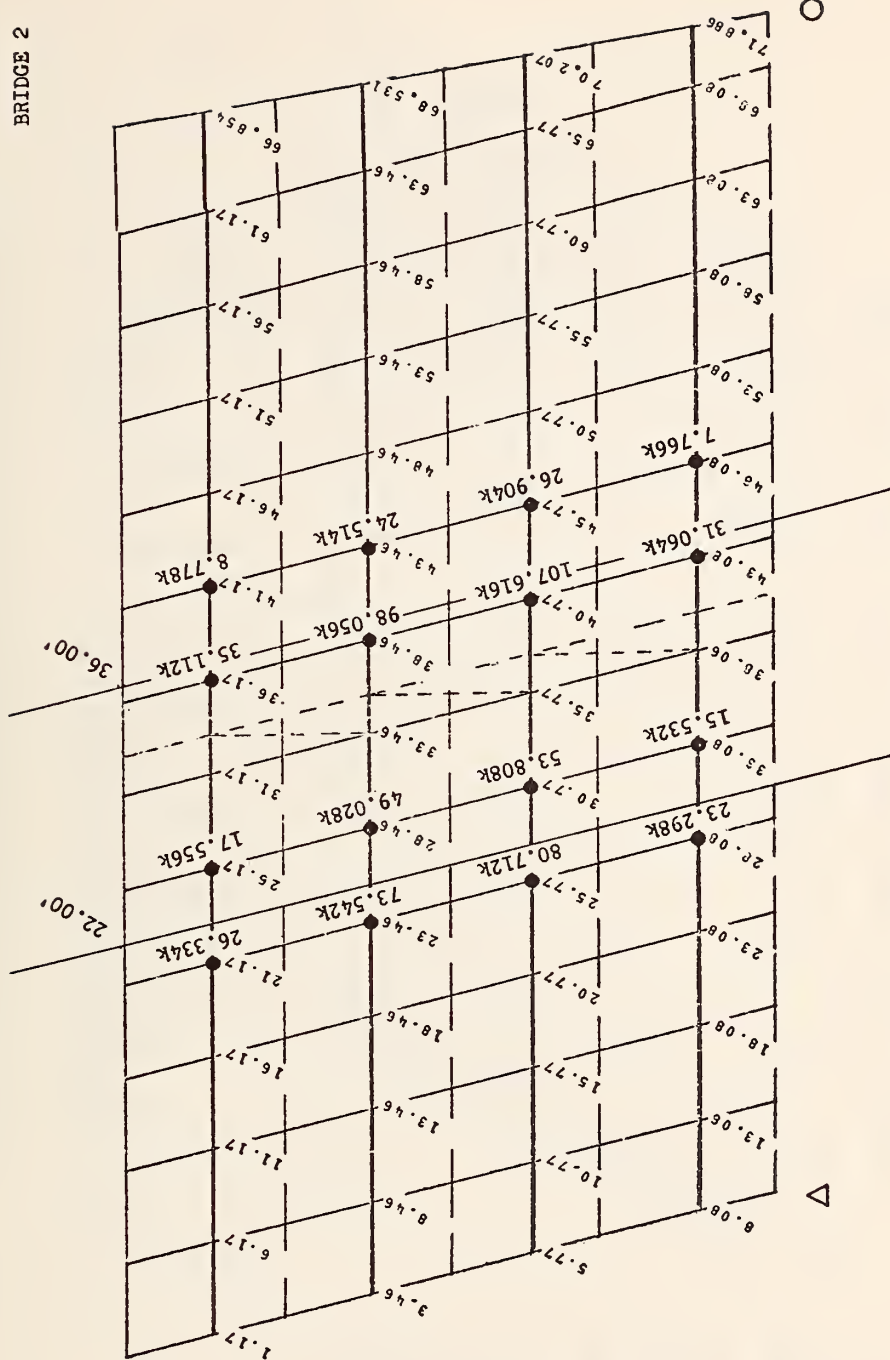


FIG. C-19. LOAD CONDITION 4, BRIDGE 2. STATIC LOADING

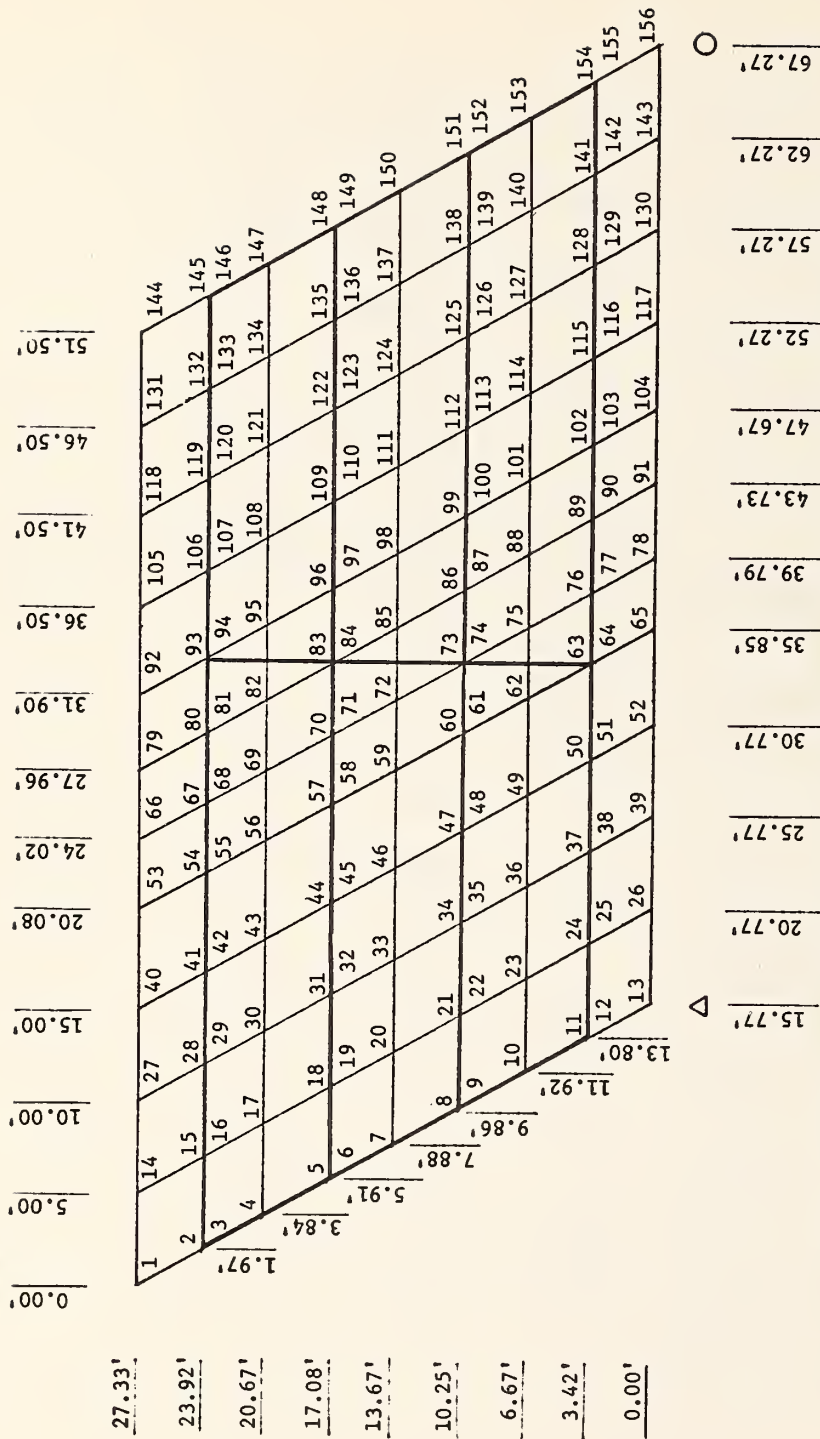


FIG. C-20 - COORDINATE LOCATION OF NODES USED FOR BRIDGE #3 FOR MILITARY LOADING

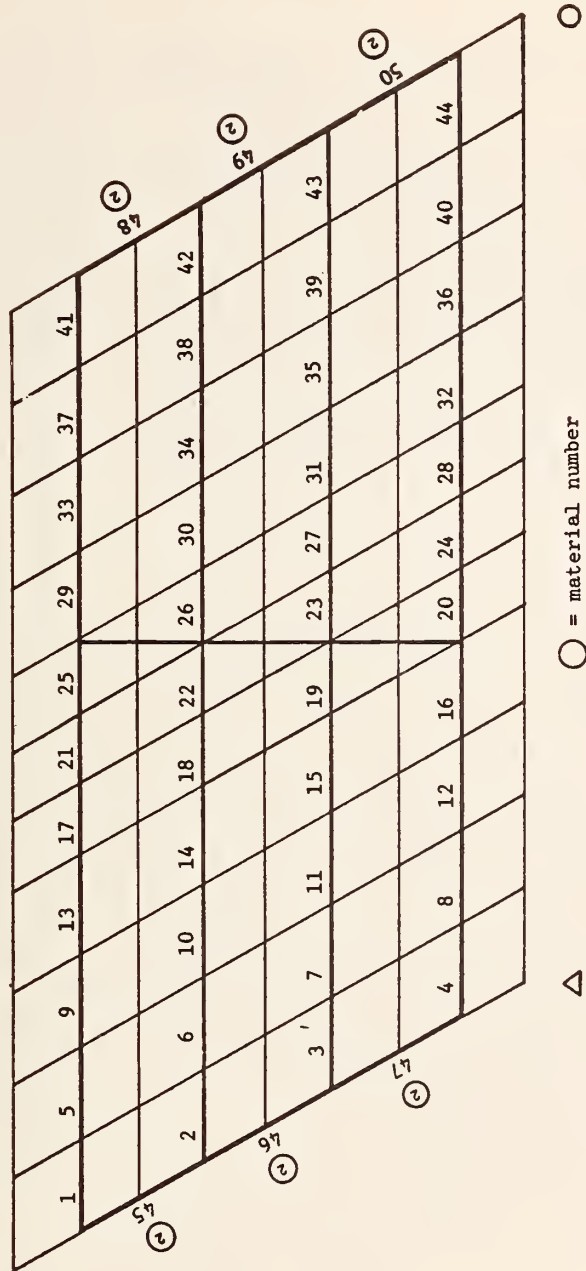


FIG. C-21 - BEAM AND DIAPHRAGM NUMBERING FOR BRIDGE #3 FOR MILITARY LOADING

1	9	17	25	33	41	49	57	65	73	81
2	10	18	26	34	42	50	58	66	74	82
3	11	19	27	35	43	51	59	67	75	83
4	12	20	28	36	44	52	60	68	76	84
5	13	21	29	37	45	53	61	69	77	85
6	14	22	30	38	46	54	62	70	78	86
7	15	23	31	39	47	55	63	71	79	87
8	16	24	32	40	48	56	64	72	80	88

○

△

FIG. C-22 - PLATE SHELL NUMBERING FOR SLAB OF BRIDGE #3 FOR MILITARY LOADING

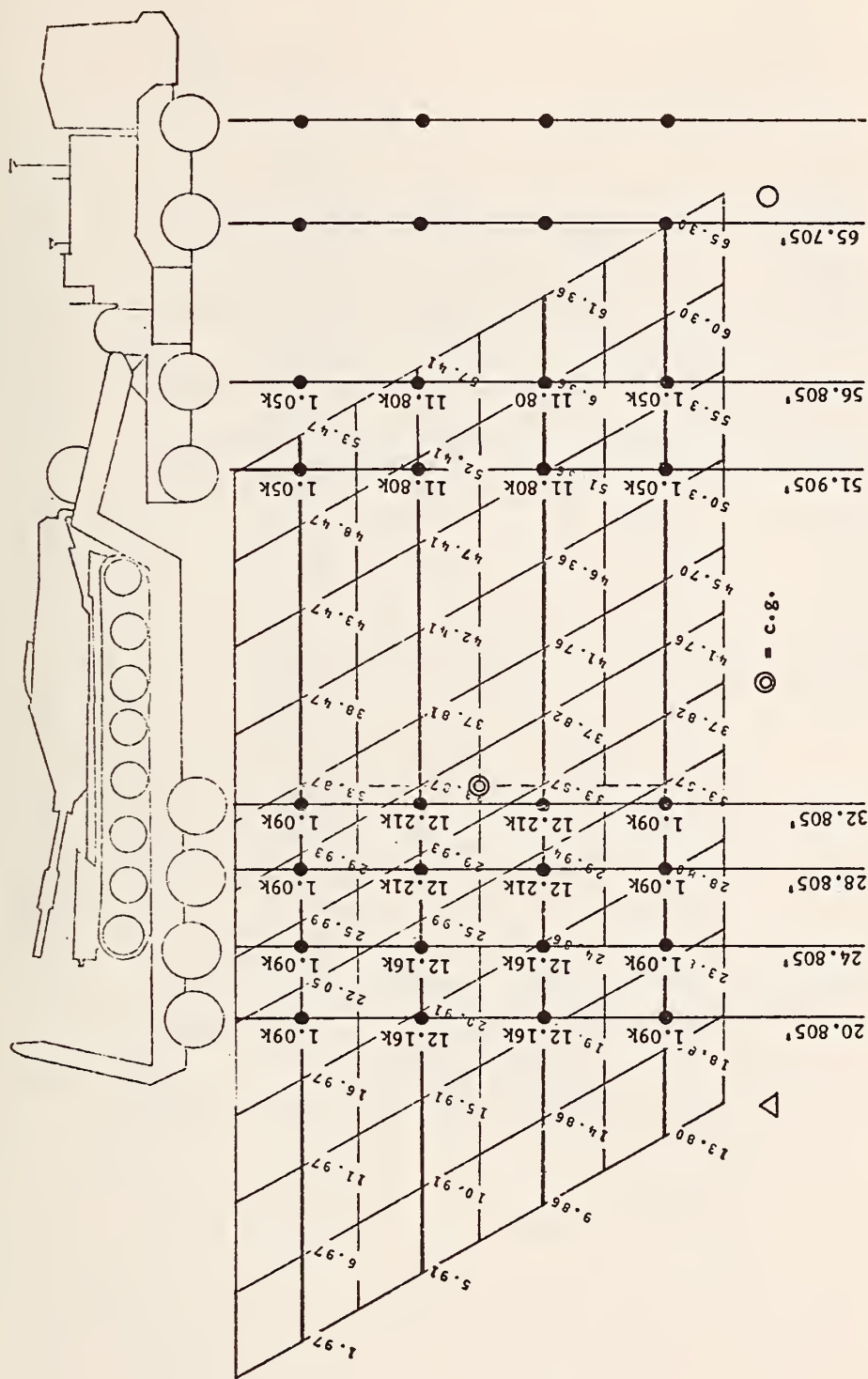


FIG. C-23 - LOAD CONDITION 1, BRIDGE 3. CENTER OF GRAVITY OF HET-70 WHEEL LOADS ON BRIDGE IN LOCATION USED TO CALCULATE THE BRIDGE MOMENT OF TABLE 1.

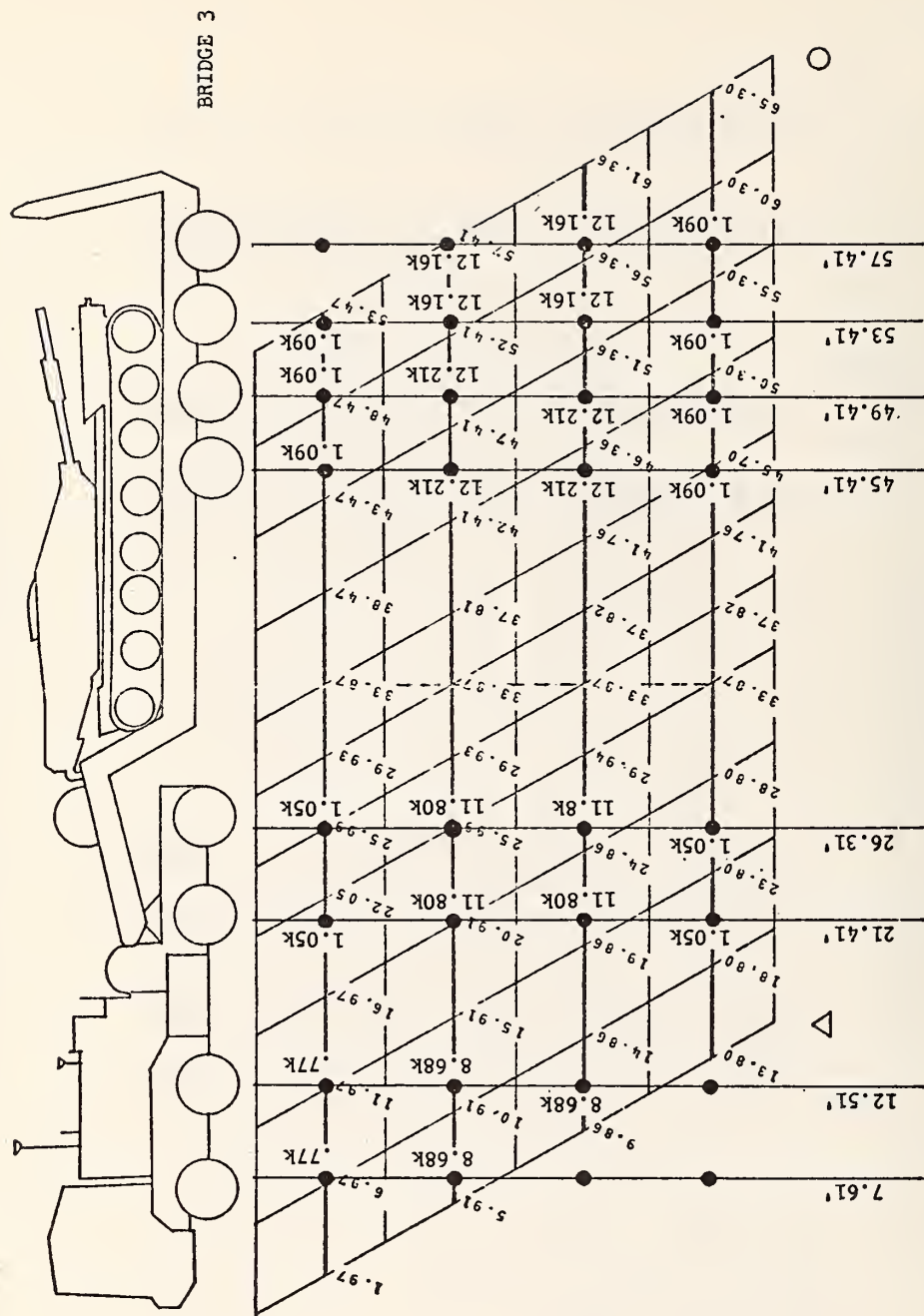


FIG. C-24. LOAD CONDITION 2, BRIDGE 3. REAR WHEEL OF TRAILER AT END OF INTERIOR GIRDER.

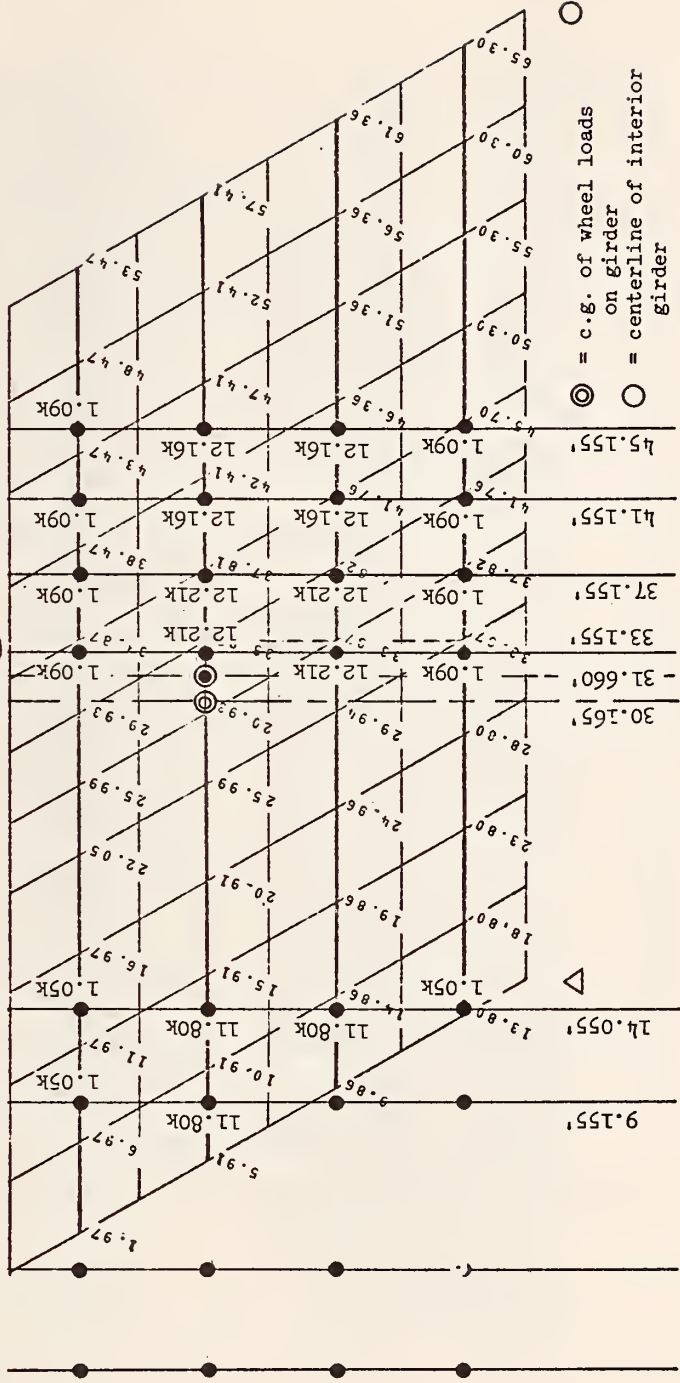


FIG. C-25. LOAD CONDITION 3, BRIDGE 3. CENTER OF GRAVITY OF HET-70 LOADS REMAINING ON INTERIOR GIRDER PLACED TO SATISFY MAXIMUM MOMENT CRITERIA FOR INTERIOR GIRDER.

BRIDGE 3

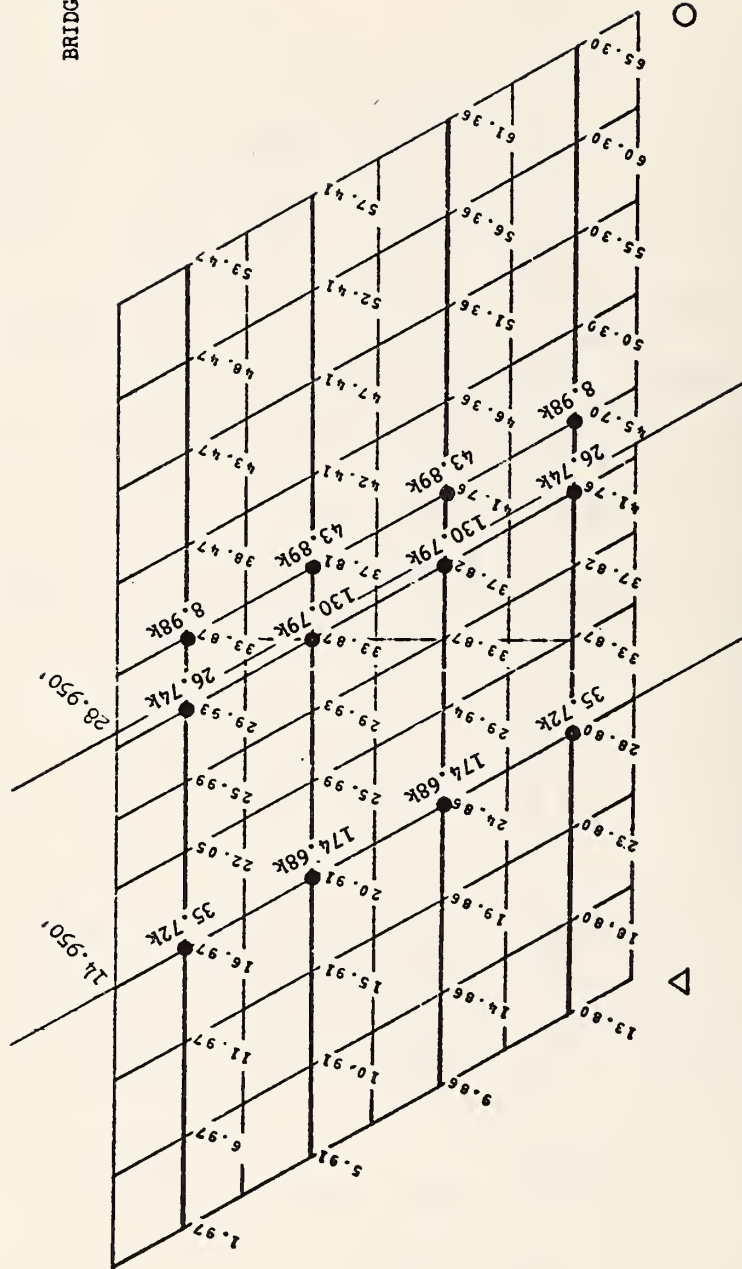


FIG. C-26. LOAD CONDITION 4, BRIDGE 3. STATIC LOADING.

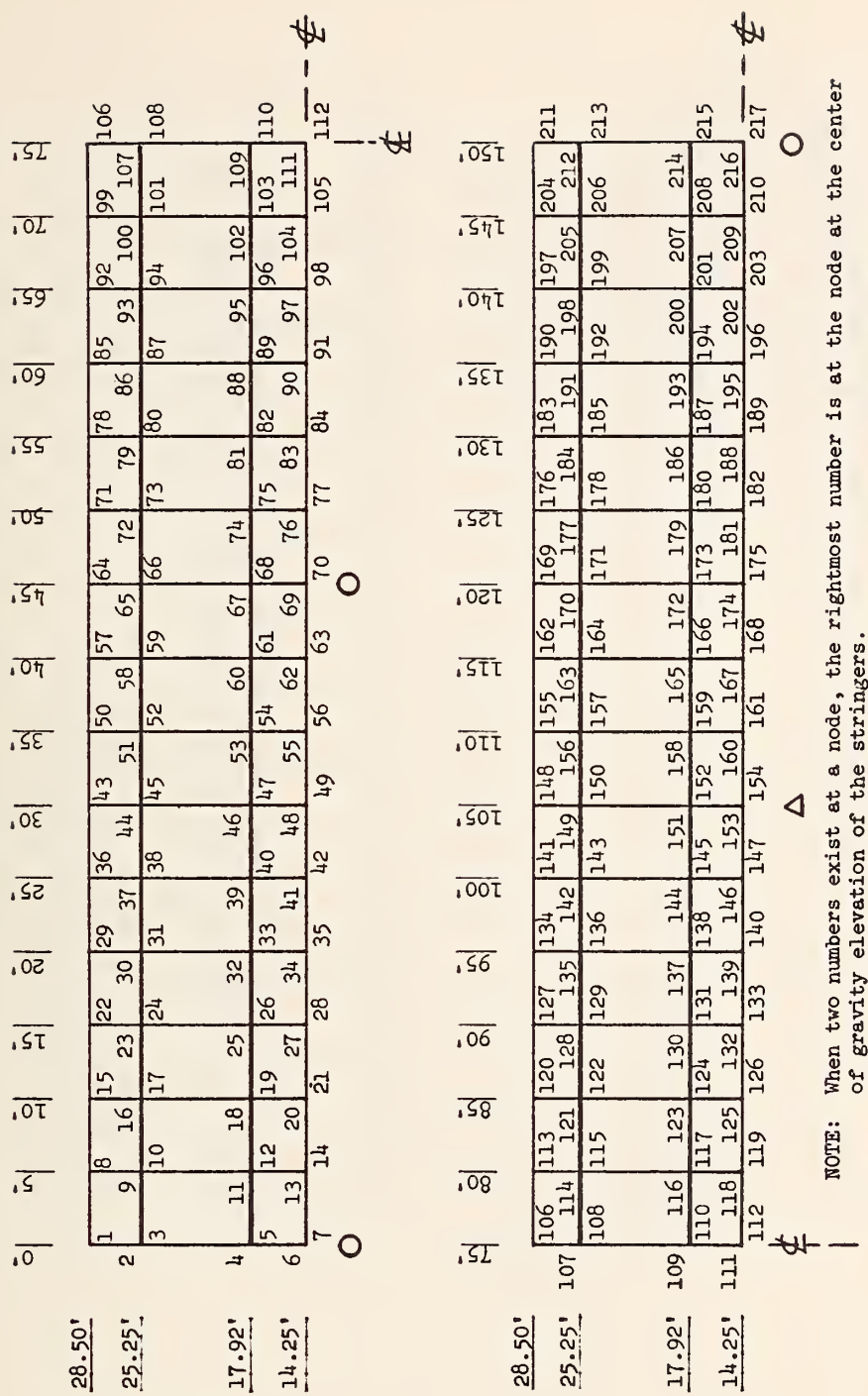


FIG. C-27 - COORDINATE LOCATION OF NODES USED FOR BRIDGE #4 FOR MILITARY LOADING

Beam Material Number
 → (1) → (3) → (1) →

1	3	5	7	9	11	13	15	17	19	21	23	25	27	29
		61			63			65			67			69
2	4	6	8	10	12	14	16	18	20	22	24	26	28	30*
		62			64			66			68			70

○

→ (1) → (3) → (1) →

31	33	35	37	39	41	43	45	47	49	51	53	55	57	59
		71			73			75			77			
32*	34	36	38	40	42	44	46	48	50	52	54	56	58	60
		72			74			76			78			

△

○

* Beams 30 and 32 have beam material no. 2
 All diaphragms have beam material no. 4

FIG. C-28 - BEAM AND DIAPHRAGM NUMBERING FOR BRIDGE #4 FOR MILITARY LOADING

1	4	7	10	13	16	19	22	25	28	31	34	37	40	43
2	5	8	11	14	17	20	23	26	29	32	35	38	41	44
3	6	9	12	15	18	21	24	27	30	33	36	39	42	45

○

46	49	52	55	58	61	64	67	70	73	76	79	82	85	88
47	50	53	56	59	62	65	68	71	74	77	80	83	86	89
48	51	54	57	60	63	66	69	72	75	78	81	84	87	90

△

FIG.C-29- PLATE SHELL NUMBERING FOR SLAB OF BRIDGE #4 FOR MILITARY LOADING

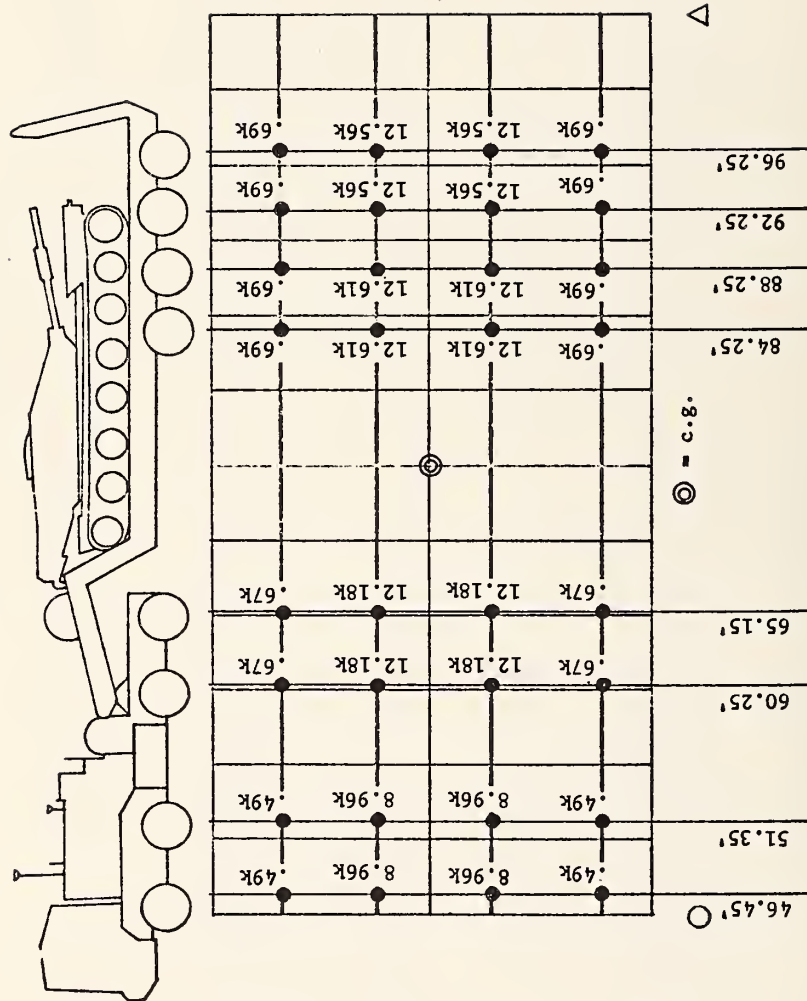


FIG. C-30. LOAD CONDITION 1, BRIDGE 4. CENTER OF GRAVITY OF HET-70 WHEEL LOADS AT THE CENTER OF THE FIRST INTERIOR 60' SPAN.

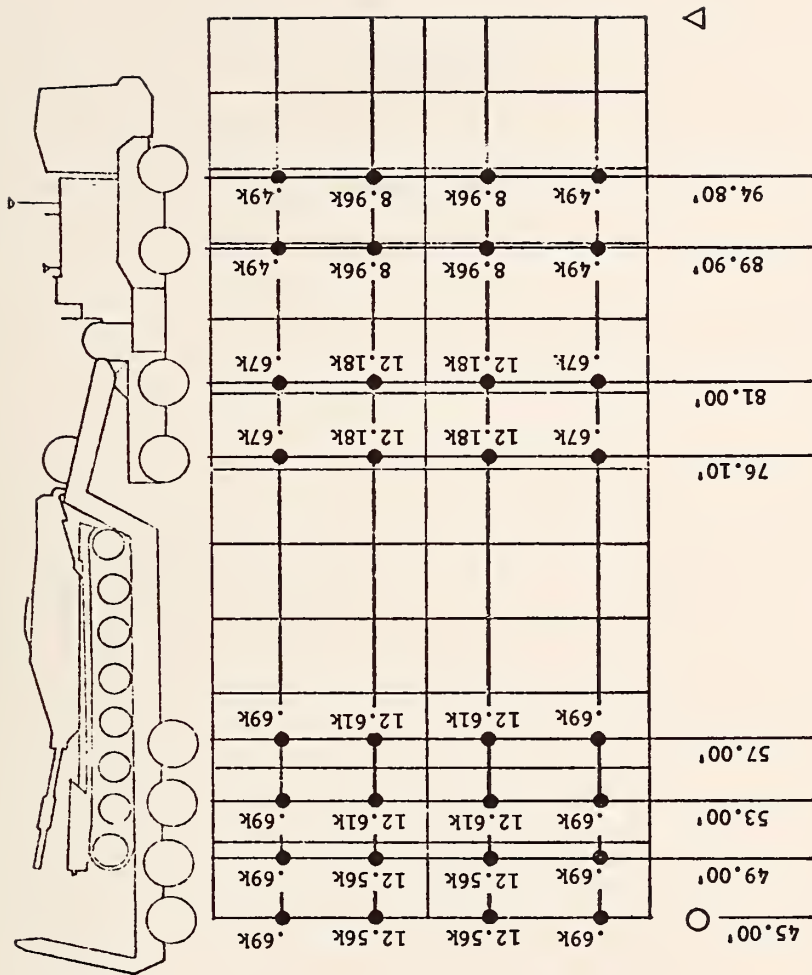


FIG. C-33. LOAD CONDITION 4, BRIDGE 4. REAR WHEEL OF TRAILER IS AT THE FIRST INTERIOR SUPPORT ON 60' SPAN.

APPENDIX D

References

APPENDIX D

REFERENCES

1. Forbes, R. C. and Heinz, C. P., Analysis Charts for Use in Issuing Vehicle Permits, Report No. 49, Civil Engineering Department, The University of Maryland, June 1973.
2. Military Fixed Bridges, Department of the Army Technical Manual TM-5-312, December 1968.
3. Standard Specifications for Highway Bridges, The American Association of State Highway Officials, 11th Edition, 1973.
4. Burdette, E.G. and Goodpasture, D.W., "FINAL REPORT ON FULL SCALE BRIDGE TESTING, AN EVALUATION OF BRIDGE DESIGN CRITERIA", a draft report submitted to the Office of Research and Planning, Tennessee Highway Department and The Department of Transportation, Federal Highway Administration, December 31, 1971.
5. Bathe, Klaus-Jurgen, Wilson, Edward L., Peterson, Fred E., "SAP IV - A STRUCTURAL ANALYSIS PROGRAM FOR STATIC AND DYNAMIC RESPONSE OF LINEAR SYSTEMS", a report to the National Science Foundation, Grant GI-36387 or Report No. EERC 73-11, College of Engineering, University of California, Berkeley, June 1973.
6. Miklofsky, H., "CORRELATION OF THEORETICAL AND EXPERIMENTAL DATA FOR HIGHWAY BRIDGES - VOLUME I - STATIC LOADING", Report No. FHWA-RD-74, May, 1974.
7. Reference 6, p E-4.
8. Standard Specifications for Highway Bridges, The American Association of State Highway Officials, 8th Edition, 1961, pp 39-40, 94, 114-116.
9. Reference 3, pp 56-58, 79, 112, 160-164.
10. Reference 3, p 80.
11. Steel Construction Manual, American Institute of Steel Construction, Seventh Edition, 1970, p. 2-210.
12. Reference 8, p 39.
13. Reference 3, p 57.
14. Reference 6, p 17.

References (Continued)

15. Reference 8, pp 126-133.
16. Reference 3, pp 95-105.
17. Reference 6, p E-9.
18. Reference 8, pp 40 and 132.
19. Reference 3, p 104.
20. Standard Specifications for Highway Bridges, The American Association of State Highway Officials, Second Edition, 1935, pp 182, 206-213.
21. Kirkham, J.E., Highway Bridges, Design and Cost, McGraw Hill, 1932, p 391.
22. Reference 21, p 54.
23. Standard Specifications for Highway Bridges, The American Association of State Highway Officials, Fifth Edition, 1949, pp 145, 149, 186-195, 203-204.
24. Reference 6, p 16.
25. Reference 4, p 28.
26. Libby, J.R. Modern Prestressed Concrete, Design Principles and Construction Methods, Van Nostrand Reinhold Company, 1971, p 410.
27. Lin, T.Y., Design of Prestressed Concrete Structures, Second Edition, John Wiley, 1963, p 562.
28. Reference 26, p 15.

APPENDIX E

Calculations Regarding Computer Predictions and AASHO Specifications

APPENDIX E

Calculations Regarding Computer Predictions and AASHO Specifications

1. AASHO Specifications for Bridge #1

Bridge #1 was designed under 1961 AASHO specifications, with the exception that A-36 steel was used for the stringers. The concrete deck was not poured until all of the structural steel was erected and all the bolting was completed (7). In this discussion both the 1961 and 1973 (latest available AASHO specifications) are considered. The following criteria are applicable:

Applicable 1961 and 1973 Specifications* (8)(9)

The dead load flexural stress shall be based on non-composite beam action for unshored bridges; while the added live plus impact flexural stress shall be based on composite beam action. If concrete is on the tension side, it is to be disregarded in computing the moment of inertia of composite beams.

The ratio of concrete modulus of elasticity to steel is taken as:

$$\begin{aligned} \text{when } f'_c &= 3000 - 3900 \text{ psi} & n &= 10 \\ f'_c &= 5000 \text{ or more psi} & n &= 6. \end{aligned}$$

Composite beams and slabs are to be designed by the composite moment of inertia method considering the elastic working stresses.

The effective flange width of the slab as a T-beam flange is limited to:

1. One-fourth the girder span.
2. The center-to-center distance between girders.
3. Twelve times the least slab thickness.

Extreme flexural compressive stress of the concrete slab is limited to $f_c = 0.4 f'_c$. Class A concrete is defined as $f'_c = 3000$ psi minimum.

Applicable 1961 Specifications (8)

The horizontal shear to be transferred by the shear connectors is computed by a formula:

$$S = \frac{V_m}{I}$$

in which

* See Table E-1, page E-3, for allowable transverse slab stresses.

- S = the horizontal shear per linear inch of the interface between the slab and girder.
- V = the total external shear due to live plus impact loading.
- m = the statical moment of the transformed concrete area about the composite section neutral axis.
- I = the moment of inertia of the transformed composite beam.

The working load for each welded stud for ratios of height/diameter equal or greater than 4.2 is given as:

$$Q = 330 d^2 \sqrt{f'_c}$$

where d is the stud diameter and f'_c is defined as above.

Applicable 1973 Specifications (9)

For A-36 steel, the allowable flexural compression stress is limited to 20,000 psi when the compression flange is embedded in the concrete deck. Such is the case in Bridge #1.

The allowable tension flexural stress also is 20,000 psi.

Shear in girder webs, based on the gross-section of the web, is limited to 12,000 psi. The girder web is to carry the total external shear.

The horizontal shear to be transferred by shear connectors is computed by the same formula as given in the 1961 specifications; however, the capacity of each welded stud is based on an ultimate strength formula:

$$S_u = 930 d^2 \sqrt{f'_c}$$

where d and f'_c are defined as above. Under these conditions a load factor is applied to the calculation of the total external shear, V, and can be calculated by the formula:

$$V = 2.17(L + I)$$

where (L + I) is the live load plus impact total external shear load.

2. Stress Calculations for Bridge #1

As an example consider the allowable bending moments and stresses listed on page B-12 of Preliminary Report No. 1. The dead load moment is listed as 1710 ft-kips for the entire bridge

TABLE 5

SUMMARY OF ALLOWABLE TRANSVERSE SLAB STRESSES UNDER
VARIOUS AASHO SPECIFICATIONS

Stress Type	1935	1950	1961	1973
Compression flexural concrete stress, f_c , for Class A concrete.	900	1,000	1,200	1,200
Tension flexural stress in the reinforcing steel, f_s . $f_{yp} = 40,000$ psi.	16,000	20,000	20,000	20,000
Shear stress, v , without web reinforcement, but longitudinal bars are hooked or anchored.	90	90	90	90
Bond stress, u , longitudinal bars anchored. $D = \text{bar diameter}$	120	$.075 f'_c$ 225 psi max	$.10 f'_c$ 350 psi max	$\frac{4.8\sqrt{f'_c}}{D}$ 500 psi max

All values are in psi units.

cross-section. Using a flexure formula and a moment of inertia of 10,500 in⁴ for each W 36 x 170 stringer (at the middle of the 90' span) the maximum fiber stress is calculated as:

$$f = \frac{Mc}{I} = \frac{1710(12000)(36.16)}{10500(2)(4)} = 8833 \text{ psi}$$

which is close to the 8900 psi listed on page B-12. Note that this calculation is based on non-composite action, and on the assumption that each stringer receives the same proportion of the total moment at the cross-section in question of the bridge. *

As a further example these calculations are repeated for a design live plus impact moment acting on a composite concrete slab-steel stringer beam. For calculations as to the neutral axis location and moment of inertia see Figure E-1. By use of the flexure formula we obtain:

$$f = \frac{Mc}{I} = \frac{2940(12000)(30.23)}{24395(4)} = 10929 \text{ psi}$$

which is in good agreement with the 11,200 psi listed on page B-12.

For the HET-70 maximum-positive moment of 530.19 ft-kips (see page 16) for the interior stringer at a point 4.8' from the center of the 90' span, we obtain for the bottom steel fiber a stress of:

$$f = \frac{Mc}{I} = \frac{530.19(12000)(30.23)}{24395} = 7884 \text{ psi (L.L. + Impact)}$$

8900	(D.L. see p. B-12)
Total Stress 16784 psi	
Total Allowable 20000 psi	

The corresponding compression stress in the concrete deck becomes:

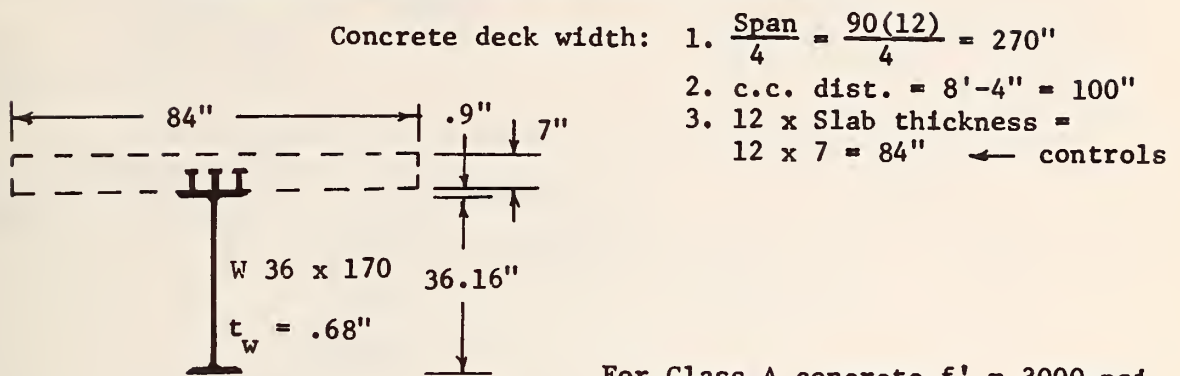
$$f = \frac{Mc}{I} = \frac{530.19(12000)(13.83)}{10(24395)} = 360 \text{ psi}$$

$$\text{Allowable} = .4f'_c = .4(3000) = 1200 \text{ psi}$$

Figure E-2 shows the calculations for maximum negative moments at the first interior support and center of Bridge #1. A maximum negative moment of 549.81 ft-kips occurs at the interior stringer at the first interior support. Substitution in the flexure formula on the basis of non-composite action yields:

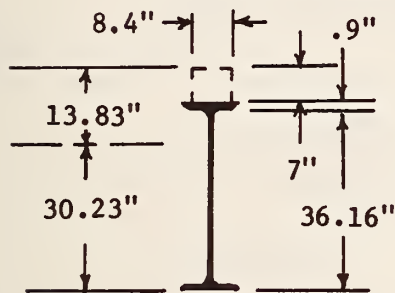
* Such is not the case as the computer analysis shows; however, further refinement, requiring a dead load input to the computer program, has not been done at this time. Note that the HET-70 maximum flexural stresses are considerably lower than the designed values for the bridge.

Composite Beam at $\frac{L}{4}$ of 90' Span - Bridge #1



For Class A concrete $f'_c = 3000 \text{ psi}$
 $n = 10$

Idealization as transformed steel: $\frac{84}{10} = 8.4''$



$$A_c = 8.4(7) = 58.8 \text{ in}^2$$

Location of Neutral Axis:

Summing moments about bottom fiber

$$58.8(36.16 + .9 + 3.5) = 2384.93$$

$$50(18.08) = 904$$

$$108.8 \quad \underline{3288.93}$$

$$\bar{y} = 30.23''$$

$$A_s = 50 \text{ in}^2$$

$$I_{so} = 10,500 \text{ in}^4$$

Calculation of moment of Inertia:

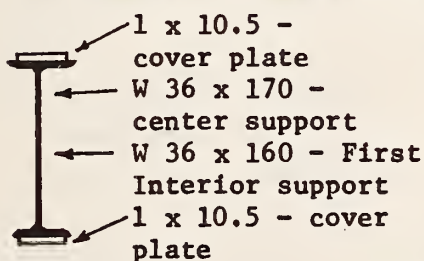
Stringer $I_o = 10,500 \text{ in}^4$

$$Ad^2 = 50(30.23 - 18.08)^2 = 7,381$$

Deck $I_o = 8.4(7)^3/12 = 240$

$$Ad^2 = 58.8(13.83 - 3.5)^2 = \frac{6,274}{24,395 \text{ in}^4}$$

Non-composite Beam at Interior Supports



$$\text{Stringer W 36 x 170} = 10,500 \text{ in}^4$$

$$\text{Cover plates} = Ad^2 =$$

$$2(10.5)(18.08 + .5)^2 = \frac{7,250}{17,750 \text{ in}^4}$$

$$\text{Total at Center} = 17,750 \text{ in}^4$$

$$\text{Stringer W 36 x 160} = 9,760 \text{ in}^4$$

$$\text{Covers } 2(10.5)$$

$$(18.08 + .5)^2 = \frac{7,187}{16,947 \text{ in}^4}$$

$$\text{Total at 1st Int. Support} = 16,947 \text{ in}^4$$

FIG. E-1 - CALCULATIONS FOR STRINGER MOMENTS OF INERTIA FOR BRIDGE #1, ACCORDING TO AASHO SPECIFICATIONS.

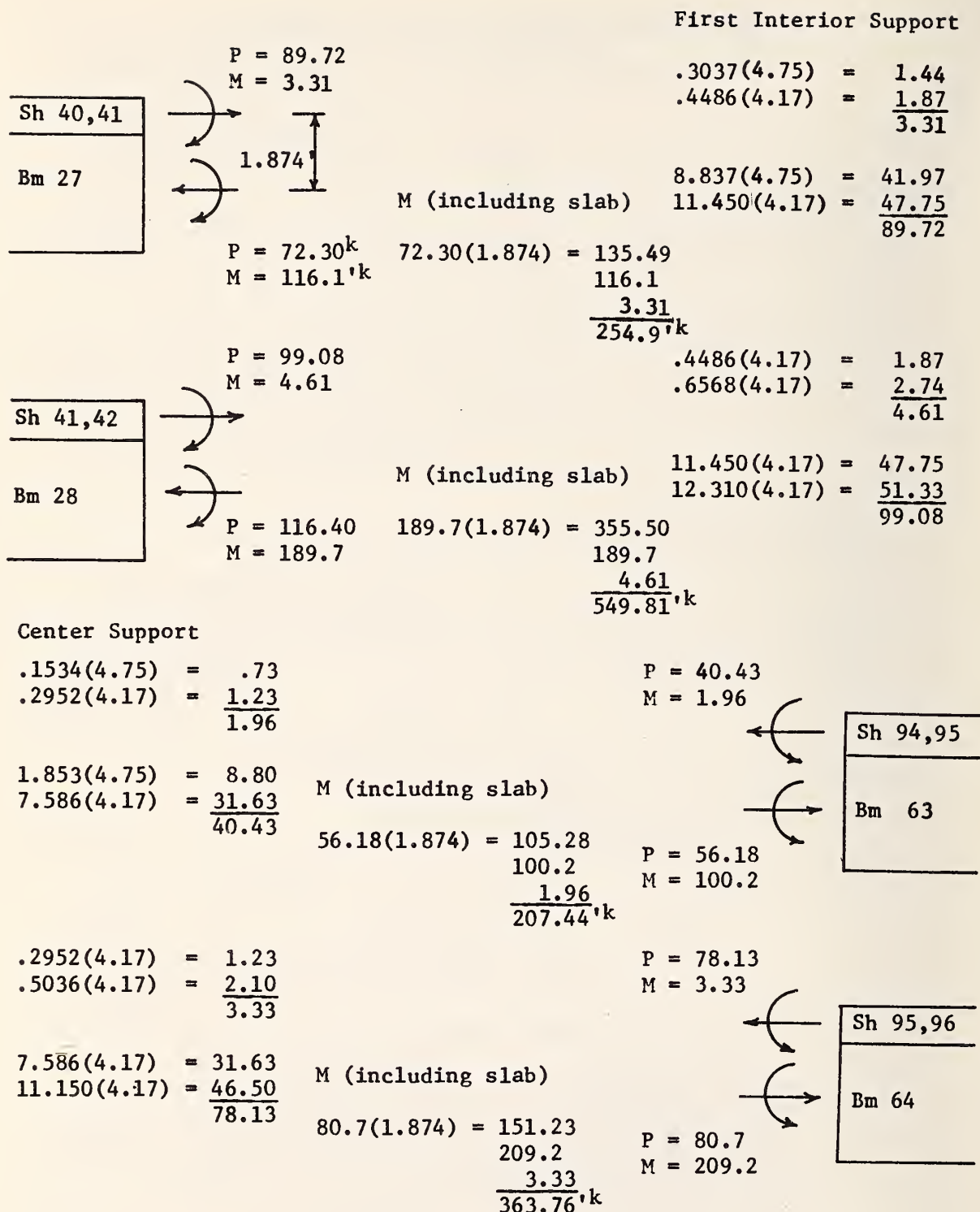


FIG. E-2 - CALCULATION OF NEGATIVE MOMENTS AT INTERIOR SUPPORTS FOR
BRIDGE #1 - FROM COMPUTER DATA, LOAD CONDITION 1

$$f = \frac{Mc}{I} = \frac{549.81(12000)(19.08)}{16947} = 7428 \text{ psi, which is not the critical live load maximum fiber stress.}$$

The maximum shear stress in the steel stringer governed by loading condition 5 is:

$$v = \frac{V}{t_w d} = \frac{65150^*}{.68(38.16)} = 2511 \text{ psi}$$

Maximum Allowable = 12000 psi.

We now examine the horizontal shear condition at the interface between deck and stringer for maximum shear force. The shear force per lineal inch is:

$$S = \frac{V_m}{I} = \frac{65150(607.4)}{17750} = 2230 \text{ \#/in}$$

where $M = 58.8(13.83 - 3.5) = 607.4 \text{ in}^3$ (See Fig. E-1)

According to 1961 AASHO specifications the allowable load per shear connector would be:

$$Q_{uc} = 330 d^2 \sqrt{f'_c} = 330(.875)^2 \sqrt{3000} = 13838^{\#}$$

Therefore, the resisting shear strength for three connectors spaced at 9" c.c. becomes:

$$\frac{3(13838)}{9} = 4613 \text{ \#/in} > 2230 \text{ \#/in}$$

which is quite adequate. A recalculation under 1973 specifications shows the shear strength per connector to be:

$$S_u = 930 d^2 \sqrt{f'_c} = 930(.875)^2 \sqrt{3000} = 38998$$

For three connectors spaced at 9" c.c. this becomes:

$$\frac{3(38998)}{9} = 12999 \text{ \#/in}$$

Using the load factor specified, the applied shear force per linear inch of interface is:

$$2.17(2230) = 4831 \text{ \#/in} < 12999$$

which also shows the design to be adequate for HET-70 loading under the 1973 specifications.

* This includes the 21,500 rear wheel load on the girder at the support moved a dx distance off of the support for maximum shear.

Last the flexural transverse stresses in the concrete slab are investigated. Both the 1961 and 1973 AASHO specifications permit a working stress method of analysis which is used here, although the 1973 specifications also present an alternate ultimate strength method. (10)

Transverse distance between girders = 8'-4".

$$M_{D.L.} \text{ of unit slab approximately} = .1wl^2 \text{ (page 2-210 AISC Manual)} \\ = (.1)\frac{7}{12} (150)(8.33)^2 = - 607 \text{ \#} \quad (11)$$

$M_{L.L.} = -3.49 \text{ 'k/ft}$ in plate-shell element No. 18 for load condition 1, accompanied by an axial load of .3426 k/ft. The axial load is so small ($\frac{P}{A} =$ approximately 10) that it can be neglected. Figure E-3 shows the transverse cross-section of a unit width of the slab. The maximum concrete stress becomes:

$$f = \frac{Mc}{I} = \frac{4.097(1.98)(12000)}{105.949} = 919 \text{ psi}$$

Allowable Stress = 1200 psi

The maximum steel stress is:

$$f = \frac{Mc}{I} = \frac{4.097(3.02)(12000)(10)}{105.949} = 14014 \text{ psi}$$

Allowable Stress = 20000 psi

The maximum shear could occur when the one maximum wheel load is adjacent to the girder. On the basis that this wheel load of 26.5^k (see page B-15) is supported by a 4' width of slab, the maximum shear stress becomes:

$$\frac{V}{bjd} = \frac{26,500}{4(12)(.875)(5)} = 126 \text{ psi.}$$

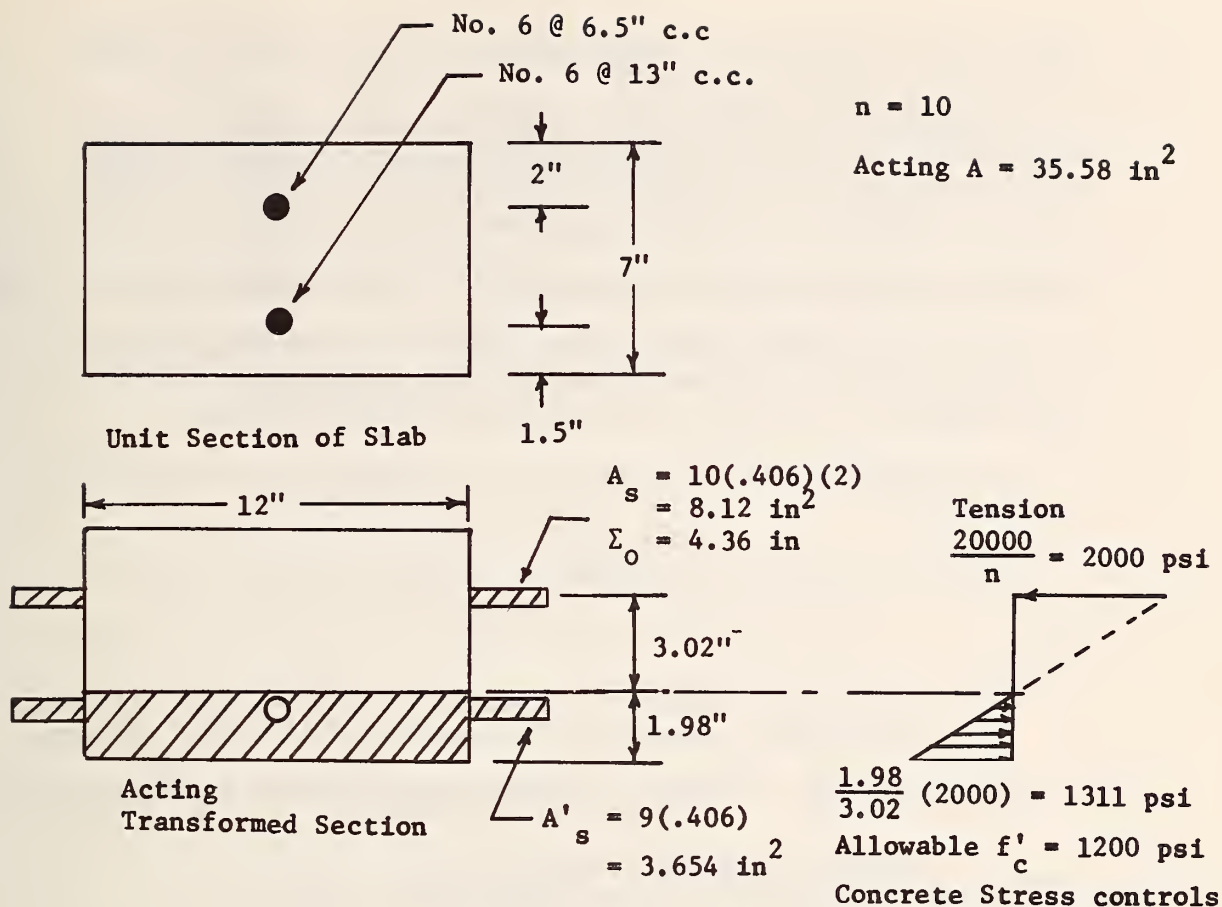
Allowable shear stress for Class A concrete = $.03f'_c = .03(3000) = 90 \text{ psi.}$

According to AASHO Specifications (12) (13), however, if we use the test value of $f'_c = 6870$ (14), the allowable stress becomes $0.03(6870) = 206 \text{ psi.}$

Bond stress is calculated by:

$$u = \frac{V}{\sum ojd} = \frac{26500}{4(4.36)(.875)(5)} = 347 \text{ psi}$$

Allowable bond stress = $.1f'_c = 300 \text{ psi}$ by 1961 specifications or = 687 psi by test value of $f'_c = 6870 \text{ psi.}$ Nevertheless, the specifications limit this to 350 psi maximum.



Σ Moments about neutral axis

$$-8.12(5 - x) + 3.654(x - 1.5) + \frac{12x^2}{2} = 0$$

$$-40.6 + 8.12x + 3.654x - 6.09 + 6x^2 = 0$$

$$6x^2 + 11.77x - 46.69 = 0$$

$$x = \frac{-11.77 \pm \sqrt{11.77^2 + 4(6)(46.69)}}{12} = +1.98" \leftarrow \text{use}$$

-3.94"

Transformed I

$$8.12(3.02)^2 = 74.058$$

$$9(.406)(1.98 - 1.5)^2 = .842$$

$$\frac{12(1.98)^3}{12} = 7.762$$

$$12(1.98) \frac{(1.98)^2}{2} = \frac{23.287}{105.949 \text{ in}^4}$$

FIG. E-3 - CALCULATIONS OF MOMENT OF INERTIA OF TRANSFORMED UNIT WIDTH OF SLAB FOR BRIDGE #1

3. AASHO Specifications for Bridge #2

Bridge #2 was designed under the 1961 AASHO specifications. This discussion considers the calculations of stresses for the HET-70 loading under the 1961 specifications, and also how they would be modified, if necessary, to meet the 1973 specifications.

Applicable 1961 and 1973 Specifications for Prestressed Girders (15)(16)

The maximum allowable concrete compression flexural stress f'_c is 5000 psi for the girders. For the deck for Class A concrete, this becomes $f_c = 0.4f'_c = 1200$ psi at the design loading.

The ultimate flexural strength for flanged sections shall be calculated as:

$$M_u = A_{sr} f_{su} d \left(1 - 0.6 \frac{A_{sr} f_{su}}{b' d f'_c} \right) + .85 f'_c (b - b') t (d - 0.5t)$$

where

$A_{sr} = A - A_{sf}$ = steel area required to develop the ultimate compressive strength of the web of the flanged section.

$A_{sf} = .85 f'_c (b - b') \frac{t}{f_{su}}$, provided the effective prestress after

losses is not less than 0.5 f'_s .

f'_s = ultimate strength of prestressing steel

$$f_{su} = f'_s \left(1 - 0.5 \frac{p f'_s}{f'_c} \right)$$

$$p = \frac{A_s}{bd}$$

t = flange thickness

b = width of flange

b' = width of web

d = distance from maximum compression fiber to centroid of prestressing steel.

The ultimate flexural strength of rectangular sections in which the neutral axis lies within the flange is given as:

$$M_u = A_s f_{su} d \left(1 - \frac{.6 p f_{su}}{f'_c} \right)$$

where M_u = ultimate moment.

For single beams carrying moving loads the maximum shear may be computed within the middle half of the beam. The web reinforcement required at the quarter points should be used for the outer quarters of the beam.

Applicable 1961 Specifications (15)

The elastic theory method shall be used for design, but the members are to be rechecked by ultimate strength procedures for compliance with specified load factors.

The design load shall consider stresses in effect after losses and under dead load.

The ultimate strength capacity shall not be less than:

$$1.5D + 2.5(L + I)$$

where

D = dead load

L + I = live load plus impact load.

For the prestressing steel the stress at design load (after losses) shall be not greater than $.6f'_s$ or $.8f_{sy}$.

f_{sy} = yield point stress of prestressing steel at 1.0% extension.

Loss of prestress due to all causes for prestressed members may be assumed as 35000 psi.

Prestressed concrete members under design flexural loading may be assumed to act as uncracked members subjected to combined axial and bending stresses. The transformed area of steel may be included in computing the moment of inertia for review under full loading.

Composite beams may have their elements tied together by extensions of the web reinforcement. The shear connection shall be designed for the ultimate load and may be computed by:

$$v = \frac{V_u \phi}{I_b'}$$

where

V_u = ultimate shear force due to load and prestressing.

ϕ = statical moment of flange about the neutral axis of the beam.

I = transformed moment of inertia of the composite section.

Shear capacity at the interface is given as:

225 psi - when the area of vertical ties \geq area of two No. 3 bars spaced at 12 inches, and the interface surface of the girder is artificially roughened.

Any excess capacity shall be obtained by shear keys.

Prestressed concrete members shall be reinforced for diagonal tension stresses. The area of web reinforcement is governed by the formula:

$$A_v = \frac{(V_u - V_c)S}{2f'_y d} \leq .0025 b'S$$

where V_c is the shear carried by the concrete, as given by:

$$V_c = .075 f'_c b_j d$$

Transverse bond stress in slab = $.1f'_c$, with maximum 350 psi.

Applicable 1973 Specifications where different from the 1961 Specifications (16)

Design is to be based on ultimate strength at service loading. The ultimate load capacity shall not be less than:

$$\frac{1.3}{\phi} [D + \frac{5}{3} (L + I)]$$

where $\phi = 1$ for flexure
 $= .9$ for shear

For the prestressing steel the stress at service loading (after losses) is limited to $.8 f_{sy}$ or $.7f'_s$.

Prestress losses are given by:

$$Af_s = SH + ES + CR_c + CR_s$$

where SH = 5000 psi minimum (Concrete shrinkage)
 ES = 4000 psi minimum (Elastic shortening of concrete)
 $CR_c = 8000$ psi minimum (Concrete Creep)
 $CR_s = 20,000 - .125 (SH + ES + CR_c)$
 $= 20,000 - .125(17000) = 17875$

Therefore, the minimum losses become 34,875 psi, say 35,000 psi; which total the same as the 1961 specs.

The area of net reinforcement for diagonal tension shall be:

$$A_v = \frac{(V_u - V_c)S}{2f'_y d} \leq \frac{100 b'S}{f'_y}$$

$$V_c = .06f'_c b_j d \leq 180 b_j d$$

Horizontal shear at the interface is calculated in the same manner as the 1961 specs; however, the shear capacity is give as:

300 psi when the area of vertical ties \geq the area of two No. 3 bars spaced at 12 inches; and the interface surface of the girder is intentionally roughened.

In addition for each percent of stirrup in excess of the above requirements, 150 psi shear resistance may be considered effective.

Alternately, full transfer of the ultimate horizontal shear forces may be assumed when:

Interface of girder is cleaned and roughened prior to slab addition;
The minimum vertical ties are provided as given above;
All stirrups are fully anchored into slab and girder;
The girder web carries the entire external shear.

Transverse bond stress in slab is:

$$4.8 \frac{\sqrt{f'_c}}{D}, \quad 500 \text{ psi maximum}$$

where D is the diameter of rod.

4. Stress Calculation for Bridge #2

From page B-12

$$\begin{aligned} \text{D.L. moment} &= 3050'k @ 1490 \text{ psi}^* \\ \text{L.L. moment} &= 3600'k @ \frac{990}{2480} \text{ psi} \\ \text{Total} & \end{aligned}$$

Non-Transformed Section (See Fig. E-4 for section properties)

D.L. (Girder only):

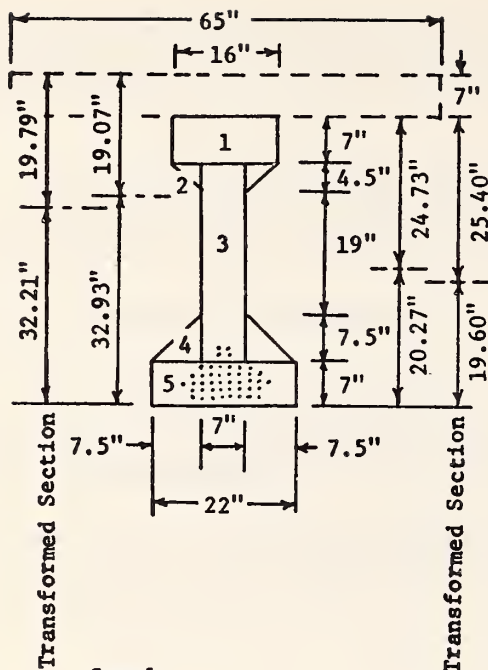
$$f = \frac{Mc}{I} = \frac{3050(12000)24.73}{125,390(4)} = -1805 \text{ psi} - \text{Top of girder}$$

L.L. (Slab and Girder):

$$f = \frac{Mc}{I} = \frac{3600(12000)19.07}{327,226(4)} = -629 \text{ psi} - \text{Top of slab}$$

$$f = \frac{Mc}{I} = \frac{3600(12000)12.07}{327,226(4)} = -398 \text{ psi} - \text{Top of girder}$$

* It appears that the stresses shown on page B-12 represent those at the bottom of the girder; probably for correlation with the strains shown on page B-21.



Girder alone

	Area	Arm	
ΣM_{base}	7(16)	(41.5)	= 4648
	4.5(4.5)	36.5	= 739.125
	7(31)	22.5	= 4882.5
	7.5(7.5)	9.5	= 534.375
	22(7)	3.5	= 539
	559.5		11343

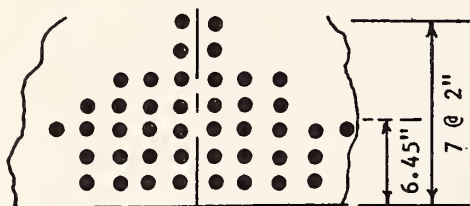
\bar{y} concrete girder from base = 20.27"

Moment of Inertia

Section	I_o	Ay'^2
1	457.33	50479.84
2	22.78	5334.11
3	17378.08	1079.12
4	175.78	6524.60
5	628.83	43309.87
	18662.80	106727.54

$$I_{na} = 125,390.34 \text{ in}^4 \text{ (26)}$$

Steel



44 Strands

Transformed c.g. of girder alone

	Area	Arm	
ΣM_{base} concrete	559.5	20.27	= 11341.065
	28.52	6.45	= 183.95
	588.02		11525.015

Trans. \bar{y} from base = 19.60"

ΣM_{base}	8 x 2 = 16
	8 x 4 = 32
	10 x 6 = 60
	8 x 8 = 64
	6 x 10 = 60
	2 x 12 = 24
	2 x 14 = 28
	44 284

\bar{y} steel from base = 6.45"
n = 6(12)

$$\text{Steel transformed area} = 44(6)(.108) = 28.512 \text{ in}^2$$

$$\frac{E_c \text{ slab}}{E_c \text{ girder}} \text{ assumed as } \frac{\sqrt{3000}}{\sqrt{5000}} = \frac{54.77}{70.71} = .775 \quad \frac{L}{4} = \frac{66}{4}$$

$$\text{Transformed width} = 84(.775) = 65" \quad \text{c.c} = 9(12) = 108" \\ 12(7) = 84" \leftarrow \text{Governs}$$

FIG. E-4 - MOMENT OF INERTIA CALCULATIONS FOR BRIDGE #2

Girder and Slab

ΣM_{base}	Area	Arm	Moments of Inertia	
			I_o	Ay'^2
	65(7)	(48.5) = 22067.5		
	559.5	20.27 = 11341.065		
	1014.5	33408.565		
\bar{y} from base 32.93"			Slab 1857.92	110303.32
			Girder 125390.34	89674.20
			I (without steel) = 327225.78 in. ⁴	

Girder alone

Moments of Inertia

	I_o	Ay'^2
Girder	125390.34	251.20
Steel	---	5447.10

I Girder with transformed steel = 131088.64 in.⁴

Girder and Slab

ΣM_{base}	Area	Arm	Moments of Inertia	
			I_o	Ay'^2
	65(7)	(48.5) = 22067.05		
	559.5	20.27 = 11341.065		
	28.52	6.45 = 183.954		
	1043.05	33592.069		
\bar{y} from base 32.21"			Slab 1857.92	120740.66
			Girder 125390.34	88967.27
			Steel ---	18925.23
			I including transformed steel = 355,881.08 in. ⁴	

FIG. E-4 (Continued)

Prestress

Initial force = 18900#/strand.(17)

Area of $\frac{7}{16}$ " ϕ 7 wire uncoated stress relieved strand = .108 in²

Loss of prestress at 35,000 psi = .108(35,000) = 3815#

Net strand force = 18900 - 3815 = 15085#

$$\frac{P}{A} = \frac{44(15085)}{559.6} = -1186 \text{ psi} - \text{Top of Girder}$$

$$\frac{Pec}{I} = \frac{44(15085)(20.27 - 6.45)(24.73)}{125390} = \frac{-1186 \text{ psi}}{+1809 \text{ psi}} - \text{Top of Girder}$$

Net = + 623 psi - Top of Girder

L.L. + D.L. = -2203 psi - Top of Girder

Non-Transformed Section

Total Stress = -1580 psi - Top of Girder

D.L. (Girder only):

$$f = \frac{Mc}{I} = \frac{3050(12000)(20.27)}{125390(4)} = +1479 \text{ psi}^* - \text{Bottom of Girder}$$

vs 1490

L.L. (Slab and Girder):

$$f = \frac{Mc}{I} = \frac{3600(12000)(32.93)}{327226(4)} = +1087 \text{ psi}^* - \text{Bottom of Girder}$$

vs 990

Prestress

$$\frac{P}{A} \text{ (Girder only)} = -1186 \text{ psi}$$

$$\frac{Pec}{I} \text{ (Girder only)} = \frac{44(15085)(20.27 - 6.45)20.27}{125390} = \frac{-1483 \text{ psi}}{\text{Bottom of Girder}}$$

Total stress = -103 psi at the bottom
(See Fig. E-5)

Transformed Section

D.L. (Girder only):

$$f = \frac{Mc}{I} = \frac{3050(12000)(25.4)}{131089(4)} = -1773 \text{ psi} - \text{Top of Girder}$$

L.L. (Slab and Girder):

$$f = \frac{Mc}{I} = \frac{3600(12000)(19.79)}{355881(4)} = -601 \text{ psi} - \text{Top of Slab}$$

$$f = \frac{Mc}{I} = \frac{3600(12000)(12.79)}{355881(4)} = -388 \text{ psi} - \text{Top of Girder}$$

* See footnote, page E-13.

Prestress

$$\frac{P}{A} \text{ (Girder only)} = \frac{44(15085)}{588.02} = -1129 \text{ psi - Top of Girder}$$

$$\frac{P_{ec}}{I} \text{ (Girder only)} = \frac{44(15085)(19.6 - 6.45)(25.4)}{131089} = +1691$$

Top of Girder

$$\begin{aligned} & -1129 \\ & +1691 \\ \text{Net} & = +562 \text{ psi - Top of Girder} \\ \text{D.L. + L.L.} & = -2161 \text{ psi} \\ \text{Total Stress} & = -1599 \text{ psi - Top of Girder} \end{aligned}$$

It doesn't seem to make much difference whether the section is transformed or not.

L.L. HET-70, Non-Transformed Section

$$M = 665.68 \text{ (See page 20)}$$

$$\begin{aligned} f &= \frac{Mc}{I} = \frac{665.68(12000)19.07}{327226} = -466 \text{ psi - Top of Slab} \\ & \quad -294 \text{ psi - Top of Girder} \\ \text{D.L. + Prestress} &= -1805 + 623 = -1182 \text{ psi - Top of Girder} \\ \text{Total} &= -1476 \text{ psi - Top of Girder} \end{aligned}$$

$$\text{Allowable slab stress } (f'_c = 3000) = -1200 \text{ psi}$$

$$f = \frac{Mc}{I} = \frac{665.68(12000)32.93}{327226} = +804 \text{ psi - Bottom of Girder}$$

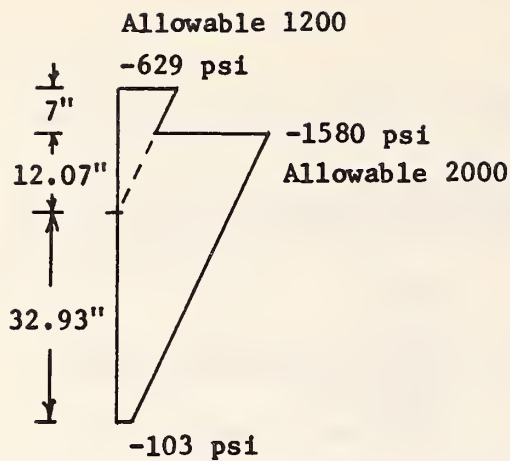
From page B-21 maximum strain = $106.2\mu"/\text{in.}^*$

If we use the test data $E = 57500\sqrt{f'_c} = 57500\sqrt{8700} = 5363025 \text{ psi (14)}$, where the average cylinder strength of girder = 8700 psi, then the actual stress = $E\epsilon = 5.363 \times 106.2 = 570 \text{ psi}$ vs. 804 psi predicted.

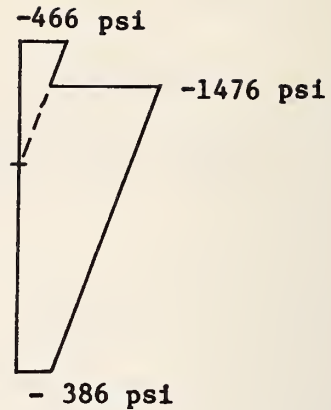
For the total stress:

$$\begin{aligned} \text{L.L. } f &= \frac{Mc}{I} = \frac{665.68(12000)(32.93)}{327226} = +804 \text{ psi - Bottom of Girder} \\ \frac{P}{A} &= -1186 \text{ psi} \quad " \\ \text{D.L.} &= +1479 \text{ psi} \quad " \\ \frac{P_{ec}}{I} &= -1483 \text{ psi} \quad " \\ \text{Total Stress} &= -386 \text{ psi - Bottom of Girder (see Fig. E-5)} \end{aligned}$$

* Refined data on Page B-58 lists maximum strain = $112\mu"/\text{in.}$



Design Loading



HET-70 Loading

FIG. E-5 - MAXIMUM FLEXURAL STRESS SUMMARIES FOR INTERIOR GIRDER OF BRIDGE #2

Steel Stress (27)(28)

Maximum prestress load after losses	= 15085 #/Strand
Prestress capacity of strand = 175000(.108)	= 18900 #/Strand
Ultimate capacity of strand = 250000(.108)	= 27000 #
Minimum load at 1% extension	= 23000 #

$$\frac{15085}{27000} = .56 f'_s \leq .6 f'_s \quad \text{o.k.}$$

$$\frac{15085}{23000} = .66 f_{sy} \leq .8 f_{sy} \quad \text{o.k.}$$

Ultimate Flexural Strength

$$f'_s = 175000 \text{ psi} \quad A_s = 44(.108) = 4.752 \text{ in}^2$$

$$P = \frac{A_s}{bd} = \frac{44(.108)}{65(52 - 6.45)} = .0016$$

$$f_{sy} = f'_s \left(1 - .5 \frac{P f'_s}{f'_c} \right) = 175000 \left(1 - .5 \frac{(.0016)(175000)}{3000} \right)$$

$$= 166,833 \text{ psi}$$

$$A_{sf} = .85f'_c \frac{(b-b')t}{f_{su}} = \frac{.85(3000)(65 - 18)7}{166,833}$$

$$= 5.03 \text{ in}^2 > A_s$$

Use flange formula

$$M_u = A_s f_{su} d \left(1 - .6 \frac{P f_{su}}{f'_c}\right)$$

$$= 4.752(166833)(52 - 6.45) \left[1 - .6 \frac{(.0016)(166833)}{3000}\right]$$

$$= 4.752 \frac{(166833)(45.55)(.9466)}{12000} = 2849 \text{ 'k}$$

			Load Factor		M_u
D.L. Moment	$\frac{3050}{4}$	= 762.5	x 1.5	=	$\frac{1143.75}{}$
L.L. Moment	= 662.7		x 2.5	=	$\frac{1656.75}{}$
			Total M_u	=	$\frac{2800.5 \text{ 'k}}{2849 \text{ 'k}}$ vs o.k.

Shear: 1961 Specifications

Maximum V (live load) occurs in beam element 55 for load condition 2, and equals $43.12 \text{ k} + 26.5 \text{ k} = 69.62 \text{ k}^*$

D.L. Estimate for Interior Girder (See page C-19 for dimensions)

$$\text{Slab} = 150 \times \text{thickness} \times \text{width} \times \frac{1}{2} \text{ length}$$

$$= 150 \left(\frac{7}{12}\right) (8.74) 33 = 25,237 \text{ \#}$$

$$\text{Girder} = 150 \times \text{area} \times \frac{1}{2} \text{ length}$$

$$= 150 \left(\frac{559.5}{144}\right) 33 = 19,233 \text{ \#}$$

$$\text{Total} = 44,470 \text{ \#}$$

$$\text{Ultimate Load } V_u = 1.5D + 2.5(L + I)$$

$$= 1.5(44.47) + 2.5(69.62) = 240.76 \text{ k}$$

Deduction for vertical prestress component:

Ten strands drop average of 27" in 27'; therefore, vertical component approximately equals:

* See footnote, page E-7.

$$\frac{27(10)(15085)}{27(12)(1000)} = -12.57^k$$

$$\text{Net } V_u = 228.19^k$$

$$V_c = .075 f'_c b_j d = .075(5000)(7)\frac{7}{8} \frac{(38.55)}{1000} = 88.54^k \quad (18)$$

No. 4 double stirrups are spaced on 15" centers.

$$A_v (\text{Req}) = \frac{(V_u - V_c)S}{2f_y j d} = \frac{(228.19 - 88.54)(15)(1000)}{2(40,000).875(38.55)} = .776 \text{ in}^2$$

$$A_v \text{ furnished} = .40 \text{ in}^2$$

$$A_v \text{ minimum required} = .0025b'S = .0025(7)15 = .26 \text{ in}^2$$

Shear: 1973 Specifications (19)

$$V_c = .06f'_c b_j d \leq 180b_j d$$

$$\text{is limited to } 180(7).875 \frac{(38.55)}{1000} = 41.40^k$$

$$A_v \text{ minimum} = \frac{100b'S}{f_{sy}} = \frac{100(7)15}{40,000} = .26 \text{ in}^2$$

Same as 1961 specs.

$$A_v (\text{Req}) = \frac{(V_u - V_c)S}{2f_{sy} j d} = \frac{(228.19 - 41.40)(15)(1000)}{2(40,000).875(38.55)} = 1.04 \text{ in}^2$$

$$A_v \text{ furnished} = .4 \text{ in}^2$$

However both 1961 and 1973 specifications allow the shear to be investigated only in the middle half of simply-supported beams for members carrying moving loads. Within the middle half:

$$\text{D.L. Shear} = \frac{44.47}{2} = 22.24^k$$

$$\text{L.L. (Beam Element 27, Load Condition 3)} = 33.96^k$$

$$V_u = 1.5(22.24) + 2.5(33.96) = 118.26^k$$

$$A_v (\text{Req}) = \frac{(V_u - V_c)S}{2f_{sy} j d} = \frac{(118.26 - 41.40)(15)(1000)}{2(40,000).875(38.55)} = .427 \text{ in}^2$$

Slightly Overstressed.

Horizontal Shear at Beam-Slab Interface

$$Q = 7(65)(19.79 - 3.5) = 7411.95 \text{ in}^3$$

$$v = \frac{V_u Q}{I_b} = \frac{174.05(7411.95)(1000)}{355,881(7)} = 518 \text{ psi}$$

where $V_u = 2.5(69.62) = 174.05^k$ due to live load.

$$\text{Area furnished by stirrup} = \frac{3}{4}(.4) = .3 \text{ in}^2/\text{foot}$$

$$\text{Minimum tie-in steel required (Two \#3 @ 12")} = .22 \text{ in}^2/\text{foot}$$

$$\text{Excess} = .08 \text{ in}^2$$

$$\% \text{ excess} = \frac{.08}{7(12)} (100) = .095$$

At 150 psi shear resistance increase per percent excess
area = $.095(150) = 14.3 \text{ psi}$.

$$300.0 \text{ psi (See page E-13)}$$

$$14.3 \text{ psi}$$

$$\text{Total Shear Capacity} = 314.3 \text{ psi vs } 518 \text{ psi (Overstressed)}$$

However see page E-13 for alternate specification which allows full transfer of ultimate shear force.

Slab Analysis (See page E-3 for applicable 1961 & 1973 specs)

The computer results show a maximum transverse slab moment of -2.002^k with an axial load of $.6779^k$ in plate-shell element No. 52 for load condition 3. We shall neglect the axial load (f_A = approximately 15 psi).

$$\text{Transverse distance between girders} = 8.74'$$

$$M_{D.L.} = .1wl^2 = .1\left(\frac{7}{12}\right)150(8.74)^2 = 669' \#$$

$$M_{L.L.} = 2.002^k$$

Fig. E-6 shows the transverse cross-section of a unit width of slab.

The maximum concrete stress becomes:

$$f = \frac{Mc}{I} = \frac{2.671(2.302)(1200)}{128.866} = 573 \text{ psi}$$

$$\text{Allowable Stress} = 1200 \text{ psi.}$$

The maximum steel stress is:

$$f = \frac{Mc}{I} = \frac{2.671(2.698)(12000)(10)}{128.866} = 6710 \text{ psi}$$

$$\text{Allowable Stress} = 20,000 \text{ psi}$$

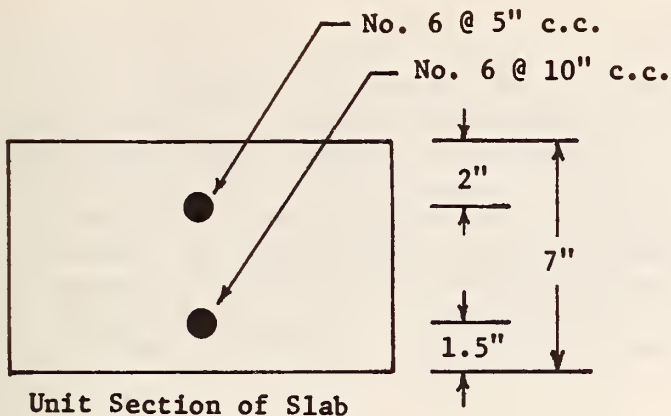
$$\text{Maximum shear (see page E-3)} = 126 \text{ psi}$$

$$\text{Allowable Shear} = 90 \text{ psi}$$

Maximum bond stress:

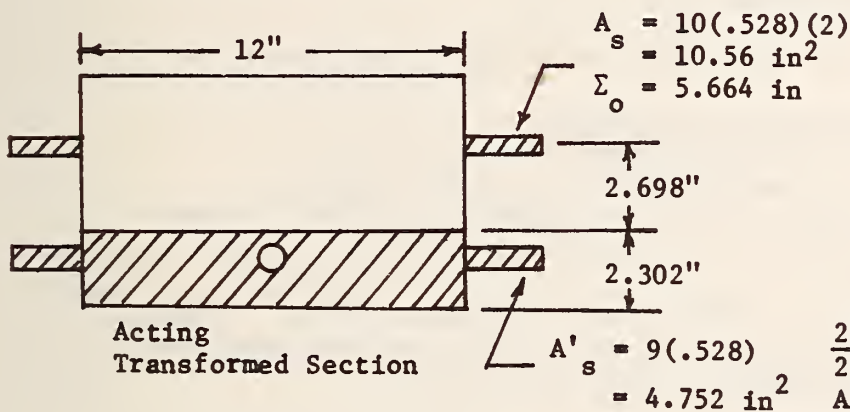
$$u = \frac{v}{\sum_o jd} = \frac{26,000}{(4)5.664(.875)(5)} = 262 \text{ psi}$$

$$\text{Allowable bond stress} = \frac{4.8\sqrt{3000}}{.75} = \frac{4.8}{.75}(54.77) = 351 \text{ psi.}$$

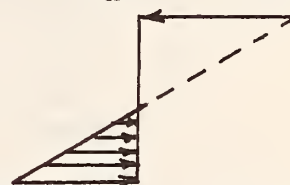


$$n = 10$$

$$\text{Acting } A = 43.16 \text{ in}^2$$



$$\text{Tension } \frac{20000}{n} = 2000 \text{ psi}$$



$$\frac{2.302}{2.698} (2000) = 1706 \text{ psi}$$

$$\text{Allowable } f'_c = 1200 \text{ psi}$$

Concrete Stress controls

Σ Moments about neutral axis

$$-10.58(5 - x) + 4.75(x - 1.5) + \frac{12x^2}{2} = 0$$

$$-59.2 + 10.58x + 4.75x - 7.92 + 6x^2 = 0$$

$$6x^2 + 15.33x - 67.12 = 0$$

$$x = \frac{-15.33 \pm \sqrt{15.33^2 + 4(6)(67.12)}}{12} = +2.302'' \leftarrow \text{use}$$

$$-4.858''$$

Transformed I

$$10.58(2.698)^2 = 77.014$$

$$9(.528)(2.302 - 1.5)^2 = 3.057$$

$$12 \frac{(2.302)^3}{12} = 12.199$$

$$12(2.302) \frac{(2.302)^2}{2} = 36.596$$

$$I = 128.866 \text{ in}^4$$

FIG. E-6 - CALCULATIONS OF MOMENT OF INERTIA OVER TRANSVERSE UNIT WIDTH OF SLAB FOR BRIDGE #2

5. Specifications for Bridge #3

Bridge #3 was designed in 1938 under the Standard Road and Bridge Specifications of the Tennessee Department of Highways and Public Works for an H-15 loading. Unfortunately, these specifications and the drawing showing the layout of the beam reinforcing was not readily available to the author; therefore, the author decided to review the stresses in this bridge under the requirements of the 1935 AASHO specifications. The allowable stresses are higher under the 1973 code; however, in view of the age of the bridge, the author considers it unwise to base strength above the 1935 specifications.

1935 AASHO Specifications (20)

The effective T-Beam flange width shall not exceed:

- a. One-fourth the span length.
- b. Center-to-center distance between beams.
- c. Six times the beam width.
- d. Eight times the slab thickness plus width of beam stem.

The flange shall not be effective in resisting shear. Flexural stress is based on the usual elastic theory of the transformed section. For approximating computations, use:

$$A_s = \frac{M}{14000d}$$

Shearing unit stresses are calculated as:

$$v = \frac{V}{bjd}$$

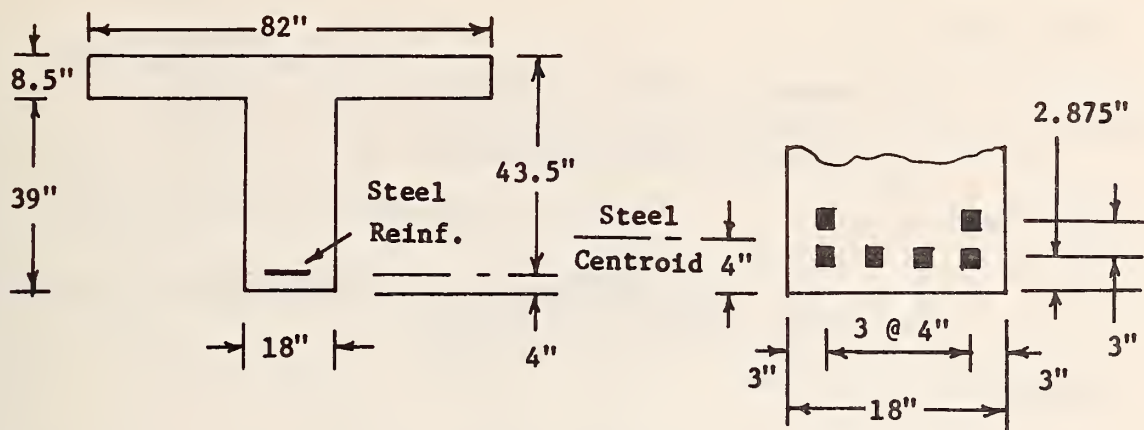
in which V is the maximum shear, b the stem width, d the distance from maximum compression fiber to the centroid of the tension steel, and j is the effective lever arm between centroid of compression area and centroid of tension steel. Webs must be reinforced.

Clearance requirements:

- = Clear distance between bars preferably not less than 3".
- Covering minimum to be 2".

6. Stress Calculations for Bridge #3

Considerable speculation is inferred in this analysis as to the arrangement of longitudinal reinforcing steel in the T-beams, since drawings were not available. Fig. E-7 shows the cross-section of a T-beam with deduced arrangement of longitudinal bars in accordance with clearance requirements specified in the 1935 AASHO Code.



1935 Specs: $\frac{L}{4} = \frac{51.5}{4} = 154.5''$

c.c. distance between beams = 6'-10" = 82" ← controls

6 x beam width = 6 x 18 = 108"

8 x slab thickness + beam width = 8(18) + 18 = 162"

Assume 4" distance between bottom fiber and centroid of reinforcing steel: $d = 43.5''$

Area of steel required for total moment = 2440 + 1400 = 3840'k
(See page B-12)

Try approximate formula:

$$A_s = \frac{M}{14000d} = \frac{3840(12000)}{14000(43.5)4} = 18.92 \text{ in}^2$$

Assume 6 bars . Page B-20 shows 4 bars in lower row. Area of each bar is:

$$\frac{18.92}{6} = 3.15 \text{ in}^2$$

The area of a 1 3/4" square rod = 3.06 in². Reference (21) shows that 1 3/4" square reinforcing rods were available at least as early as 1932. The figure above shows clearance requirements are adequate, and also shows a possible arrangement of bars.

$$\Sigma O = 6(1.75)(4) = 42 \text{ in.}$$

$$\frac{d}{t} = \frac{43.5}{8.5} = 5.1, \quad \text{Use } j = .91 \text{ (22)}$$

FIG. E-7 - ONE POSSIBLE ARRANGEMENT OF REINFORCING STEEL FOR THE T-BEAM OF BRIDGE #3

From page B-12:

$$\text{D.L. Moment} = 2440'k @ 10100 \text{ psi}$$

$$\text{L.L. Moment} = 1400'k @ 5900 \text{ psi}$$

Dead load check:

$$f_s = \frac{M}{A_{sjd}} = \frac{2440(12000)}{6(3.06)(.91)(43.5)(4)} = 10072 \text{ psi vs } 10100 \text{ psi}$$

Design live load check:

$$f_s = \frac{M}{A_{sjd}} = \frac{1400(12000)}{6(3.06)(.91)(43.5)(4)} = 5944 \text{ psi vs } 5900 \text{ psi}$$

L.L. - HET-70 loading, load condition 1:

$$\text{From page 25, } M = 366.71'k$$

$$f_s = \frac{M}{A_{sjd}} = \frac{366.71(12000)}{6(3.06)(.91)(43.5)} = 6055 \text{ psi}$$

$$\text{D.L.} = \underline{10072}$$

$$\text{Total Stress} = \underline{16127} \text{ psi}$$

$$\text{Allowable Stress} = 16000 \text{ psi}$$

Shear - Load Condition 2, Beam Element 42

$$V = 29.22 + 26.5 = 55.72'k$$

$$v = \frac{V}{b_{jd}} = \frac{55.72(1000)}{18(.875)(43.5)} = 81.33 \text{ psi}$$

$$\text{Allowable Stress} = 90 \text{ psi}$$

Bond Stress

$$v = \frac{V}{\Sigma o_{jd}} = \frac{55.72(1000)}{55(.875)(43.5)} = 26.62 \text{ psi}$$

Minimum bond stress - longitudinal:

$$\text{Bars not anchored} = 80 \text{ psi}$$

$$\text{With bars anchored} = 120 \text{ psi.}$$

Test Data for Stress

Page B-20 shows a maximum live load stress on one of the bottom bars of only 3450 psi for the HET-70 loading.

Slab Stresses in Transverse Direction.

Transverse distance between beams = 6.833'

$$M_{D.L.} = .1wl^2 = .1\left(\frac{8.5}{12}\right)150(6.833)^2 = 496 \text{ 'k}$$

$M_{L.L.} = 1.813^{\text{'k}}$ for load condition 3, shell-plate element 53, with axial load $P = .8943^{\text{k}}$. Neglect P .

Maximum Concrete Stress

$$f = \frac{Mc}{I} = \frac{2.309(1.96)12000}{148.748} = 365 \text{ psi}$$

Allowable Stress = 1200 psi

Maximum Steel Stress

$$f = \frac{Mc}{I} = \frac{2.309(4.54)12000(10)}{148.748} = 8457 \text{ psi}$$

Allowable Stress = 20,000 psi

Maximum Shear (See page E-3)

$$v = \frac{V}{bjd} = \frac{26,500}{4(12)(.875)(6.5)} = 97 \text{ psi}$$

Allowable Shear = 90 psi

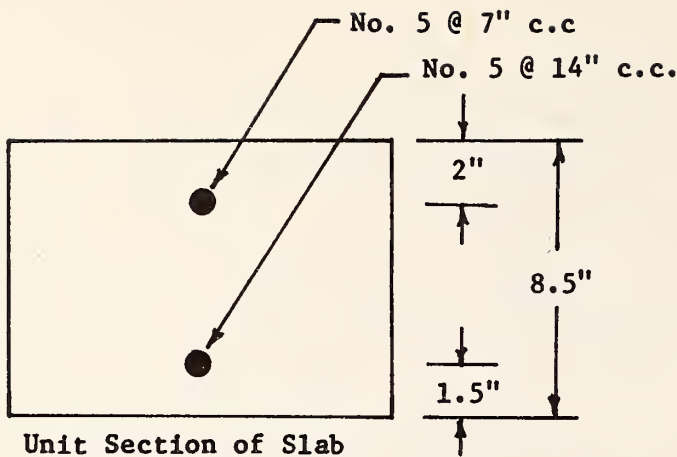
Maximum Bond Stress

$$u = \frac{V}{\sum o_j d} = \frac{26,500}{4(3.36)(.875)(6.5)} = 347 \text{ psi}$$

1935 AASHO Allowable Stress = 120 psi Overstressed

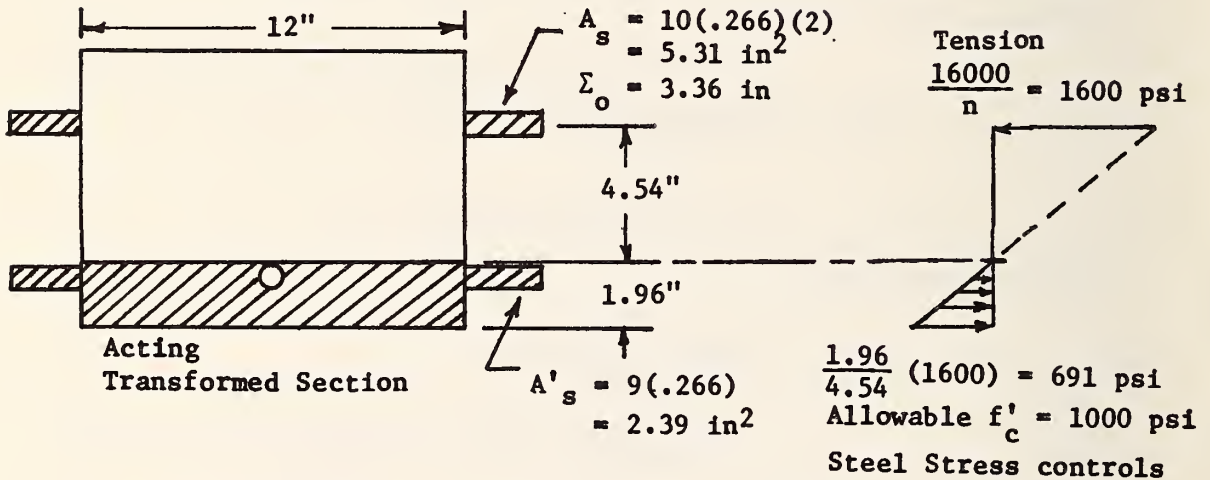
As a matter of interest, the 1973 specifications would allow:

$$\frac{4.8\sqrt{f'_c}}{D} = \frac{4.8(54.77)}{.625} = 420 \text{ psi}$$



$$n = 10$$

$$\text{Acting } A = 31.22 \text{ in}^2$$



Σ Moments about neutral axis

$$-5.31(6.5 - x) + 2.39(x - 1.5) + \frac{12x^2}{2} = 0$$

$$-34.515 + 5.31x + 2.39x - 3.585 + 6x^2 = 0$$

$$6x^2 + 7.7x - 38.1 = 0$$

$$x = \frac{-7.7 \pm \sqrt{7.7^2 + 4(6)(38.1)}}{12}$$

$$= +1.96'' \leftarrow \text{use}$$

$$-3.24''$$

Transformed I

$$5.31(4.54)^2 = 109.448$$

$$2.39(1.96 - 1.5)^2 = 9.181$$

$$12 \frac{(1.96)^3}{12} = 7.530$$

$$12(1.96) \frac{(1.96)^2}{2} = 22.589$$

$$I = 148.748 \text{ in}^4$$

FIG. E-8 - CALCULATIONS OF MOMENT OF INERTIA OVER TRANSVERSE UNIT WIDTH OF SLAB FOR BRIDGE #3

7. AASHO Specifications for Bridge #4

Bridge #4 was built in 1950 under the Standard Road and Bridge Specifications of the Tennessee Department of Highways and Public Works. For this report the review for HET-70 loading is made under the 1949 AASHO specifications and 1973 specifications. For 1973 specs see page E-2.

Applicable 1949 AASHO Specifications (23)

Allowable stresses:

Flexural tension or compression Embedded upper flange considered fully supported laterally - A-7 steel assumed.	18000 psi
Shear in girder webs, gross section.	11000 psi
Concrete flexure in compression.	1000 psi
Concrete shear in beams without web reinforcement, longitudinal bars anchored.	90 psi
Bond stress in reinforced steel, bars anchored by hooks.	225 psi
Tension in reinforcing steel - Although type of steel was not given on the plans, reference 1 shows the yield point to be 40,000 psi. (24)	20000 psi

8. Stress Calculations for Bridge #4

In the Tennessee report (4) it was stated that "the bridge was designed to act non-compositely; however, the experimental located position of the neutral axis clearly indicated that a considerable degree of composite action did exist." It was for that reason that the computer program used slave nodes tying the stringers to the deck when comparing the deflections versus test data for Volume I. (25) The same type of computer format, however, is used for the HET-70 loading, although no test data exists, with the advantage that this type of format enables one to obtain the transverse slab moments directly without computing a new set of data for the slab alone resting on yielding supports. For the girder moments, we simply compute the composite moment as in the previous examples (bridges #1 through #3) and apply this to the non-composite girder.

In bridges #1 through #3, the dead load girder moments were furnished. For this bridge we must first compute them; either by input loading in the computer program or by hand. The author has used the latter method here. Fig. E-9 shows the calculation of

dead load moment at the critical positive moment section in the 60' span, as indicated by load condition 1, page 27. The method of *moment distribution* is used for this calculation.

Live Plus Dead Load Stresses for Maximum Positive Moment in 60' Span

$$M_{L.L.} = 181.53^k \text{ (See page 28)}$$

$$f = \frac{Mc}{I} = \frac{(181.53 + 94.57)}{3610} \left(\frac{27.02}{2} \right) 12000 = 12,399 \text{ psi}$$

$$\text{Allowable Stress} = 18,000 \text{ psi}$$

where $I = 3610 \text{ in}^4$ for the W 27 x 94 girder (see Fig. E-10).

Shear

$$V_{D.L.} = 24.24^k$$

$$V_{L.L. \text{ max}} = 27.65^k + 26.5^k = \underline{54.15^k} - \text{beam element 20,}$$

Total $V = 78.39^k$ load condition 4

$$v = \frac{V}{t_w d} = \frac{78.39(1000)}{27.07(.518)} = 5590 \text{ psi}$$

$$\text{Allowable} = 11,000 \text{ psi}$$

Maximum Negative Moment

Fig. E-11 shows the maximum negative moment for HET-70 loading of 196.5^k occurring in beam element 20 under load condition 1. For negative live plus dead load moment the stress becomes:

$$f = \frac{Mc}{I} = \frac{(196.5 + 229)}{6512.3} \frac{27.77}{2} (12000) = 10,887 \text{ psi}$$

(not the critical stress)

where $I = 6512.3$ for the W 27 x 94 girder with cover plates (see Fig. E-10).

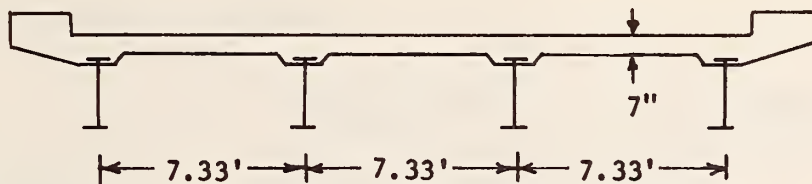
Transverse Slab Stresses

$$\text{Transverse distance between girders} = 7.33'$$

$$M_{D.L.} = .1w\ell^2 = .1\left(\frac{7}{12}\right)(150)7.33^2 = 470 \text{ \#}$$

$$M_{L.L.} = -2.711^k \text{ for element 48 under load condition 1,}$$

with an axial load of $.06453^k$. Neglect axial load.



$$w = \frac{7}{12}(150) = 87.5 \text{ \#/ft}^2$$

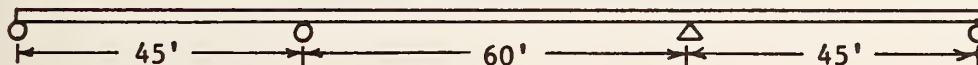
From page 2-210, AISC Manual, reaction of interior stringer is:

$$1.1w\ell = 1.1(87.5)7.33' = 706 \text{ \#/ft.}$$

$$\text{D.L. Girder} = \frac{102}{808} \text{ \#/ft.}$$

$$\begin{aligned} \text{FEM} &= \frac{w\ell^2}{12} = \frac{.808}{12}(60)^2 = 242.40 \text{ 'k} \\ &= \frac{.808}{12}(45)^2 = 136.35 \text{ 'k} \end{aligned}$$

$$\frac{w\ell^2}{8} = \frac{.808}{8}(60)^2 = 363.6 \text{ 'k}$$



1.0		.57	.43		.43	.57	1.0
+136.35	-136.35	242.40		-242.40	136.35	-136.35	
-136.35	-60.45	-45.60		+45.60	+60.45	+136.35	
-30.23	-68.18	+22.80		-22.80	+68.18	+30.23	
+30.23	+25.87	+19.51		-19.51	-25.87	-30.23	
+12.94	+15.12	-9.76		+9.76	-15.12	-12.94	
-12.94	-3.06	-2.30		+2.30	+3.06	+12.94	
	-6.47				+6.47		
	+3.69	+2.78		-2.78	-3.69		
	-229.83	229.83		229.83	-229.83		

Moment Distribution

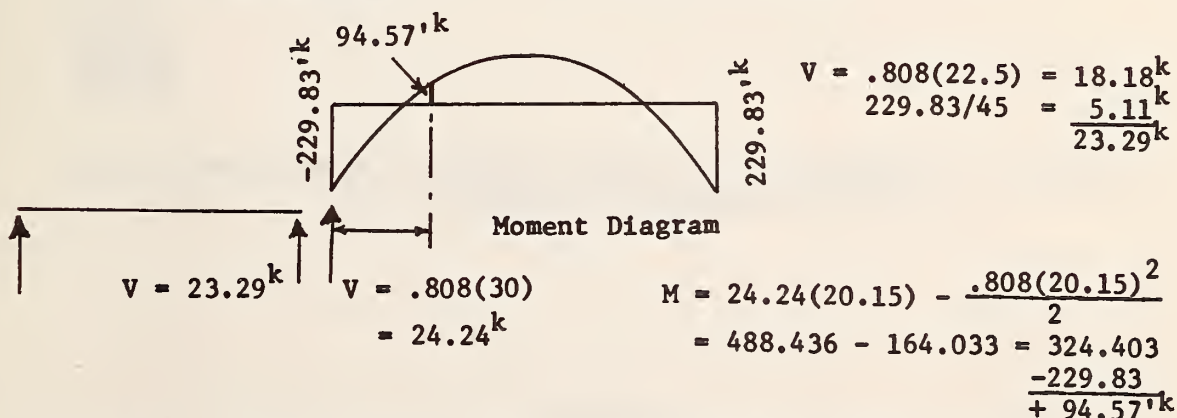
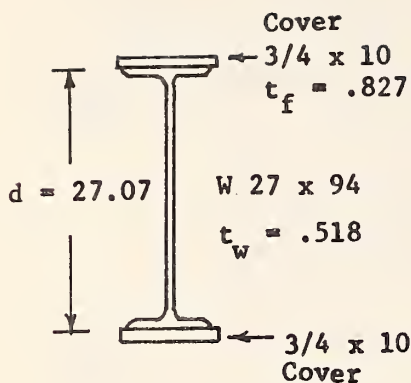


FIG. E-9 - CALCULATIONS OF DEAD LOAD MOMENTS AND SHEARS FOR THE INTERIOR GIRDER OF BRIDGE #4



$$\begin{aligned}
 I_o &= 3610 \text{ in}^4 \text{ for pos. moment} \\
 \text{Covers} &= 2(10)(.75)(13.91)^2 = \underline{2902.3} \\
 I &= 6512.3 \text{ in}^4 \text{ (for neg. moment)}
 \end{aligned}$$

FIG. E-10 - MOMENTS OF INERTIA OF GIRDER AND COVER PLATES FOR BRIDGE #4

BRIDGE #4 - Load Condition 1

<div style="border: 1px solid black; padding: 5px; display: inline-block;"> Sh 29,30 Bm 20 </div>	$P = 4.481$ $M = 2.74$	$.2712(3.67) = .9953$ $.4757(3.67) = \underline{1.7458}$ 2.7411
	$1.63'$	$5.882(3.67) = 21.587$ $6.328(3.67) = \underline{23.224}$ 44.811
	$P = 53.15^k$ $M = 107.10^k$	$M \text{ (including slab)}$ $53.15(1.63) = 86.63$ 2.74 $\underline{107.10}$ 196.47

FIG. E-11 - CALCULATIONS OF MAXIMUM NEGATIVE MOMENT AT ONE OF THE INTERIOR SUPPORTS FOR BRIDGE #4

Maximum Concrete Stress

$$f = \frac{Mc}{I} = \frac{3.181(1.74)12000}{129.15} = 514 \text{ psi}$$

$$\text{Allowable Stress} = 1000 \text{ psi}$$

Maximum Steel Stress

$$f = \frac{Mc}{I} = \frac{3.181(3.26)12000(10)}{129.15} = 9635 \text{ psi}$$

$$\text{Allowable Stress} = 20,000 \text{ psi}$$

Shear (See page E-3)

$$\frac{v}{b_j d} = \frac{26,500}{4(12)(.875)(6.5)} = 97 \text{ psi}$$

$$\text{For } f'_c = 3000 \text{ psi} - \text{Allowable} = 90 \text{ psi}$$

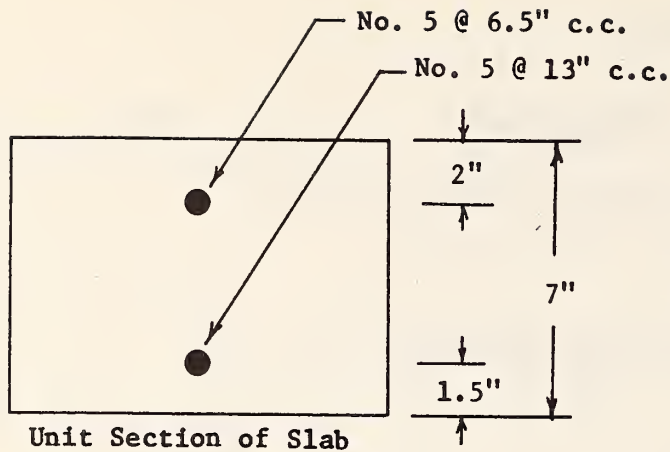
$$\text{For test } f'_c = 6500 \text{ psi} - \text{Allowable} = 195 \text{ psi}$$

Bond Stress (See page E-3)

$$u = \frac{V}{\sum o_j d} = \frac{26500}{4(3.36)6.5} = 303 \text{ psi}$$

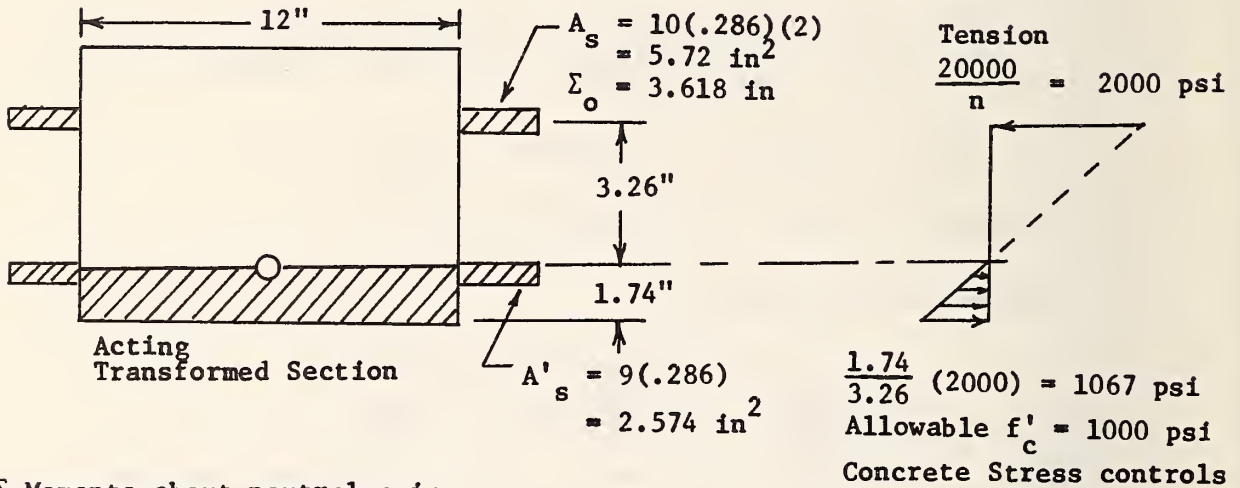
Allowable bond stress = $.075f'_c = 225 \text{ psi}$ - by 1950 specifications, or = 420 psi by test value of $f'_c = 5600 \text{ psi}$. Since the specs state a maximum of 225 psi, the slab would be overstressed in bond. Under 1973 specifications, however, the allowable bond stress would be:

$$\frac{4.8\sqrt{3000}}{.625} = 420 \text{ psi.}$$



$$n = 10$$

$$\text{Acting } A = 29.174$$



Σ Moments about neutral axis

$$\begin{aligned} -5.72(5 - x) + 2.574(x - 1.5) + 6x^2 &= 0 \\ -28.6 + 5.72x + 2.57x - 3.861 + 6x^2 &= 0 \\ 6x^2 + 8.294x - 32.461 &= 0 \end{aligned}$$

$$x = \frac{-8.294 \pm \sqrt{8.294^2 + 4(32.461)6}}{12} = \begin{matrix} +1.74 \\ -3.12 \end{matrix} \leftarrow \text{use}$$

Transformed I

$$\begin{aligned} 5.72(3.26)^2 &= 60.79 \\ 2.574(1.74 - 1.5)^2 &= .15 \\ 12 \frac{(2.574)^3}{12} &= 17.05 \\ 12(2.574) \frac{(2.574)^2}{2} &= 51.16 \\ I &= 129.15 \text{ in}^4 \end{aligned}$$

FIG. E-12 - CALCULATIONS OF MOMENT OF INERTIA OVER TRANSVERSE UNIT WIDTH OF SLAB FOR BRIDGE #4

TE 662

.A3

no. FHWA-RD-75-

BORROWER

K. J. H. H.

DOT LIBRARY



00054989

